UNIVERSITY OF MODENA AND REGGIO EMILIA

Doctorate School in Clinical and Experimental Medicine

Curriculum: Translational Medicine

PhD Cycle: XXXV

Role of miRNAs in predicting Growth Hormone (GH) response in children with Growth Hormone Deficiency (GHD) and their relationship with oncogenesis: miRNA profiling, *in silico* and *in vitro* studies.

Candidate: Dr. Cecilia Catellani

Tutor: Dr. Maria Elisabeth Street

Co-Tutor: Dr. Stefania Croci

PhD School Coordinator: Prof. Marco Vinceti

Index

Abstract ……3

List of abbreviations ...……..……5

1. Background ……..8

1.1 Growth hormone (GH) and the GH/IGF-I axis …….. 8

1.2 The role of GH in longitudinal growth and GH deficiency……13

1.2.1 GH deficiency ……15

1.2.2 The potential oncogenic effect of GH treatment ……17

1.3 The epigenetic regulation of growth: focus on microRNAs……...18

1.3.1 miRNA biogenesis and functions……18

1.3.2 miRNAs in the regulation of growth……22

1.3.3 miRNAs in cancer……24

2. Aims of the study……26

3. Patients and methods ……27

3.1 Patients ……...27

3.1.1 Ethical approval……....27

3.1.2 Collection of auxological parameters and bone age……30

3.1.3 Collection of biochemical parameters……..30

3.2 Blood sample processing ……...……..…..30

3.3 RNA isolation and cDNA preparation……31

3.3.1 Total RNA isolation from serum samples……31

3.3.2 Preparation of cDNA for miRNA profiling analysis and validation step……32

3.4 Real-time qRT-PCR……33

3.4.1 MiRNA profiling analysis in serum……33

3.4.2 MiRNA validation step in single assay in serum……34

3.5 MiRNA target prediction and pathway analysis……35

3.6 *In vitro* study……...36

3.6.1 Cell cultures……..…36

3.6.2 GH treatment *in vitro* …….....36

3.6.3 Transfections with miRNA mimics and inhibitors……..36

3.6.4 MiRNA target prediction……37

3.6.5 Total RNA isolation from cells……37

3.6.6 Preparation of cDNA for the analysis of miRNA levels *in vitro*……38

3.6.7 Preparation of cDNA for gene expression analysis *in vitro*…….39
3.6.8 MiRNA expression analysis *in vitro*……40
3.6.9 Gene expression analysis *in vitro* of miRNA target genes and differentiation markers …….40
3.6.10 Cell viability/proliferation assay ..…….....41
3.6.11 Cell lysis in situ……..42
3.6.12 Western blot analysis……42
3.7 Statistical analysis……...43
4. Results……..46
4.1 Growth and biochemical parameters during the first 12 months on GH treatment……46
4.2 Discovery miRNA profiling step……48
4.3 Pathway enrichment analysis……..49
4.4 miRNA validation step……52
4.5 Simple linear regression analysis and multiple stepwise linear regression models to explain growth response……57
4.6 *In vitro* study……...63
4.6.1 miR-199a-5p, miR-335-5p and miR-494-3p are expressed in HOB cells ….....63
4.6.2 Study of the effects of GH treatment on miRNA levels in HOB cells ..……..63
4.6.3 *In silico* analysis of predicted targets of miR-199a-5p, miR-335-5p and miR-494-3p within bone……...65
4.6.4 Analysis of CLOCK, ROCK1 and CRIM1 gene expression levels in HOB cells.....65
4.6.5 Analysis of transfection efficiency……...66
4.6.6 Analysis of the effects of the miRNAs mimics and inhibitors on CLOCK, ROCK1, and CRIM1 gene expression levels……67
4.6.7 Analysis of the effects of the miRNA mimics and inhibitors on CLOCK and ROCK1 protein levels ……...…...68
4.6.8 Analysis of the effects of miRNA mimics and inhibitors on gene expression levels of the differentiation markers SPP1, COL1A1 and COL1A2……71
4.6.9 Analysis of the effects of miRNAs on cell viability/proliferation..…….72
5. Discussion……73
6. Conclusions……..79
7. References……80
List of papers published during the 3 years of PhD……...108

Abstract

Growth Hormone (GH) and its main peripheral effector, insulin-like growth factor (IGF)-I, play a fundamental role in growth processes and metabolism. Pediatric subjects diagnosed with GH deficiency (GHD) undergo long-term GH replacement therapy at dosages that are currently not individualized and growth rates do not always coincide with the expected. The role of GH in the regulation of cell proliferation, differentiation and apoptosis leads to consider possible oncogenic effects. MicroRNAs (miRNAs) are post-transcriptional regulators of gene expression, which are involved in many biological processes such as body growth and cancer. Moreover, miRNAs are studied as biomarkers of diseases and as markers to optimize administration of pharmaceutical agents.

This project aimed at identifying circulating miRNAs varying in prepubertal GHD patients undergoing GH treatment by using a miRNA profiling approach and at evaluating whether they could be useful to predict the clinical outcome in terms of growth. Furthermore, it aimed at evaluating the impact of the identified miRNAs on pathways related with cancer by using an *in silico* approach and functional assays *in vitro* on primary cells.

The miRNA profiling analysis on serum samples from 10 GHD patients (5 males, 5 females) at two time points before starting GH treatment (i.e. the baseline), and at 3 months on treatment allowed to identify 16 miRNAs which were upregulated and 2 miRNAs which were downregulated. The *in silico* analysis evidenced the involvement of these miRNAs in growth and cancer and allowed to select a subset of 8 miRNAs with a putative role in growth and bone metabolism, which underwent a validation step in 25 GHD patients. MiR-199a-5p, miR-335-5p, and miR-494-3p were confirmed to be upregulated after 3 months on GH treatment.

The analysis of miRNA expression over 12 months of GH treatment evidenced that miRNA variability tends to decrease after 12 months on treatment. No differences in miRNA levels

between responder and non- responder patients were observed. These 3 miRNAs contributed to explain growth response on GH treatment in terms of height variation (0-12 months) (Adj.R^2=0.79; R^2CV=0.43) and growth velocity variation (0-6 months) (Adj.R^2=0.75; R^2CV=0.63). A target prediction analysis of these 3 miRNAs evidenced that miR-335-5p and miR-199a-5p are predicted to target CRIM1 which binds with both BMP4 and BMP7 in the Golgi and determines a reduction in the production and processing of preproteins to mature BMPs and a reduction of secretion of mature BMPs. Moreover, miR-199a-5p, miR-335-5p, and miR-494-3p are predicted to target CLOCK, which is involved in circadian clock regulation known to be linked to bone development and cancer and ROCK1, which is increased in many tumors and related to metastasis. The *in vitro* study of the effects of these miRNAs on HOB osteoblasts evidenced that these miRNAs had no effects on cell viability after miRNA transfection. Moreover, osteopontin (SPP1), COL1A1 and COL1A2 were analyzed as markers of cell differentiation in HOB cells after miRNA transfection and their expression levels did not change. Furthermore, the 3 miRNAs showed to have no effects on CLOCK, CRIM1, and ROCK1 gene expression nor CLOCK and ROCK1 protein levels. To conclude, this project led to the identification of 18 miRNAs that change in response to GH treatment and among these miR-199a-5p, miR-335-5p, and miR-494-3p were confirmed to change. The early change in these miRNAs contributes to explain growth response in terms of height variation 0-12 months and growth velocity variation 0-6 months, and they could be used in future for prediction models to customize treatment. Current data do not indicate a role of these miRNAs in increasing the risk for cancer.

List of abbreviations

AC: adenylate cyclase

ACTB: β-actin

AKT: AKT Serine/Threonine Kinase

BMI: Body mass index

C/EBP: CCAAT-enhancer-binding protein

CA: chronological age

cAMP: cyclic AMP

CCND1: Cyclin D1

CDK6: Cyclin Dependent Kinase 6

CDKN1A: Cyclin Dependent Kinase Inhibitor 1A

circRNA: Circular RNA

CLOCK: Circadian Locomoter Output Cycles Protein Kaput

COL1A1: Collagen Type I Alpha 1 Chain

COL1A2: Collagen Type I Alpha 2 Chain

CRE: CAMP Responsive Element

CREB: CAMP Responsive Element Binding Protein

CRIM1: Cysteine Rich Transmembrane BMP Regulator 1

CSH1: Chorionic Somatomammotropin Hormone 1

CSH2: Chorionic Somatomammotropin Hormone 2

CSHL: Chorionic Somatomammotropin Hormone Like 1

ERK 1/2: extracellular signal-regulated kinase 1/2

GAPDH: Glyceraldehyde-3-Phosphate Dehydrogenase

GH: growth hormone

GH1: Growth Hormone 1

GH2: Growth Hormone 2

GHR: Growth Hormone Receptor

GHRH: Growth Hormone Releasing Hormone

GHRHR: Growth Hormone Releasing Hormone Receptor

GHS-R1a: Growth Hormone Secretagogue Receptor 1a

GPCR: G protein-coupled receptors

GRB2: Growth Factor Receptor Bound Protein 2

GTP: Guanosine-5'-triphosphate

IGF1R: Insulin Like Growth Factor 1 Receptor

IGFBP 1-6: Insulin Like Growth Factor Binding Protein 1-6

IGF-I: Insulin Like Growth Factor I

IGF-II: Insulin Like Growth Factor II

IIGHD: idiopathic isolated growth hormone deficiency

IP3: Inositol 1,4,5-Trisphosphate

IRS: Insulin receptor substrate

JAK2: Janus Kinase 2

KRAS: Kirsten Rat Sarcoma Proto-Oncogene

MAPK: Mitogen-Activated Protein Kinase

MAPK1: Mitogen-Activated Protein Kinase 1

MDM2: MDM2 Proto-Oncogene

MEK: Mitogen-Activated Protein Kinase Kinase

miRNA: microRNA

PDK1: Pyruvate Dehydrogenase Kinase 1

PI3K: phosphoinositide 3-kinase

PIAS: Protein inhibitor of activated STAT

PIP2: Phosphatidylinositol 4,5-bisphosphate

PIP3: Phosphatidylinositol (3,4,5)-trisphosphate

PKA: protein kinase A

PKC: Protein Kinase C

PLC: Phospholipase C

PLCγ: Phosphoinositide-specific phospholipase C

pri-miRNA: primary miRNA

PTP: Protein tyrosine phosphatase

RAN: RAS-related Nuclear protein

RAS: Rat Sarcoma Proto-Oncogene

ROCK1: Rho Associated Coiled-Coil Containing Protein Kinase 1

SAGhE: Safety and Appropriateness of Growth hormone treatments in Europe

SDS: standard deviation score

SFK: Src family kinases

SOCS: suppressor of cytokine signaling

SPP1: Secreted Phosphoprotein 1 - Osteopontin

STAT: signal transducer and activator of transcription

TNRC6A: Trinucleotide Repeat Containing Adaptor 6A

WST-1: water-soluble tetrazolium salt-1

XPO5: exportin 5

yr: years

1. Background

1.1 Growth hormone and the GH/IGF-I axis

Growth hormone (GH), also known as somatotropin, is a peptide hormone composed by 191 amino acids with a molecular weight of about 22 kDa which was firstly isolated in 1944 (*1*,*2*). In humans, GH is encoded by a gene located in a locus composed by five genes on chromosome 17q22 (*3*). GH1 gene encodes for GH produced mainly in somatotropic cells in the anterior pituitary in children and adults, while the other four genes (GH2, CSH1, CHS2 and CSHL) are typical of placental tissue (*4*).

GH synthesis occurs after activation of G-protein coupled receptor (GPCRs) by the hypothalamic Growth hormone releasing hormone (GHRH); this determines, at the intracellular level, the stimulation of adenylyl cyclase (AC) activity which converts ATP to cAMP and allowing for protein kinase A (PKA) activation that in turn phosphorylates several target substrates (*5*). Among these, cAMP responsive element binding protein (CREB) binds to cAMP responsive elements (CRE) promoting the transcription of *pit-1*, a transcription factor that subsequently induces the expression of the GH gene (*5*).

GH release is pulsatile and follows a circadian rhythm having the maximal release in the second half of the night (*3*). GH secretion is promoted by cAMP which stimulates calcium influx from Ca^{2+} membrane channels and induces GH exocytosis. Moreover, at the intracellular level, βγ subunits of G-proteins can activate protein lipase C (PLC) leading to an increase in inositol triphosphate 3 (IP3), and to the activation of protein kinase C (PKC) also promoting the mobilization and the influx of Ca^{2+}. Besides GHRH, GH synthesis and release is directly promoted also by ghrelin, a protein produced by the stomach which binds GH secretagogue receptor 1a (GHS-R1a) in the pituitary somatotropic cells, and by many other stimulators (*6*).

On the contrary, GH synthesis and secretion is inhibited by somatostatin, an hypothalamic peptide, and by many other inhibitors (*6*). Moreover, at the intracellular level, PKA can limit cAMP levels through the stimulation of phosphodiesterases or through desensitization of GPCRs, thus inhibiting GH synthesis.

GH regulates IGF-I (or somatomedin) synthesis in the liver, which in turns regulates GH release in a negative feedback loop (*7*) (**Figure 1**). IGF-I is known to be the main mediator of the anabolic and mitogenic activity of GH (*8*), however GH has also IGF-independent effects (*9*). The bioavailability of both IGF-I and IGF-II a protein that belongs to IGF family that mainly regulates fetal development, is regulated by six IGFBPs (IGFBP1-6) which regulate the free plasma IGF fraction and transport in different tissues (*10*). Interestingly, about 75% of IGF-I is bound to IGFBP-3 and IGFBP-3 synthesis is also regulated by GH (*11*).

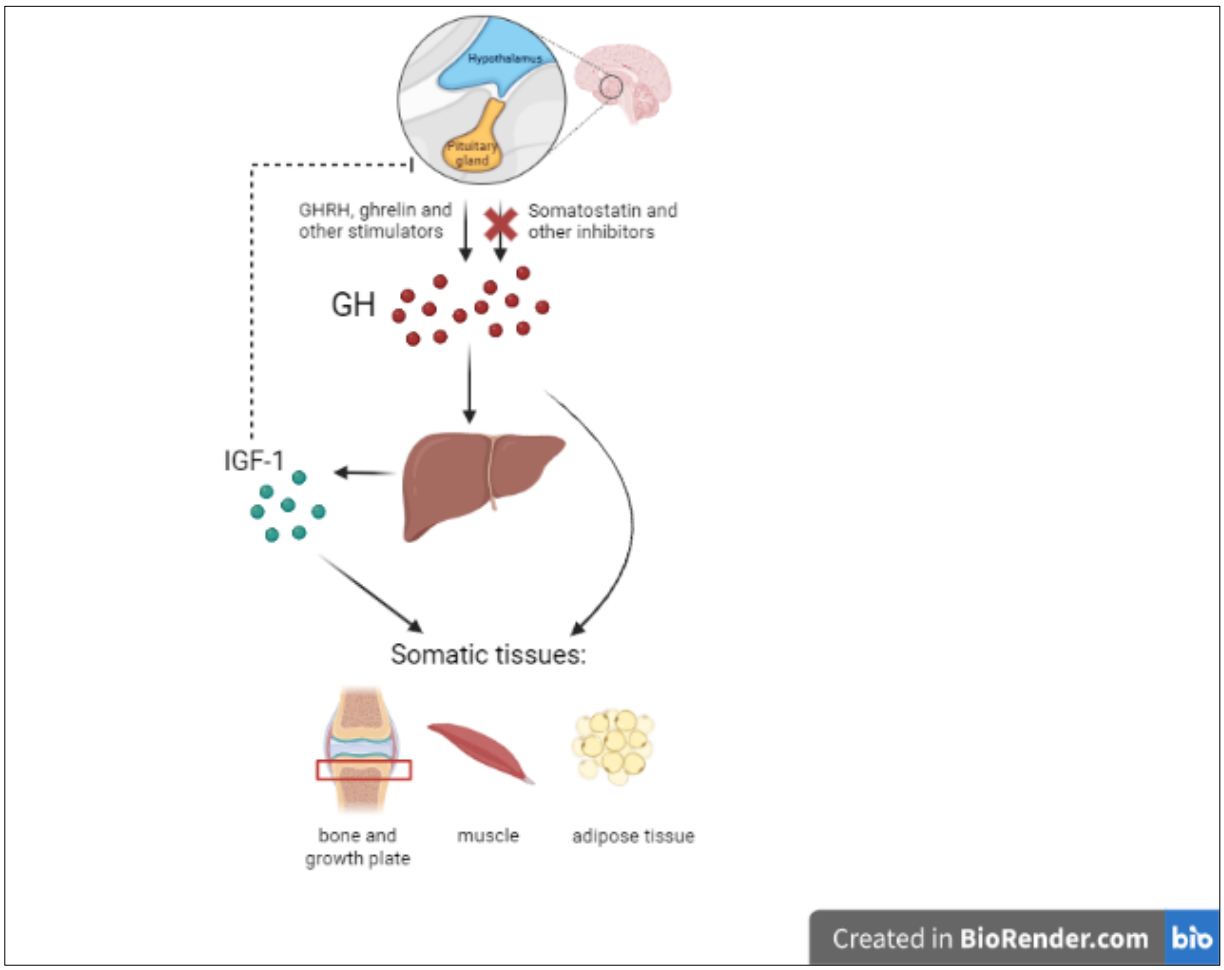

Figure 1. Schematic representation of the GH/IGF-I axis. *GH synthesis mainly occurs in the pituitary gland under the action of GHRH and other stimulators, while is blocked by somatostatin and other inhibitors. Released GH promotes IGF-I synthesis in the liver, which in turn inhibits GH synthesis in a negative feedback loop. Furthermore, GH directly acts on other somatic tissues, such as bone and especially the growth plate, skeletal muscle, and adipose tissue.*

At cellular level, the interaction between GH and GH receptor (GHR), a class I cytokine membrane receptor of about 110 kDa composed by two monomers, induces a conformational change in the receptor which leads to the juxtaposition of catalytic domains and to the phosphorylation of Janus-kinase-2 (JAK2) (*12,13*). Indeed, the catalytic domain of the JAK2 kinase is usually maintained in an inactive form by autoinhibition exerted by its pseudokinase domain and by the SH2-pseudokinase linker which is important for transmitting the ligand binding signal (*5,14*). Besides JAK2, which represents the classical GHR signaling kinase, Src family kinases (SFK) can be directly activated by GHR independently from JAK2 and activate GH signaling pathways (*15,16*). The extent of JAK2 or SFK activated signaling depends on conformational changes occurring in GHR and on the expression levels of these kinases in different cell types (*16)*.

This leads to the activation of three main intracellular signaling pathways: Signal transducer and activator of transcription (STAT), Rat sarcoma protein/Extracellular signal-regulated kinase (Ras/MEK/ERK) and phosphoinositide 3-kinase/AKT serine/threonine kinase (PI3K/AKT). The activation of different pathways depends on the cell type and on the relative expression of the components (*5,12*) (**Figure 2**).

The STAT pathway involves different signaling molecules such as STAT 1, 3, 5a and 5b. In particular, activated JAK2 phosphorylates multiple tyrosine residues in the intracellular domain of GHR which provide a docking site for both STAT5a and 5b and this facilitates their

phosphorylation by JAK2. Otherwise, STAT1 and 3 are directly phosphorylated by JAK2, without docking to GHR. Phosphorylated STAT proteins can dimerize and translocate to the nucleus where they activate gene transcription. In particular, STAT5a and 5b are the main transcription factors that carry out the cell-proliferative action of GH (*12,17*). Moreover, STAT5b can bind to the promoters of both IGF-I and ALS, a critical component of the IGF binding protein (IGFBP) complex, inducing their transcription (*18,19*). This pathway can also be activated by SFK that phosphorylates STAT5 in specific cell types (*20*). The attenuation of JAK-STAT signaling is mediated by tyrosine phosphatases (PTP), by the action of the Suppressors of cytokine signaling (SOCS) protein family, or by protein inhibitor of activated STAT (PIAS) (*5,21).*

The Ras/MEK/ERK pathway can be activated by phosphorylation of JAK2 which activates the adaptor protein SHC that binds with SOS and GRB2 and starts the signaling cascade *(12*). This pathway can be activated also by the phosphorylation of Src which, in turn, induces the activation of phospholipase Cγ (PLCγ)-RAS pathway *(12*).

The activation of the PI3K/AKT pathway accounts for the role of GH in the stimulation of glucose transport (*22).* This pathway involves IRS proteins which are activated by phosphorylation and recruit multiple PI3K proteins which convert Phosphatidylinositol (4,5)-bisphosphate (PIP2) in PIP3 leading to the recruitment of AKT to the plasma membrane. AKT is then partially activated by kinase PDK1 and phosphorylates GSK3 inhibiting its activity. This event reduces the phosphorylation of C/EBP beta determining an increase in C/EBP binding to the *c-fos* promoter, inducing its transcription (*23*). The proto-oncogene *c- fos* is involved in cell metabolism is also an interesting example of how these three different signaling pathways can work together (*22*). Indeed, the *c-fos* gene expression depends on the binding to the promoter region of proteins belonging to the STAT, and MAPK pathways and PI3K/AKT pathway (*22*). Moreover, many intracellular proteins belonging to these three pathways

represent a point of convergence between GH and insulin signaling pathways; indeed, STAT5, SOCS proteins, IRS proteins, PI3K/AKT and ERK1/2 are shared between the pathways (*24,25*). A possible competition for intracellular substrates could be an explanation of the negative effect of GH on insulin signaling (*26,27).* Another possible explanation is that GH could increase the expression of *socs* genes which negatively regulate the insulin singnaling pathway (*28*).

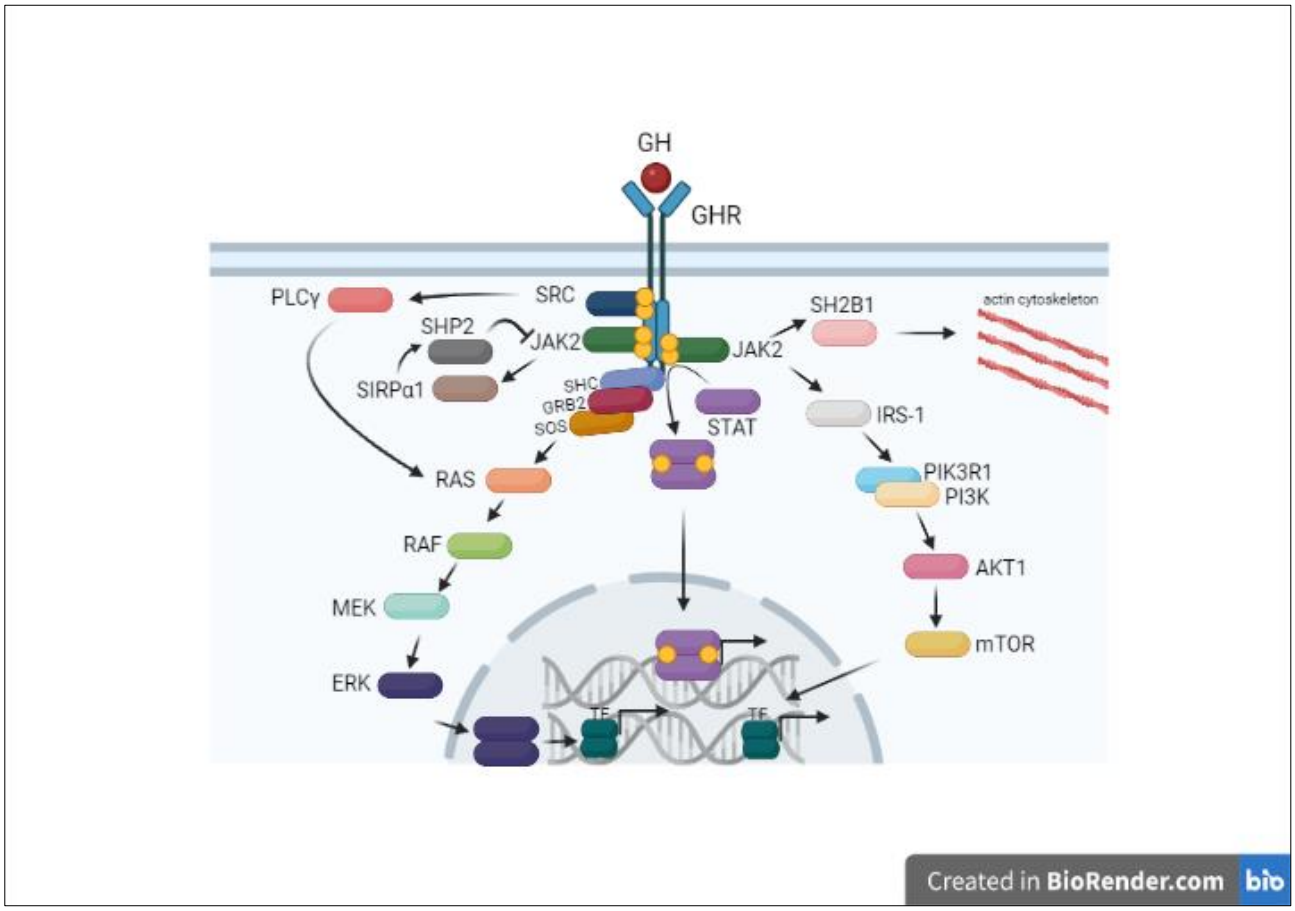

Figure 2. GH signaling pathways. *The binding of GH to GHR leads to the activation of three main intracellular signaling pathways: Signal transducer and activator of transcription (STAT), Rat sarcoma protein/Extracellular signal-regulated kinase (Ras/MEK/ERK) and phosphoinositide 3-kinase/AKT serine/threonine kinase (PI3K/AKT). The activation of different pathways depends on cell type and on the relative expression of the components and ultimately induces the activation of specific transcription factors and contributes to multiple responses in GH targeted cells.*

GH is a pleiotropic hormone which plays a fundamental role in many biological processes such as chondrogenesis and longitudinal bone growth (*29,30*). Moreover, GH is important for metabolism, particularly related with the liver and adipose tissue where it promotes gluconeogenesis and lipolysis respectively, for the immune, reproductive and cardiovascular systems, for the nervous system during neural stem cell proliferation and synapsis connection formation, and for kidney and gut functions (*31,32*).

1.2 The role of GH in longitudinal growth and GH deficiency

Human growth is a multifaceted process which involves sequential modifications in an individual's functions that are controlled by the combination of different factors starting from the genetic background and then continuing with the endocrine system, the environment, and the epigenetic regulation of gene expression (*33*).

The most relevant mechanism involved in the longitudinal growth of the skeleton is endochondral ossification which is responsible of the growth of long bones, skull base bones, and vertebral formation. This process occurs in the growth plate, a thin layer of cartilage which is located in the metaphyses of long bones and on the surface of plates between vertebral bodies. The growth plate is histologically subdivided in three distinct zones: the germinal (or resting) zone composed by progenitor chondrocytes, the proliferative zone formed by chondrocytes that proliferate unidirectionally and produce extracellular matrix proteins, and the hypertrophic zone in which chondrocytes exit the cell cycle and undergo hypertrophic differentiation and synthesis of collagen type 10 (*34*). Finally, chondrocytes undergo apoptosis, cartilage becomes mineralized and is subsequently resorbed by osteoclasts, and new bone tissue is formed by osteoprogenitors (*34*). Proliferation of chondrocytes in the epiphyseal side and chondrocyte degeneration with the progressive replacement with bone tissue in the diaphyseal side occur at the same rate; this allows bone elongation during human growth (*35*). At the end of puberty the

rate of growth division decreases while ossification rate remains the same and this induces a thinning of growth plate until it disappears along with cessation of longitudinal growth (*35*).

GH is the main endocrine regulator of human growth and exerts its effect promoting growth plate chondrogenesis both directly and indirectly via IGF-I (*36*). The original "somatomedin hypothesis" argued that GH induces longitudinal bone growth by stimulating IGF-I synthesis in the liver, which in turn determines longitudinal bone growth in the growth plate (*37,38*). In particular, IGF-I induced chondrocyte proliferation, endochondral ossification ultimately resulting in linear bone growth (*38*).

GH was further proposed to induce IGF-I expression also in extra-hepatic tissues and locally in the growth plate (*39,40*). Many years later, the contribution of different extra-hepatic IGF-I sources but also a direct impact of GH on bone were reported (*41*). Indeed, a transgenic mouse model developed with a selective *Igf-I* deletion in the liver had reduced circulating IGF-I levels and a huge increase in circulating GH levels also due to the loss of IGF-I feedback inhibition, with no significant reduction in body growth and femoral growth compared with wild-type mice suggesting a direct impact of GH on bone growth (*41*).

Consistently, the "dual effector theory" substained a direct action of GH on cell proliferation and differentiation (*42-44).* This theory was supported by the fact that direct growth promoting effects of GH have been documented by the injection of GH in a rat tibial growth plate resulting in the induction of growth, limited only to the injected bone (*45,46*). Moreover, in *igf-I* null mice, growth plate germinal zone was expanded and given the absence of IGF-I, high circulating GH levels may be responsible of this effect (*47*). In particular, GH was reported to be mainly involved in chondrocyte proliferation, while IGF-I was mainly involved in the increase of chondrocyte size (*47*). To further elucidate this aspect, *Igf-I*-null and *Ghr*-null mice were generated and a comparison of long bone growth was performed. Interestingly, in

complete absence of IGF-I but with elevated GH circulating levels only the hypertrophic zone was reduced, while in complete absence of GHR both germinal zone and hypertrophic zone were reduced leading to corroborate the dual role of GH, both IGF-I-dependent and IGF-I-independent (*30*). However, it must be taken into account that in *Igf-I*-null mice, IGF-II mRNA levels were increased with respect to *Ghr*-null mice, so the observed IGF-I-independent effects of GH could be partially due also to the stimulation of *igf-II* expression (*30*).

More recently, the generation of conditionally postnatally ablated mice for *Igf1r* only in chondrocytes allowed to evaluate that the lack of IGF1R in the growth plate resulted in reduced body and tibial growth. However, the injection of GH induced body and tibial growth as well as cartilage formation establishing an IGF-independent role of GH in promoting longitudinal growth (*9*). Indeed, the injection of GH in *Igf1r KO* mice induced the phosphorylation of only JAK2, indicating the activation and binding only to GHR (*9*).

Besides cartilage, direct effects of GH on osteoblastogenesis and bone formation were reported (*48,49*). Moreover, the GH-IGF-I axis is involved in bone turnover (*50,51*).

To recapitulate, GH exerts both IGF-I dependent and IGF-I-independent actions that, during childhood and adolescence, promote longitudinal bone growth and somatic maturation (*3*).

1.2.1 GH deficiency

GH deficiency (GHD) is a rare disorder with incidence and prevalence that vary based on the considered period (*52,53*). Specifically, since the second half of the 20th century, in the *pituitary-hGH era* when human and monkey pituitary GH started to be administered in humans, only very short children (height < -3 SDS) were diagnosed, and a GH test cut-off < 5 ng/mL was considered, an incidence of 1:4000 and a prevalence of 1:5,000-30,000 were documented (*54,55*). Later, during the *recombinant-human GH (rhGH) era* when rhGH became available thanks to recombinant DNA technology, and the GH test cut-off for the diagnosis was increased

to 10 ng/ml, a doubling of the incidence in childhood-onset GHD in both Denmark and Germany was observed (*56,57*). GHD can be subdivided into congenital, acquired, or idiopathic based on the etiology (*58).* Moreover, GHD can be isolated or part of a multiple pituitary hormone deficiency syndrome (*59*).

Congenital GHD presents at birth and can be due to genetic mutations and/or structural brain malformations (*60*). Mutations in known genes pivotal for GH action, pituitary development, or transcription factors (e.g. GH1, GHRH, GHRH receptor (GHRHR)) are identified in a relatively small portion of patients about 11%, suggesting the involvement of other factors (*59*).

Acquired GHD can be caused by midline tumours, cranial irradiation, traumatic brain injury, central nervous system infections and inflammatory conditions (*60).*

However, in the majority of children diagnosed with GHD, specific causes of short stature are unknown and they receive a diagnosis of an "idiopathic growth hormone deficiency" (*61*). Idiopathic isolated GH deficiency (IIGHD) is a not inherited condition characterized by growth failure and consequent short stature with normal proportions and appropriate body weight (*61).* Patients with childhood-onset IIGHD usually have no additional pituitary hormone deficiencies, and no identifiable etiology for the condition (*62*). IIGHD, when not diagnosed and treated, results in short stature, decreased bone turnover, reduced bone mineral density, decreased muscle strength, and increased fracture risk in adulthood (*63).* Moreover, IIGHD can result in delayed puberty, thin skin and hair, increased adiposity and hepatic steatosis (*12,50,63*).

Pediatric subjects diagnosed with IIGHD undergo long-term GH replacement therapy; the observed growth response in these patients depends both on the patient's basal conditions and on a personal innate sensitivity to therapy (*64*). Often, during treatment, the measured growth rate does not correspond with the expected one and the degree of correlation between clinical–

auxological parameters, and GH dose and peak at testing is extremely variable both inter- and intra-individually. Thus, patients run the risk of receiving an excessively low or high dose of GH (*65-67*). In recent years, with the intention to improve growth response in children, some prediction models and medical devices on web platforms have become available in clinical practice (*68-74*). However, these interactive tools use universal algorithms based on growth prediction models built by collecting clinical data stored in international databases, and they can be used only after the first year of treatment (*68*).

The use of complex mathematical models has been observed to be difficult in the clinical setting (*52)* and the development of easy to use prediction models still remains an unmet clinical need in a perspective of individualization of care and personalized medicine with respect to the current approach of standard care for all patients.

1.2.2 The potential oncogenic effect of GH treatment

The role of GH in the regulation of cell proliferation, differentiation, apoptosis and angiogenesis leads to consider its possible oncogenic effect (*7,75,76*). Morever, the components of GH and IGF system are also locally produced by cancer cells and exert both autocrine and paracrine actions (*7,77).* In particular, autocrine GH has been reported to be involved in neoplastic transformation (*78*) contributing to create a favourable microenvironment (*79*). Consistently, GHR deficiency is associated with reduced aging and cancer risk (*80*). Moreover, a prolonged activation of GHR due to a variant in the sequence of the intracellular domain, prevents the binding of the negative regulator SOCS2 and is associated with an increased risk of lung cancer (*21,81*). Interestingly, pegvisomant, a specific antagonist of GHR, has been proposed as treatment for different types of cancer (*82*).

Interestingly, GH-resistant and humans with IIGHD have been reported to be partially protected from cancer (*80,83*).

Although GH treatment is considered safe (*84*), a potential oncogenic risk in those patients treated with GH still remains debated (*85-88*). In order to evaluate any potential oncological risk in GHD patients who underwent GH replacement therapy in childhood, a European consortium was created in 2009 defined SAGhE (Safety and Appropriateness of GH treatment in Europe). The SAGhE study conducted in France showed an increased risk of mortality for bone tumors in those patients who had been treated with GH in childhood and expecially in those patients who received the highest doses in childhood (*87*). A further and more recent study confirmed an increased risk of bone tumors but not an overall increased cancer risk in subjects treated with GH in childhood (*85*). Cancer risk seems increased particularly in those patients having a moderate/elevate risk of developing tumors due to specific basal conditions (*86*) but the molecular mechanisms underlying the potential association GH-oncogenesis remain to be elucidated.

1.3 The epigenetic regulation of growth: focus on microRNAs

In 1939, Waddington introduced the term "epigenetic" to describe those mechanisms that lead from a genetic trait to a phenotype (*89*) and, over years, this definition has narrowed to those heritable changes in gene function that do not involve changes in the DNA sequence (*29*). During the last two decades, knowledge on epigenetics has increased with the identification of three main mechanisms of epigenetic modifications: DNA methylation, histone modifications and microRNAs (miRNAs).

1.3.1 miRNA biogenesis and functions

MiRNAs are small non-coding RNAs about 22 nucleotide long that act as post-transcriptional regulators in a very specific and context-dependent manner (*90-92*). It has been estimated that miRNAs can regulate up to the 60% of protein coding genes and up to the 30% of the entire mammalian genome (*93,94*).

MiRNAs coding sequences are often organized in clusters and are localized in intergenic regions, with their own individual promoters, or in intragenic regions of the genome; in this latter case they overlap exons and/or introns of annotated genes and are under the same transcriptional regulation of their host genes. Moreover, miRNA expression is tightly regulated by post-transcriptional mechanisms that could influence their stability and processing, and also by epigenetic mechanisms (*95-97*).

In the canonical miRNA biogenesis pathway, miRNA sequences are transcribed by the RNA polymerase II which synthetizes a primary miRNA (pri-miRNA), a relatively long transcript which includes many miRNA sequences folded in hairpins. Pri-miRNAs are processed by a microprocessor complex which includes Drosha, an enzyme which belongs to the RNAse III family of endoribonucleases, complexed with the cofactor Dgcr8 (*98,99*). The processing results in a stem-loop structured pre-miRNA which is exported by the exportin 5 (XPO5):RAN-GTP complex to the cytosol, where it is further cleaved near the loop in a double stranded miRNA by the endoribonuclease DICER1 associated with cofactors such as TRBP (*100*). The miRNA duplex is complexed with Argonaute proteins with the help of chaperone proteins and forms the miRNA-induced silencing complex (miRISC) which performs miRNA strand displacement and strand selection. The miRNA selected strand (-5p or -3p), also known as guide strand, defines the set of target mRNAs. Besides this canonical miRNA biogenesis pathway, summarized in **Figure 3**, several non-canonical pathways have been also documented and they can be grouped as Drosha/Dgcr8-independent and Dicer-independent pathways (*90*). The mature miRNA contains the so called “seed region” of about 7 nucleotides at the 5’-end which guides the miRNA to its target (*100,101*). The hybridization typically occurs at the 3’ untranslated region (UTR) of the mRNA, but miRNAs can also interact with the 5’ UTR, the coding sequence, or the promoter region of target mRNAs (*90,102*). This latter aspect highlights that miRNAs can also exert a co-transcriptional regulation of gene expression by binding to

gene promoters (*103,104*). The mRNA alternative splicing, the different polyadenylation of 3'-UTR sequences, and the presence of RNA binding proteins can modify the availability of miRNA responsive elements (MRE) making miRNA-mediated gene regulation very cell type and cell state specific (*105,106*).

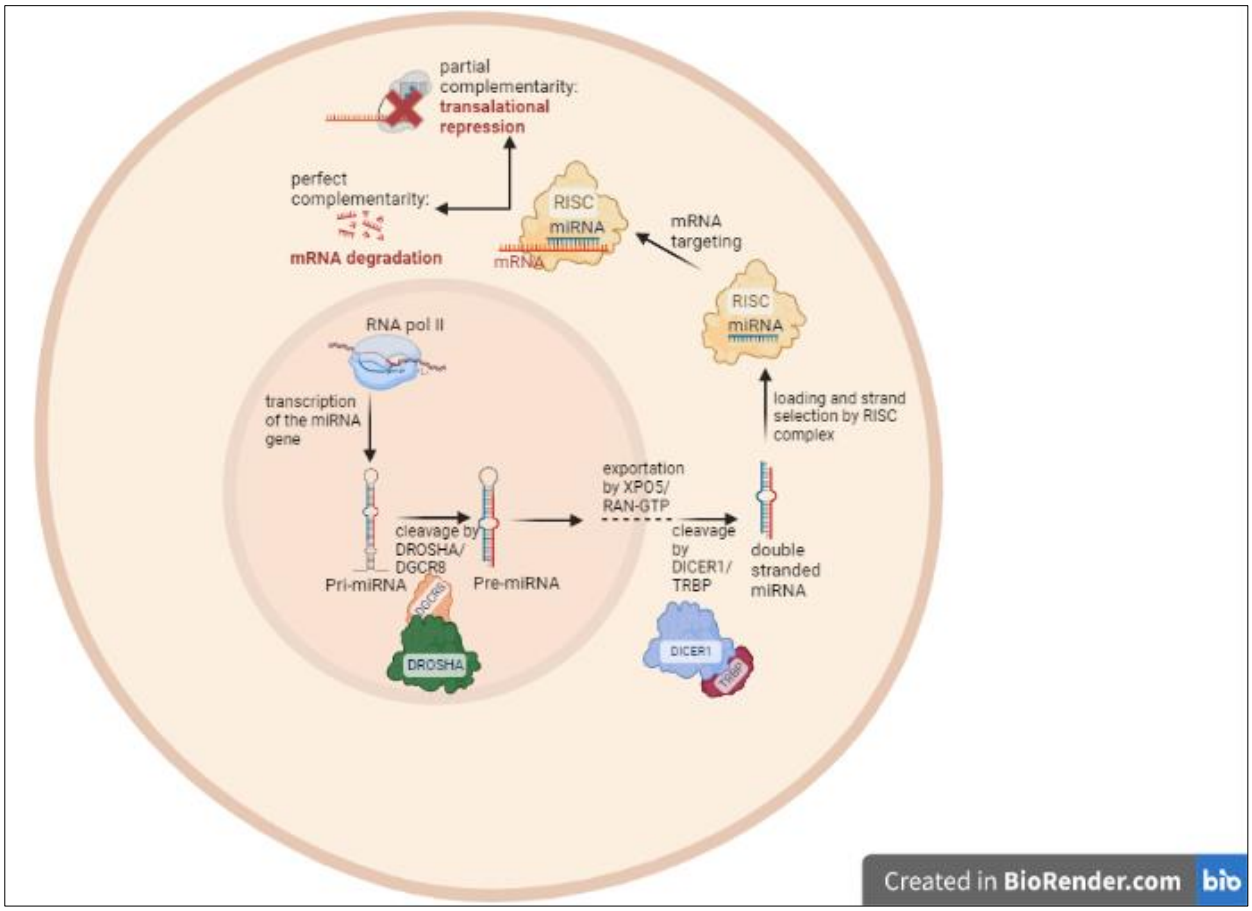

Figure 3. miRNA biogenesis and functions. *RNA pol II transcribes miRNA genes and forms a pri-miRNA which contains many miRNA sequences. The pri-miRNA is cleaved by Drosha:Dgcr8 in a pre-miRNA. The pre-miRNA is exported to the cytosol by XPO5:RAN-GTP and is further processed by DICER1:TRBP in a double stranded miRNA. The miRNA duplex is loaded in RISC where strand displacement and selection is performed. The mature miRNA binds, with a partial or perfect complementarity, to the mRNA target and determines translational repression or mRNA degradation, respectively.*

The complementarity between the miRNA and its targets can be either partial or perfect, determining respectively translational repression of the mRNA or its ubiquitination and

consequent degradation (*94,107*). Interestingly, under specific conditions (*e.g.* starvation, cell cycle arrest and quiescence) miRNAs can also activate translation of target mRNAs (*108,109*).

A single miRNA can regulate many target mRNAs and a single transcript can be modulated by different miRNAs outlining a regulatory network which is pivotal for the maintenance of physiological cell and tissue functions (*99,110*). Moreover, miRNAs participate with other regulators of gene expression, such as transcription factors, in the reinforcement of transcriptional programs, in the limitation of aberrant transcripts and, in some case, help in buffering out random fluctuations in transcript copy number (*111,112*). As a consequence, miRNAs and other proteins may compete for a specific mRNA and modifications in the stoichiometry of mRNA targets, or their localization in different cellular compartments can influence and modify the expected miRNA:target interactions. Moreover, these interactions can be impaired by other competing RNAs (ceRNAs), circular RNAs, long non-coding RNAs which act as molecular "sponges" for miRNAs, or by AU-rich element binding proteins (AUBPs) which can interact with mature miRNAs.

At the intracellular level, miRISC:mRNA complexes can be localized in different compartments which are enriched in components that facilitate miRNA action (*113-115*). For example, at the rough endoplasmic reticulum (rER), miRISC:mRNA complexes are associated to membrane-bound polysomes and can induce translational inhibition of the target. In the cytoplasm, miRNAs can exert their activity in processing (P)-bodies which are cytoplasmic foci enriched in decapping and decay enzymes pivotal for mRNA translational inhibition or degradation. MiRNAs can also be secreted as paracrine factors and transported in exosomes, microvesicles, apoptotic bodies, lipoproteins and ribonucleoproteins, or passively released from cells and mediate intercellular interactions (*116,117*). The presence of miRNAs in blood and other body fluids has opened important venues of research regarding the potential to be used as biomarkers of disease and as markers of administration of pharmaceutical agents (*98, 118-120*).

Indeed, miRNAs fulfill the four most important features of a biomarker: specificity, sensitivity, stability and non-invasive quantification (*121*). Even though miRNA concentrations in body fluids are relatively low, in the order of femtomolar, they can be easily quantified in small sample volumes by means of qRT-PCR, microarrays or RNAseq and a growing body of evidence links changes in miRNA levels to different kind of diseases (*116*).

1.3.2 miRNAs in the regulation of growth

The involvement of miRNAs in the regulation of growth is known since 1993, when the first discovered miRNA, lin-4, was found to regulate growth and development in *Caenorhabditis elegans* (*122*).

At the tissue level, miRNAs are pivotal for longitudinal bone growth and regulate cell growth particularly of chondrocytes (*123*). Indeed, the deletion of Dicer, a crucial enzyme for miRNA biogenesis (*see paragraph 1.3.1*), in murine cartilage evidenced that Dicer-null mice had severe skeletal growth defects and premature death (*124*). In particular, cartilage sections of these mice presented a reduction in proliferative chondrocytes and an increase in hypertrophic chondrocytes accounting for the skeletal growth defects and evidencing the importance of Dicer-dependent events in the regulation of chondrocyte proliferation and differentiation during skeletal development (*124)*. Consistently, a miRNA profiling study on growth plate zones in rat evidenced a differential expression of 34 miRNAs between the proliferative and hypertrophic zones suggesting that miRNA expression patterns could control cell fate of the specific growth plate zones (*125*). Moreover, miRNAs regulate skeletal development and exert their role at different bone developmental stages and in different bone cell types (*126,127*). Consistently, many miRNAs have been reported to be critical in the regulation of GH-IGF1 axis, pituitary development, and growth plate function in different *in vivo* and *in vitro* models (*128*). In particular, miR-141 and miR-429 were reported to reduce the expression of GH and

GHR determining a drastic reduction in body length of zebrafish embryos (*129*). Consistently, other two studies showed that GHR can be regulated by specific miRNAs both *in vivo* and *in vitro* confirming that miRNA regulatory system is of importance for the GH signaling pathway (*130,131*). In detail, let-7b was found to directly target GHR and a specific deletion of let-7b target site at the 3'-UTR induced growth retardation in dwarf chicken as this determines the loss of let-7e regulatory site (*131).* More recently, also miR-129-5p, miR-142-3p, miR-202, and miR-16 were found to inhibit GHR in *in vitro* cell lines (*130*). A profiling analysis of miRNAs in rat pituitary gland highlighted that 15 miRNAs, which were differentially expressed during growth process, were involved in GH signaling and miR-141-3p reduced GH1 mRNA levels (*132*). Moreover, the treatment of swine primary pituitary cells with GHRH which promotes GH secretion and corticostatin, which negatively regulates GH secretion, showed that 19 miRNAs and 35 miRNAs were differentially expressed in response to the two treatments, respectively. In particular, miR-361-5p and miR-127 were regulated in opposite ways under the two treatment indicating a potential role in GH regulation (*133*). Moreover, let-7c was upregulated after CTS treatment and directly regulates both GH1 and GHRH (*133*). Moreover, let-7e, miR-98, miR-193-3p, and miR-195 were associated with a decreased GH secretion from the pituitary in dwarf pigs with respect to healthy control animals (*134*).

In humans, studies on the role of miRNAs in the regulation of growth are lacking. However, an interesting study evidenced different expression patterns of circulating miRNAs between children and adults, suggesting that miRNAs could be involved in growth and development (*135*).

GH itself exerts a role in the regulation of miRNAs. Interestingly, in chicken heaptocytes, GH treatment lead to the up-regulation of 16 miRNAs and to the down-regualtion of 1 miRNA. These miRNAs were predicted to regulate genes involved in both growth and metabolism (*136*). In GH deficient mice, GH replacement treatment induced the down-regulation of miR-29a

which regulates PTEN, involved in the regulation of IGF1 and insulin signaling, as well as genes involved in the extracellular matrix organization important for bone development (*137*). Consistently, the profiling of circulating miRNAs in adult patients and mice with untreated isolated congenital GHD highlighted that 14 miRNAs were regulated by both age and genotype and 19 were regulated only by genotype suggesting that miRNA expression is modulated by GH deficiency (*138*). Moreover, miR-193b-5p, hsa-miR-199a-5p, hsa-miR-654-3p, and hsa-miR-4732-5p emerged to be also associated with glucose metabolism (*138*).

Finally, one study in adult patients reported the reduction of miR-663, miR-2861, miR-3152, and miR-3185 in response to GH treatment (*139).*

1.3.3 miRNAs in cancer

MiRNAs were firstly identified as key players in cancer in 2002 by Calin et al. which showed that miR-15a/16-1 cluster was frequently deleted in chronic lymphocytic leukemia, and assigned to these miRNAs a tumor suppressor role (*140*). Since then, miRNAs have been extensively studied in the context of cancer due to their important regulatory role (*141*).

MiRNAs act in a very specific and context specific manner as onco-miR or tumor-suppressor miRNAs based on the modulatory effect that they exert on the expression of target genes: the up-regulation of onco-miRs tends to suppress the expression of tumor suppressor target genes possibly leading to tumor formation. The the down-regulation of tumor-suppressor miRNAs promotes the translation of oncogenes also leading to tumor formation (*142*).

The most recent findings on miRNAs regulating GH and IGF system in the cotext of cancer have been recently reviewed (*143*) focusing in particular on osteosarcoma which is the most prevalent bone tumor in children and adolescent (*144*) and it has been related with GH treatment (*85,87).* Indeed, an increased risk of osteosarcoma in adults treated with GH in childhood was reported (*85,87).* Moreover, both PI3K/AKT and RAS/MAPK signaling pathways pivotal for

both GH and IGF signaling are over activated during osteosarcoma progression and metastasis (*145,146*).

Several miRNAs have been reported in the literature to be involved in the regulation of the GH/IGF1 axis and IGF system in osteosarcoma. MiR-16 was reported to be downregulated in osteosarcoma cell lines and tissue (*147*). Consistently, miR-16 overexpression induced a reduction in cell proliferation *in vitro* and tumor growth in mice directly targeting IGF1R and inhibiting RAF-MEK1/2-ERK1/2 pathway (*147*). Similar results were obtained for miR-100 which was found to be reduced in osteosarcoma and its overexpression reduced cancer cell proliferation, invasion and migration (*148*). Moreover, it directly targeted IGF1R and inhibited PI3K/AKT and MAPK/ERK pathway (*148*). A further study evidenced that miR-133a was decreased in osteosarcoma cell lines and was reported to control cell proliferation, migration and invasion in vitro and growth and metastasis in vivo (*149*). MiR-133a overexpression reduced these effects and its injection both subcutaneously and systemically in nude mice decreased tumor size and metastases in lung and liver (*149*). IGF1R was reported to be a target of miR-133a (*149*). MiR-335-5p was shown to be reduced in osteosarcoma both *in vitro* and in tissue samples from patients (*150-152*) and its overexpression reduced invasivity and migration of osteosarcoma cells (*150,152)*. However, the observed effects of miR-335-5p on proliferation and apoptosis were different among the different studies and somehow opposite (*150-152)*. Interestingly, miR-335-5p was also reported to directly target IGF1R (*153*).

2. Aims of the study

To date, there is a need to improve growth response in GHD patients and this objective can be reached by ensuring the most tailored GH treatment as possible. In this view, some prediction models and medical devices on web platforms have been developed, however these interactive tools use universal algorithms based on growth prediction models built by collecting clinical data stored in international databases and can be used only after one year of treatment.

Due to the involvement of miRNAs in the regulation of growth and their easyness to measure, the first aim of this study was to identify in IIGHD patients undergoing GH treatment, the miRNAs in serum that changed early using a miRNA high throughput profiling approach.

The second aim consisted in identifying a subgroup of these miRNAs targeting genes relevant for growth using an *in silico* approach.

The third aim consisted in exploring, if and how the changes in these selected miRNAs contributed to explain the clinical outcome in terms of growth considering both changes in height and growth velocity. Moreover, any other relationships among the changes in specific miRNA levels and all the other recorded clinical and biochemical parameters were explored.

Finally, considering the role of GH in cell proliferation, differentiation and apoptosis, a possible oncogenic effect of GH is still debated, especially concerning the risk of osteosarcoma. Thus, the last aim of this study was to evaluate the impact of the miRNAs, identified in the first part of the research project, on pathways related with cancer by using an *in silico* approach and to study whether they could have a role in oncogenic processes *in vitro*.

3. Patients and methods

3.1 Patients

Ten prepubertal patients were diagnosed with isolated idiopathic growth hormone deficiency (IIGHD), according to official indications and were enrolled in a preliminary profiling step [chronological age (CA): 8.80 ± 2.60 years; 5 males (M) and 5 females (F)]. Twenty-five prepubertal patients were included in the following validation step (CA: 9.08 ± 3.05 years); the main characteristics of the patients are reported in **Table 1**.

Children with ascertained or probable genetic syndromes (e.g. skeletal dysplasia, Silver-Russell syndrome) and/or obesity were excluded to reduce the possibility of confounding factors. At diagnosis 24 subjects underwent an arginine stimulation test and 1 underwent clonidine stimulation test as the first test to evaluate GH deficiency. Nineteen underwent a glucagon stimulation test and 6 underwent a clonidine stimulation test as the second test. All the subjects underwent a magnetic resonance imaging (MRI) scan of the hypothalamus and pituitary gland.

Patients were enrolled at the pediatric endocrine centers in Reggio Emilia and Modena. The patients have been treated with growth hormone, according to Indications of the Italian Regulatory Agency (AIFA Note 39), and underwent routine practice for GH treatment. Both biosimilar and recombinant human GH were used in the study. The miRNA profiling analysis was performed in 10 patients, 5 males and 5 females. The validation step was performed in 25 patients.

3.1.1 Ethical Approval

The study has been approved by the local Ethical Committee (Project title: “Role of miRNAs as predictors of response to growth hormone (GH) in patients with GH deficiency” Prot no.

2016/0002409). Written informed consent was obtained from all participants and their parents as appropriate. The workflow of the study in IIGHD patients is resumed in **Figure 4**.

Table 1. Auxological and biochemical features of patients at baseline, and at 6 and 12 months on GH treatment.

	Baseline	**6 months on treatment**	**12 months on treatment**
Sex, M/F	17/8		
CA, years	9.08±3.05		
Target Height, cm	166.1±8.12		
Target Height SDS	-0.96±0.81		
Highest GH peak N<5 ng/ml / N>5 ng/ml	7/18		
GH peak at first test, ng/ml	4.23±2.06		
GH peak at second test, ng/ml	5.14±2.01		
Bone age, years	7.35±2.77		8.41±2.88
Height, cm	119.22±16.79	124.22±16.88	127.96±16.78
Height SDS	-1.92±0.37	-1.61±0.39*	-1.48±0.39#
Weight, kg	23.17±7.39	25.38±8.51	27.39±9.10
Weight SDS	-1.79±0.74	-1.62±0.79*	-1.45±0.79#
BMI, kg/m^2	15.85±1.48	15.92±1.78	16.21±1.93
BMI SDS	-0.49±0.79	-0.61±0.88	-0.55±0.91
Growth velocity, cm/year §	4.49±1.59	8.03±1.69	7.19±1.51
Growth velocity SDS §	-1.60±1.04	2.78±1.99*	1.82±2.40#
IGF-I, ng/ml	150.96±62.86	281.22±127.69	284.33±113.92
IGF-I SDS	-0.03±0.59	0.88±0.76*	0.79±0.63#
Fasting blood glucose, mg/dl	81.44±4.75	85.44±8.61	86.07±7.14
Insulin, µU/ml		7.73±4.41	8.83±5.30
HbA1c, mmol/mol		33.18±3.00	32.83±2.96
Alkaline phosphatase, U/L	267.43±136.97	603.59±216.75	448.33±227.44
Drug, N recombinant/N biosimilar	11/14		
GH dose, mg/kg/day	0.028±0.004	0.023±0.004	0.023±0.004
Hypothalamus-pituitary MRI	N=1 Rathke's cleft cyst N=2 small pituitary gland N=22 normal		

*Abbreviations: BMI: body mass index; CA: chronological age; FGB: fasting blood glucose; GH: growth hormone; HbA1c: glycated hemoglobin; IGF-I: insulin-like growth factor 1; M: mean; SD: standard deviation; N: number; SDS: Standard deviation score. §calculated on the previous 6 months. *p<0.0001 baseline vs 6 months on treatment. #p<0.0001, baseline vs 12 months on treatment. Data are reported as mean ± SD. From: Catellani et al. Front Endocrinol (Lausanne). 2022 Jun 22;13:896640. doi: 10.3389/fendo.2022.896640 (154).*

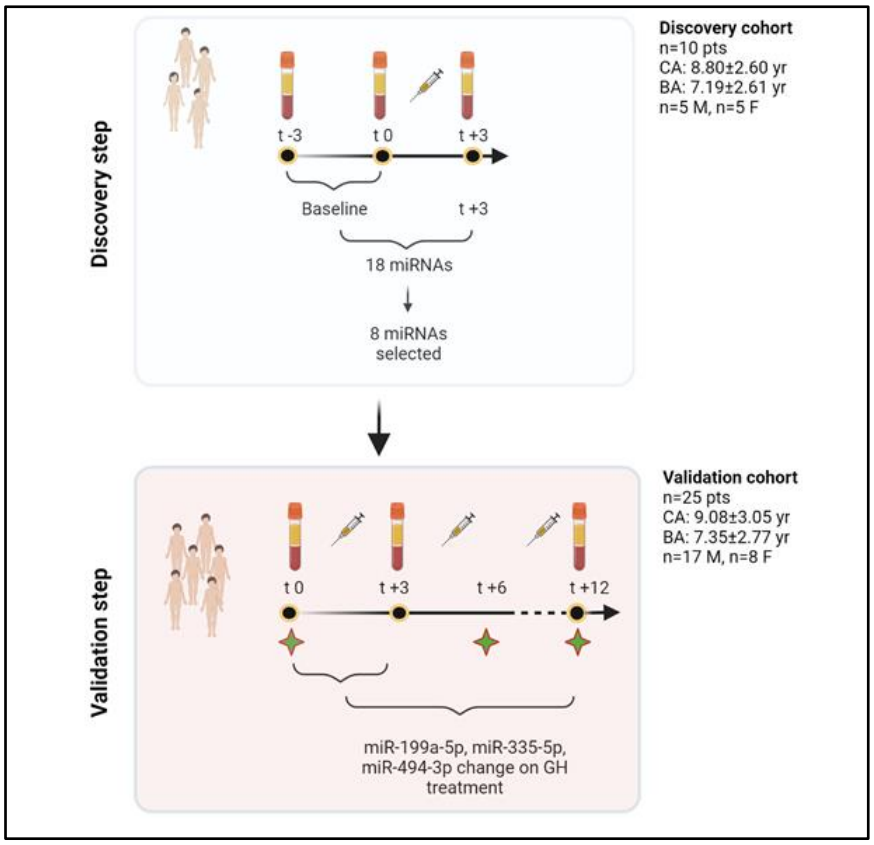

Figure 4. Workflow of the study in IIGHD patients. *In the discovery step, a miRNA profiling approach was adopted. All miRNAs showing variations independent of treatment (-3, 0 months) were excluded from further analyses. Eighteen miRNAs showed changes after 3 months on treatment. 8 miRNAs were selected for the following validation step based on their biological functions. The validation step was performed in single assay by means of Real-time qRT-PCR and evaluated the response of these 8 selected miRNAs at 3 months on GH treatment. Three miRNAs were confirmed to change significantly on treatment and were included in multiple linear regression models to contribute to explain growth response after 1 year on treatment. Green stars represent time points in which clinical and biochemical parameters have been recorded (0, +6, +12 months). BA, bone age; CA, chronological age; F, females; GH, growth hormone; M, males; n, number; pts, patients; yr, years. Created with BioRender.com From: Catellani et al. Front Endocrinol (Lausanne). 2022 Jun 22;13:896640. doi: 10.3389/fendo.2022.896640. (154)*

3.1.2 Collection of auxological parameters and bone age

A full auxological assessment of patients was done at each time point (baseline, +6 months, +12 months on treatment) and medical history was taken. Body Mass Index (BMI), calculated as weight/height^2 (kg/m^2), and weight were converted to Standard Deviation Scores (SDS) using the references of Cole et al. (*155*). Height (Ht) and target height (THt) were recorded and expressed as SDS, using the Tanner reference data (*156*). Height velocity SDS was calculated using Tanner's references (*156*). Bone age was assessed according to the Greulich and Pyle Atlas reference (*157*). Puberty in all subjects was staged according to the criteria of Marshall and Tanner for males and females (*158,159*).

3.1.3 Collection of biochemical parameters

Alkaline phosphatase and blood glucose were measured using Atellica CH Alkaline Phosphatase Concentrated (ref. 11097600) and Atellica CH Glucose Hexokinase 3 (ref. 11097592) assays on the Atellica CH Analyzer, respectively. HbA1c was measured by HPLC on the D-100 System (Bio-Rad). Insulin, GH, and IGF-I levels were measured by using chemiluminescence methods: LIAISON Insulin (ref. 310360), LIAISON hGH (ref. 310340), and LIAISON IGF-I (ref. 313231) immunoassays on the LIAISON Analyzer, Diasorin. IGF-I concentrations were converted to Standard Deviation Scores (SDS) based on the reference values provided by the manufacturer.

3.2 Blood Sample Processing

Whole blood was drawn in BD Vacutainer Serum Separator Tubes (SST^{TM}) II Advanced Plus with clot activator and separator gel, and processed within 2 hours from collection. Whole blood was then centrifuged at 2000 g for 10 min at 4°C. Serum was aliquoted in 1.5 ml sterile RNAse-free tubes and further centrifuged at 2500 g for 10 min at 4°C to remove any contaminant cell

and debris. Serum was then collected in sterile RNAse-free tubes and finally stored at -80°C. Blood samples were taken before the beginning of treatment (t-3, t0), and at 3 and 12 months after the beginning of the treatment (t+3 and t+12) in the context of routine controls.

3.3 RNA isolation and cDNA preparation

3.3.1 Total RNA isolation from serum samples

Serum samples where thawed on ice. Total RNA was isolated from 400 µl of serum using miRVana PARIS kit (Invitrogen cat no. AM1556) according to the manufacturer's protocol. In detail, 400 µl of serum were mixed with an equal volume of 2X denaturing solution at RT. Then, 800 µl of Acid-Phenol:Chloroform were added to the mix and vortexed for 60 sec. Samples were centrifuged 5 min at 10.000 g at RT or until the interphase was compact. The aqueous upper phase was collected and transferred in a fresh tube, registering the recovered volume. A volume of 100% ethanol equal to 1.25X volume of the aqueous phase, was added and thoroughly mixed. For each sample, 700 µl of the mix were added on a filter cartridge placed in a fresh collection tube, centrifuged at 10.000 g for 30 sec and the flow-through was discarded. The procedure was repeated until all the mixture was passed through the filter. Subsequently, 700 µl of Wash solution 1 were applied to the filter, centrifuged at 10.000 g for 15 sec, and the flow-through was discarded. Then, 500 µl of Wash solution 2/3 was applied to the filter, centrifuged at 10000 g for 15 sec, and the flow-through was discarded; this passage was repeated by adding a second 500 µl of Wash solution 2/3. After discarding the flow-through from the last wash the filter was spun in the same collection tube at 10000 g for 1 min to remove residual fluid. Finally, the filter was placed in a fresh collection tube and 20 µl of preheated nucleas-free water (95°C) was added to the center of the filter and incubated 1 min at RT. Then each tube was centrifuged at 10.000 g for 30 sec to recover the total RNA and the eluate was stored at -80°C.

3.3.2 Preparation of cDNA for miRNA profiling analysis and validation step

RNA from serum samples was reverse-transcribed using TaqMan™ Advanced miRNA cDNA Synthesis Kit (Applied Biosystems Cat no. A28007). Samples and reagents were thawed on-ice, gently vortexed to thoroughly mix, and then centrifuged briefly to spin down the contents.

The poly(A) tailing reaction mix was prepared in RNAse-free tubes by using 0.5 µl of 10X Poly(A) Buffer, 0.5 µl of ATP, 0.3 µl of Poly(A) Enzyme, 1.7 µl of RNAse-free water. Then, the reaction mix was vortexed to thoroughly mix the contents and centrifuged briefly. Subsequently, 3 µl of the poly(A) tailing reaction mix were added to 2 µl of RNA sample to a final volume of 5 µl. The reaction mix was vortexed to thoroughly mix the contents and centrifuged briefly, then the following settings were applied to perform the reaction in the Thermal Cycler T100 (Biorad): Polyadenilation step at 37°C for 45 min, Stop reaction step at 65°C for 10 minutes, Hold step at 4°C.

Then, the following adaptor ligation reaction was immediately performed. Each adaptor ligation reaction mix was prepared in RNAse-free tubes by using 3 µl of 5X DNA ligase buffer, 4.5 µl of 50% PEG 8000, 0.6 µl of 25X Ligation Adaptor, 1.5 µl of RNA ligase, 0.4 µl of RNAse-free water. Then, the reaction mix was vortexed to thoroughly mix the contents and centrifuged briefly. Subsequently, 10 µl of the adaptor ligation reaction mix were added to 5 µl of the poly(A) tailing reaction product to a final volume of 15 µl. The reaction mix was vortexed to thoroughly mix the contents and centrifuged briefly, then the following settings were applied to perform the reaction in the Thermal Cycler T100 (Biorad): Ligation step at 16°C for 60 min, Hold step at 4°C.

Then, the following reverse transcription (RT) reaction was immediately performed. Each reverse transcription (RT) reaction mix was prepared in RNAse-free tubes by using 6 µl of 5X

RT buffer, 1.2 µl of dNTP Mix (25 mM each), 1.5 µl of 20X Universal RT Primer, 3 µl of 10X RT Enzyme Mix, 3.3 µl of RNAse-free water, the reaction mix was vortexed to thoroughly mix the contents and spinned. Subsequently, 15 µl of the RT reaction mix were added to 15 µl of the Adaptor ligation reaction mix to a final volume of 30 µl. The reaction mix was vortexed to thoroughly mix the contents and centrifuged briefly, then the following settings were applied to perform the reaction in the Thermal Cycler T100 (Biorad): Reverse Transcription step at 42°C for 15 min, Stop reaction step at 85°C for 5 min, Hold step at 4°C. Then the following miR-Amp reaction was performed.

Each miR-Amp reaction mix was prepared in RNAse-free tubes by using 25 µl of 2X miR-Amp Master Mix, 2.5 µl of 20X miR-Amp Primer Mix, 17.5 µl of RNAse-free water. The reaction mix was vortexed to thoroughly mix the contents and centrifuged briefly. Subsequently, 45 µl of the miR-Amp Primer Mix were were added to 5 µl of the RT reaction product to a final volume of 50 µl. The reaction mix was vortexed to thoroughly mix the contents and centrifuged briefly, then the following settings were applied to perform the reaction in the Thermal Cycler T100 (Biorad): Enzyme Activation step at 95°C for 5 min, (Denature step 95°C for 3 sec, Anneal/Extend step at 60°C for 30 sec) x 16 cycles, Stop reaction step at 99°C for 10 min, Hold step at 4°C.

3.4 Real-time qRT PCR

3.4.1 MiRNA profiling analysis in serum

The miR-Amp reaction product (*see section 3.3.2*) was diluted 1:10 with 0.1X TE pH 8.0 (Invitrogen). The TaqMan™ Advanced miRNA Human A Cards (Cat no. A34714, Applied Biosystems) allow the evaluation of pre-spotted TaqMan Advanced miRNA assays in a 384-well microfluidic card format. The TaqMan Array Real-Time qPCR reaction mix for each card was prepared in RNAse-free tubes by using 450 µl of 2X TaqMan Fast Advanced Master Mix

(Cat no. 4444557, Applied Biosystems), 225 µl of diluted miR-Amp reaction product, and 225 µl of RNAse-free water. The reaction mix was vortexed to thoroughly mix the contents and centrifuged briefly. Then 100 µl of the TaqMan Array qPCR reaction mix were pipetted into each of the eight reservoirs in the array card. Subsequently, the filled cards were centrifuged two times for 1 min at 1200 rpm**.** Finally, each card was sealed in the Array Card Sealer (Cat no. 4331770, Applied Biosystems) and the reservoirs were trimmed from the array card using scissors. Subsequently, the following settings were applied to perform the reaction in the 7900HT Fast Real-Time PCR System (Cat no. 4329001, Applied Biosystems): Enzyme activation step at 92°C for 10 min, (Denature step at 95°C for 1 sec, Anneal/extend step at 60°C for 20 sec) X 40 cycles. The threshold was adjusted at 0.1 and the outliers were excluded from the analysis. Array data were normalized using hsa-miR-16-5p (477860_mir) as endogenous control, and the data were analyzed using the $2^{-\Delta\Delta Ct}$ method (*160,161*). miRNAs with Ct>35 were considered as not expressed and excluded from further analysis. Moreover, those miRNAs changing significantly (p-value ≤0.05) in the two time points before starting treatment were excluded, in order to exclude those miRNAs changing for others causes independently from treatment, and those miRNAs having a fold-change (FC) ($\log_2 2^{-\Delta\Delta Ct}$) >1.5 or FC ($\log_2 2^{-\Delta\Delta Ct}$) <-1.5 were considered as differentially expressed.

3.4.2 MiRNA validation step in single assay in serum

The miR-Amp reaction product (*see section 3.3.2*) was diluted 1:10 with 0.1X TE pH 8.0 (Invitrogen). The TaqMan™ Advanced miRNA Assays (Cat no. A25576, Applied Biosystems) allow the analysis of specific miRNAs and the 8 TaqMan Advanced miRNA Assay (20X) chosen for the validation step were: hsa-miR-22-3p (Assay ID: 477985_mir), hsa-miR-30c-5p (Assay ID: 478008_mir), hsa-miR-106a-5p (Assay ID: 478225_mir), hsa-miR-140-5p (Assay ID: 477909_mir), hsa-miR-199a-5p (Assay ID: 478231_mir), hsa-miR-335-5p (Assay ID: 478324_mir), hsa-miR-340-5p (Assay ID: 478042_mir), hsa-miR-494-3p (Assay ID:

478135_mir). MiRNA assays were chosen based on fold-change between baseline and 3 months after treatment (>1.5 or <-1.5) and based on miRNA target gene analysis.

Each TaqMan Real-Time qPCR reaction mix was prepared in RNAse-free tubes by using 10 µl of 2X TaqMan Fast Advanced Master Mix (2X), 1 µl of TaqMan Advanced miRNA Assay (20X), and 4 µl of RNAse-free water. The reaction mix was gently mixed and centrifuged briefly. Then, 20 µl of the reaction mix were pipetted in each well of a 96-well plate and 5 µl of 1:10 diluted miR-Amp reaction product was added. Subsequently, the following settings were applied to perform the reaction in the 7900HT Fast Real-Time PCR System (Applied Biosystems): Enzyme activation step at 92°C for 20 sec, (Denature step at 95°C for 1 sec, Anneal/extend step at 60°C for 20 sec) X 40 cycles. The threshold was adjusted at 0.1. The data were analyzed with SDS Relative Quantification Software version 2.4. (Applied Biosystems**)** and miRNAs with Ct>35 were considered as not expressed and excluded from further analysis. miRNA expression levels were normalized using hsa-miR-16-5p (477860_mir) as endogenous control and the data were analyzed using the $2^{-\Delta\Delta Ct}$ method (*160,161*).

3.5 MiRNA target prediction and pathway analysis

An *in silico* analysis was performed to identify the validated target genes and pathways for each differentially expressed miRNA in order to select those expected to be involved with growth. In particular, the network which represents miRNA:target interactions and highlights the most impacted pathways was obtained from the miRNet v2.0 online tool (*162*) which collects data from three well-annotated databases miRTarBase v8.0, TarBase v8.0 and miRecords. The significance was set at a p-value of 0.05.

3.6 *In vitro* study

3.6.1 Cell cultures

HOB primary osteoblasts isolated from femoral trabecular bone tissue from the knee or hip joint region were purchased from PromoCell (Cat. No. C-12720). They were cultured in Osteoblast Basal Medium (Cat. No. C-27010, Promocell) supplemented with Growth Medium Supplement Mix (Cat. No. C-39615, Promocell), without antibiotics. Cells were grown at 37°C in a 5% CO2 atmosphere and were harvested by using the ReagentPack™ Subculture Reagents for primary cell subculturing (Cat. No. CC-5034, Lonza). The experiments have been performed within the 9th passage.

3.6.2 GH treatment *in vitro*

Cells were seeded at a density of 30.000 cells/well in 24-well plates. After 24 h, growth medium was replaced with 500 µl of fresh medium containing recombinant human GH (Cat. No. 1067-GH-025/carrier free, R&D Systems) at the concentrations of 20 ng/ml, 100 ng/ml and 500 ng/ml. After 24 h of treatment, cells were harvested by trypsin/EDTA and pellets were stored at -80°C.

3.6.3 Transfections with miRNA mimics and inhibitors

Cells were seeded at a density of 30.000 cells/well in 24-well plates. After 24 h, growth medium was replaced with 450 µl of fresh medium. For each assay, 2 µl of Lipofectamine RNAiMAX (cat no. 13778-075, Invitrogen) were diluted in 23 µl of Opti-MEM™ I Reduced Serum Medium without phenol red (cat. no. 11058021). The following miRNA mimics and inhibitors were used in the experiments and diluted in Opti-MEM to a concentration of 2 nM: hsa-miR-199a-5p mirVana® miRNA mimic (ID: MC10893, cat no. 4464066), hsa-miR-335-5p mirVana® miRNA mimic (ID: MC10063, cat no. 4464066), hsa-miR-494-3p mirVana®

miRNA mimic (ID: MC12409, cat no. 4464066), hsa-miR-199a-5p mirVana® miRNA inhibitor (ID: MC10893, cat no. 4464084), hsa-miR-335-5p mirVana® miRNA inhibitor (ID: MC10063, cat no. 4464084), hsa-miR-494-3p mirVana® miRNA inhibitor (ID: MC12409, cat no. 4464084), mirVana™ miRNA Negative Control #1 (cat no. 4464076). Then 25 µl of Lipofectamine RNAiMAX solution were incubated with 25 µl of diluted miRNA mimics and inhibitors for 5 min at RT to allow the formation of complexes. Subsequently, 50 µl complexes were added in the respective wells. After 48 h of transfection, cells were harvested by trypsin/EDTA and pellets stored at -80°C.

3.6.4 MiRNA target prediction

Moreover, Targetscan v8.0 (*101,163,164*) was used to evaluate the predicted targets of these miRNAs by searching for the presence of conserved 8mer, 7mer, and 6mer sites that match the seed region of each miRNA (*164*). In mammals, the prediction ranking is obtained considering the predicted efficacy of targeting which is calculated by using a biochemical model of miRNA-mediated repression. A convolutional neural network allows to extend the prediction to all miRNA sequences (*101*).

3.6.5 Total RNA isolation from cells

Total RNA was isolated from cell pellets cells using miRVana PARIS kit (Invitrogen cat no. AM1556) according to the manufacturer's protocol. In detail, pellets were thawed on ice and centrifuged at 10.000g for 1 min to carefully remove any residual of medium.

Then, 150 µl of ice-cold Cell Disruption Buffer were added to the cells and, after vigorously vortexing and pipetting, omogeneous lysates were obtained. Cell lysates were then mixed with 150 µl of 2X denaturing solution at RT and after thoroughly mixing, were incubated on-ice for 5 min. Then, 300 µl of Acid-Phenol:Chloroform were added to the mix and vortexed for 60 sec. Samples were centrifuged 5 min at 10.000 g at RT or until the interphase was compact. The

aqueous upper phase was collected and transferred in a fresh tube, registering the recovered volume. A volume of 100% ethanol equal to 1.25X volume of the aqueous phase, was added and thoroughly mixed. For each sample, up to 700 µl of the mix were added on a filter cartridge placed in a fresh collection tube, centrifuged at 10.000 g for 30 sec and the flow-through was discarded. Subsequently, 700 µl of Wash solution 1 were applied to the filter, centrifuged at 10.000 g for 15 sec, and the flow-through was discarded. Then, 500 µl of Wash solution 2/3 was applied to the filter, centrifuged at 10.000 g for 15 sec, and the flow-through was discarded; this passage was repeated by adding a second 500 µl of Wash solution 2/3. After discarding the flow-through from the last wash the filter was spun in the same collection tube at 10.000 g for 1 min to remove residual fluid. Finally, the filter was placed in a fresh collection tube and 20 µl of preheated nucleas-free water (95°C) were added to the center of the filter and incubated 1 min at RT. Then each tube was centrifuged at 10.000 g for 30 sec to recover the total RNA which was quantified at the Nanodrop 2000 spectrophotometer (Thermofisher).The eluate was stored at -80°C.

3.6.6 Preparation of cDNA for the analysis of miRNA levels *in vitro*

RNA extracted from cultured cells was reverse-transcribed using TaqMan™ microRNA reverse transcription Kit (Cat. No. 4366596). Samples and reagents were thawed on-ice, gently vortexed to thoroughly mix, and then centrifuged briefly to spin down the contents. Samples were diluted at 10 ng/µl with RNAse-free water. Then each reverse transcription (RT) reaction mix was prepared in RNAse-free tubes by using 0.15 µl dNTP mix w/dTTp (100 M total), 1 µl Multiscribe RT enzyme (50U/µl), 1.5 µl 10X RT Buffer, 0.19 RNase Inhibitor (20 U/µl), 8.16 µl RNAse-free water. Then, the reaction mix was vortexed to thoroughly mix the contents, and centrifuged briefly. Subsequently, 11 µl of the RT reaction mix were dispensed into fresh RNAse-free tubes and 3 µl of each specific TaqMan miRNA assay 5X , and 1 µl of diluted RNA were added to a final volume of 15 µl.

The following TaqMan miRNA assays 5X were used in the experiments: hsa-miR-199a-5p (Assay ID: 000498 Cat. no.: 4427975), hsa-miR-335-5p (Assay ID: 000546 Cat. no.: 4427975), hsa-miR-494-3p (Assay ID: 002365 Cat. no.: 4427975), U6 snRNA (Assay ID: 001973 Cat. no.: 4427975).

The reaction mix was vortexed to thoroughly mix the contents and centrifuged briefly, then it was incubated on-ice for 5 min. Subsequently, the following settings were applied to perform the reaction in the Thermal Cycler T100 (Biorad): 16°C for 30 min, 42°C for 30 min, 85°C for 5 min, hold step at 4°C and the obtained cDNA was stored at -20°C.

3.6.7 Preparation of cDNA for gene expression analysis *in vitro*

Total RNA obtained from cultured cells was reverse-transcribed using PrimeScript RT Reagent Kit with gDNA Eraser (Cat. No. RR047A, Takara). Samples and reagents were thawed on-ice, gently vortexed to thoroughly mix, and then centrifuged briefly to spin down the contents. A volume of sample containing 62.5 ng of total RNA was collected in RNA-free tubes and the volume was taken up to 7 µl with RNAse-free water, based on sample concentration. Genomic DNA was eliminated by adding to the RNA a mix of 2 µl of gDNA Eraser Buffer (5X) plus 1 µl of dgDNA Eraser and by incubating samples at 42°C for 2 min in the Thermal Cycler T100 (Biorad), then hold at 4°C.

Subsequently, the following RT reaction mix was prepared: 4 µl of 5X Prime Script Buffer, 1 µl of Prime Script Enzyme, 1 µl of RT Primer mix, and 4 µl of RNAse free H2O. Then, 10 µl of the mix were added to 10 µl of RNA depleted from gDNA and the following settings were applied to perform the reaction in the Thermal Cycler T100 (Biorad): 15 min at 37°C, 5 sec at 85°C to inactivate the Reverse Transcriptase and then hold 4°C. The obtained cDNA was diluted 1:2 with 20 µl of RNAse free H2O and stored at -20°C.

3.6.8 MiRNA expression analysis *in vitro*

To evaluate miRNA levels *in vitro*, a reaction mix containing 10 µl TaqMan Universal Master Mix II, no UNG (Cat. No. 4440040, Applied Biosystems), 1 µl of a specific TaqMan miRNA Assay 20X, and 7.67 µl of nuclease free water was prepared. In particular, the following TaqMan miRNA assays 20X were used: hsa-miR-199a-5p (Assay ID: 000498 Cat. no.: 4427975), hsa-miR-335-5p (Assay ID: 000546 Cat. no.: 4427975), hsa-miR-494-3p (Assay ID: 002365 Cat. no.: 4427975), U6 snRNA (Assay ID: 001973 Cat. no.: 4427975). The reaction mix was vortexed to thoroughly mix the contents and centrifuged briefly. Then, 18.67 µl of the reaction mix were pipetted in the respective well of a 96-well plate and 1.33 µl of cDNA (*see section 3.6.6*) was added. Subsequently, the following settings were applied to perform the reaction in a 7300HT Fast Real-Time PCR System (Applied Biosystems): 95°C 10 min, (95°C 15 sec; 60°C 1 min) x 40 cycles. The threshold was adjusted at 0.2. The data were normalized using U6 snRNA (Assay ID: 001973) as endogenous control, and the data were analyzed using the $2^{-\Delta\Delta Ct}$ method.

3.6.9 Gene expression analysis *in vitro* of miRNA target genes and differentiation markers

To analyse gene expression levels *in vitro*, a reaction mix containing 12.5 µl SYBR Premix Ex Taq II (2X) (Cat. No. RR039A, Takara), 2.5 µl of a specific primer 10X, 0.5 µl of ROX reference dye (50X), and 8.5 µl of nuclease free water was prepared. In particular, the following Sybr Green QuantiTect primer assays (Cat. No. 249900, Qiagen) were used: CRIM1 (ID: QT00047887), CLOCK (ID: QT00054481), ROCK1 (ID: QT00034972), osteopontin (SPP1 ID: QT01008798), collagen type I α1 chain (COL1A1; ID: QT00037793), and collagen type I α2 chain (COL1A2; ID: QT00072058). SPP1 was selected as a differentiation marker since it is expressed by mature osteoblasts, regulates bone mineralization toward terminal

differentiation into osteocytes and is not expressed in precocious and less differentiated stages of osteoblast lineage (*165,166*). COL1, the main component of the osteoid matrix is structured as a triple helix composed by two alpha 1 chains (COL1A1) and one alpha 2 chain (COL1A2) which is highly expressed by osteoblasts and is low in osteoprogenitors (*165,166)*.

The real-time PCR reaction mix was vortexed to thoroughly mix the contents and centrifuged briefly. Then, 24 µl of the reaction mix were pipetted in the respective well of a 96-well plate and 1 µl of cDNA (*see section 3.6.7*) was added. Subsequently, the following settings were applied to perform the reaction in a 7300HT Fast Real-Time PCR System (Applied Biosystems): 95°C 30 sec, (95°C 5 sec; 60°C 35 sec) x 40 cycles. The threshold was adjusted at 0.2. The data were normalized using GAPDH (ID: QT00079247) as endogenous control. The data were analyzed using the $2^{-\Delta\Delta Ct}$ method.

3.6.10 Cell viability/proliferation assay

The effects of miRNA mimics and inhibitors on cell viability were evaluated by means of WST1 reagent (Cat. No. 11644807001, Roche). This assay is based on the cleavage, exerted only by viable cells, of red tetrazolium salt WST-1 in a soluble dark-red formazan dye whom absorbance is spectrophotometrically quantified. Absorbance results directly correlate with the number of living cells that is the overall activity of mitochondrial dehydrogenases in the samples/metabolically active cells.

Cells were seeded at a density of 4.500 cells/well in 96-well plates. After 24 h, cells were transfected with the specific miRNA mimics and inhibitors (*see section 3.6.3*). Then, after 48 h of transfection, growth medium was changed in each well with 100 µl of fresh growth medium containing 10 µl of WST-1. After 4 hours of incubation at 37°C in a 5% CO2 atmosphere, the absorbance of each sample was measured at both 450 nm and at 600 nm in the Glomax Discover multimode microplate reader (Promega). For each sample, absorbance at 600 nm was

subtracted to the absorbance at 450 nm, data were blank corrected and were normalized with respect to the absorbance of the sample treated with lipofectamine only.

3.6.11 Cell lysis *in situ*

After transfection with miRNA mimics and inhibitors (*see section 3.6.3*), cell lysis was performed *in situ* by using RIPA lysis buffer (SC-24948, Santa Cruz Biotechnology) complemented with phenylmethylsulfonyl fluoride (PMSF), sodium orthovanadate, proease and phosphatase inhibitors. In detail, adherent cells were washed with 300 µl of PBS 1X, then 100 µl of complete RIPA lysis buffer were added in each well and the plate was incubated 10 min on-ice to obtain complete cell lysis. Then, cell lysates were carefully collected in 1.5 ml tubes and were centrifuged at 14.000 g x 15 min at 4°C. A translucid pellet of insoluble material was observed in each tube, and the surnatant was transferred in fresh 1.5 ml tubes and stored at -80°C. The absorbance of each lysate was determined by using the DC protein assay (Bio-Rad) and was measured at 750 nm in the FLUOstar Omega (BMG Labtech) spectrophotometer. The protein concentration of each sample was determined by the interpolation of the OD values in a standard curve made by measuring the absorbance of a dilution series of BSA protein standards at known concentrations.

3.6.12 Western blot analysis

Cell lysates of HOB were separated by gel electrophoresis using Mini-PROTEAN TGX gels 8-16% (cod 4561104, Bio-Rad). For each sample, 10 µg of proteins were loadead in the gel with 9 µl Laemmli 4X (cod 1610747, Bio-rad), 1 µl of 2-mercaptoethanol (cod 1610710, Bio-rad), and ddH20 to a final volume of 40 µl. Then, samples were denaturated at 95°C and the cooled on ice. Gels were run at 80 V for 2 min and then at 100 V for 2 hours in a Tris/Glycine/SDS running buffer (Cod 1610772 Bio-Rad) 1X.

Subsequently, proteins were blotted to 0.2 µm PVDF membranes (cod 1704156 Bio-Rad) by using the Trans-Blot Turbo transfer system (cod 1704150 Bio-Rad) for 3 min at 2.5 A constant.

Aspecific sytes of the membrane were blocked with 20 ml T-TBS + 5% BSA for 90 min with gentle rocking agitation. Then the membrane was washed 3 times for 5 min in T-TBS.

Then the membranes were incubated with the following primary antibodies overnight at 4°C in T-TBS +5% BSA with gentle rocking agitation: ROCK1 (#4035 Cell Signalling Technology) 1:1000, CLOCK (sc-271603, Santa Cruz Biotechnology) 1:400, β-Actin (#3700 Cell Signalling Technology) 1:1000.

The membranes were washed 3 times for 10 min in T-TBS and were incubated with gentle rocking agitation for 90 min with the appropriate secondary antibodies: Anti-Rabbit IgG HRP-linked antibody 1:5000 (cod ab6013, Abcam) or Anti-mouse IgG HRP-linked antibody 1:3000 (#7076 Cell Signalling Technology).

After 3 washes in T-TBS for 10 min, membranes were incubated for 5 min in the dark with Pierce ECL Plus (cat no. 32132, Thermo Scientific), or Pierce ECL (cat no. 32109, Thermo Scientific) for β-Actin (ACTB) signal, and then the hybridization signals were detected using the ChemiDoc Imaging System (cod 17001401, Bio-Rad).

3.7 Statistical analysis

Paired Student's t-test ($p \leq 0.05$) was used to identify miRNAs that were differentially expressed after 3 months of GH treatment with respect to the baseline (t0, t+3). Moreover, paired Student's t-test was used to evaluate differences between baseline patient's characteristics and after 6 and 12 months of treatment. These comparisons were made only on the standardized parameters.

The associations of miRNA values at baseline, at 3 months and their change during this time frame (delta 0–3 months) with baseline clinical features, and with 6- and 12-month recorded

clinical and biochemical data were analyzed. In addition, the associations of 12-month miRNA levels with clinical and biochemical parameters at 12 months were investigated by means of simple linear regression analysis.

The distribution of height SDS and growth rate SDS at baseline and at 6 and 12 months were also analyzed (**Figures 5, 6**) in order to select the meaningful time horizon for measuring the two outcomes.

Multiple linear regression models were performed in order to investigate the major determinants of height variations between 0 and 6 months and between 0 and 12 months, and the variance of growth rate variation between 0 and 6 months. A set of models that considered only auxological parameters at baseline were estimated: the first one included only auxological parameters; the other models were estimated by adding, one by one, as independent variables, GH peaks at testing, GH dose at the beginning of treatment, IGF-I SDS at baseline, the difference between CA and bone age at baseline, and baseline levels and change in miRNA levels during the first 3 months of treatment. Finally, the models were estimated with a backward stepwise selection estimation method with significance level for removal from the model set to 0.2 considering the following as independent variables: sex, CA at the beginning of treatment, genetic target SDS, treatment dose (mg/kg/day), height SDS at baseline, weight SDS at baseline, peak at first GH stimulation test (ng/ml), peak at second GH simulation test (ng/ml), IGF-I SDS (t0), difference between CA and bone age at baseline, miR-199a-5p (t0), delta (0–3) miR-199a-5p, miR-355-5p (t0), delta (0–3) miR-335-5p, miR-494-3p (t0), and delta (0–3) miR-494-3p.

To define the degree of accuracy or predictive effectiveness of the model, leave-one-out cross-validation analysis was performed for each model. Specifically, we reported the variations in adjusted R^2, meaning the percentage of variance in the outcome explained by the variable

included in the model adjusted for the number of degrees of freedom spent by the model parameters, and R^2 CV as a measure of the variance, explained by the models corrected with the cross-validation method. In this way, we built 25 models excluding patients one by one, and we predicted the growth parameter of the excluded patient with the parameters estimated by the model. The best models obtained are reported in the text. For the associations explored in these models, we did not perform a formal statistical test of hypothesis, and p-values should be interpreted as continuous variables without any threshold. Furthermore, p-values should be interpreted cautiously because there is an issue of multiple testing, but no easy solutions for false discovery rate adjustments were identified since it is not possible to determine the total set of independent comparisons. Comparison of miRNA expression levels in responders vs. non responders was also performed, as well as a comparison according to GH peak concentrations as specified above. Statistical analyses were performed using STATA v16.0 (STATA Corp., College Station, TX, USA).

The data obtained *in vitro* were analysed by means of GraphPad Prism v.8 as appropriate, by using one-column Student's t-test.

4. Results

4.1 Growth and biochemical parameters during the first 12 months on GH treatment

The cohort of 25 patients was characterized in terms of auxological parameters (height, weight, BMI, target height, height velocity, bone age, pubertal stage), biochemical parameters (GH levels at peaks during stimulation tests, IGF1, fasting blood glucose, insulin, HbA1c) and MRI. The recorded clinical and biochemical parameters of patients are reported in **Table 1**.

Height SDS at both 6 and 12 months on GH treatment was significantly increased with respect to the baseline (-1.61 ± 0.39 vs -1.92±0.37, p<0.0001), and (-1.48 ± 0.39 vs -1.92±0.37 p<0.0001, respectively) (**Figure 5**).

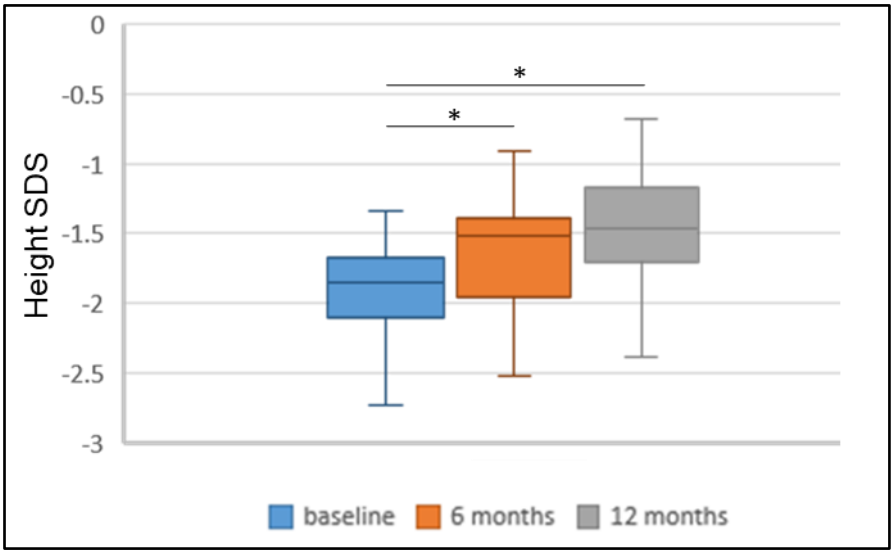

Figure 5. Height trend over time. *Height is represented over the previous 6 months. Height was standardized according to Tanner's standards and is reported as SDS. The box plots represent in blue the height SDS values at baseline, in orange the height SDS values at 6 months on GH treatment and in grey the height SDS values at 12 months on treatment. SDS: standard deviation score. *p<0.0001 vs baseline at paired Student's t-test. From: Catellani et al. Front Endocrinol (Lausanne). 2022 Jun 22;13:896640. doi: 10.3389/fendo.2022.896640 (154).*

The BMI SDS slightly decreased on GH treatment, however no significant changes were observed at both 6 (-0.61±0.88 vs -0.49±0.79, n.s.) and 12 months (-0.55±0.91 vs -0.49±0.79, n.s.) with respect to the baseline.

Growth velocity (GV) SDS after 6 months (2.78±1.99 vs -1.60±1.04, p<0.0001) and 12 months (1.82±2.40 vs -1.60±1.04, p<0.0001) on GH treatment increased with respect to pre-treatment growth velocity. However, growth velocity SDS tended to decrease during the second six months on GH treatment (2.78±1.99 vs 1.82±2.40) (**Figure 6**).

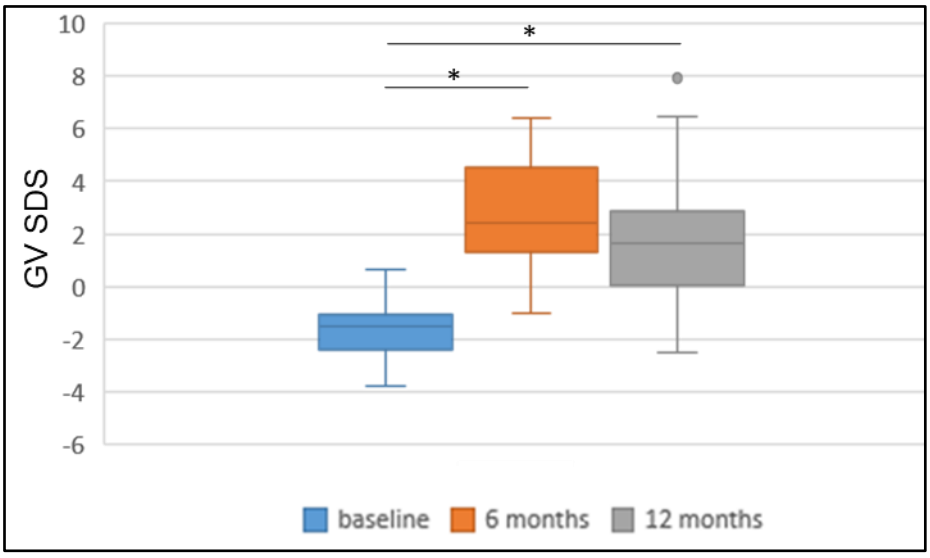

Figure 6. Growth velocity trend over time. *Growth velocity (GV) is represented with respect to the previous 6 months. GV was standardized according to Tanner's standards and is reported as SDS. The box plots represent in blue the GV SDS values at baseline, in orange the GV SDS values at 6 months on GH treatment and in grey the GV SDS values at 12 months on treatment. SDS: standard deviation score. *p<0.0001 vs baseline at paired Student's t-test. From: Catellani et al. Front Endocrinol (Lausanne). 2022 Jun 22;13:896640. doi: 10.3389/fendo.2022.896640 (154).*

IGF-I SDS values increased after 6 months on GH treatment with respect to the baseline (0.88±0.76 vs -0.03 ±0.59, p<0.0001) and remained almost stable over the following 6 months (0.88±0.76 vs 0.79 ± 0.63, n.s.).

Alkaline phosphatase increased on treatment although not significantly (603.59±216.75 vs 267.43±136.97, n.s and 448.33±227.44 vs 267.43±136.97 n.s.), whereas fasting blood glucose, insulin, and HbA1c remained stable on treatment.

4.2 Discovery miRNA profiling step

The miRNA profiling step was preliminarly performed in order to allow to select a pool of miRNAs of interest for subsequent analyses.

A total of 384 miRNAs were analysed, of which 186 were detectable and measured in serum samples of patients. MiRNAs that changed significantly ($p<0.05$ at paired Student's *t*-test) between the two time points before starting GH treatment (t-3, t0) were excluded, as these changes were considered as random fluctuations independent from treatment.

Sixteen miRNAs (hsa-let-7a-5p, hsa-let-7e-5p, hsa-miR-30c-5p, hsa-miR-34a-5p, hsa-miR-132-5p, hsa-miR-140-5p, hsa-miR-199a-5p, hsa-miR-330-3p, hsa-miR-335-5p, hsa-miR-340-5p, hsa-miR-369-3p, hsa-miR-375, hsa-miR-450-5p, hsa-miR-494-3p, hsa-miR-582-5p, hsa-miR421) had a FC>1.5 and were considered as upregulated after 3 months of GH treatment with respect to the baseline. Two miRNAs (hsa-miR-22-3p and hsa-miR-106a-5p) had a FC<-1.5 and were considered to be downregulated after 3 months of GH treatment with respect to the baseline (**Table 2**).

Table 2 Differentially expressed miRNAs after 3 months of GH treatment with respect to the baseline in 10 prepubertal patients with IIGHD. Fold change (FC) was calculated as $\log_2 2^{-\Delta\Delta Ct}$. miRNAs with a FC>1.5 were considered as upregulated and miRNAs with a FC<-1.5 were considered as downregulated. *From: Catellani et al. Front Endocrinol (Lausanne). 2022 Jun 22;13:896640. doi: 10.3389/fendo.2022.896640 (154).*

miRNA	**Fold Change ($\log_2 2^{-DDCt}$)**	**Up/Down**
hsa-miR-375	3.1	Up
hsa-let-7e-5p	2.5	Up
hsa-miR-340-5p	2.4	Up
hsa-miR-494-3p	2.1	Up
hsa-miR-34a-5p	2.1	Up
hsa-miR-30c-5p	1.9	Up
hsa-let-7a-5p	1.8	Up
hsa-miR-140-5p	1.8	Up
hsa-miR-421	1.8	Up
hsa-miR-132-3p	1.7	Up
hsa-miR-330-3p	1.7	Up
hsa-miR-369-3p	1.7	Up
hsa-miR-582-5p	1.7	Up
hsa-miR-450a-5p	1.6	Up
hsa-miR-335-5p	1.6	Up
hsa-miR-199a-5p	1.6	Up
hsa-miR-106a-5p	-1.8	Down
hsa-miR-22-3p	-3.1	Down

4.3 Pathway enrichment analysis

Pathway enrichment analysis of these 18 miRNAs with the miRNet online tool highlighted that they were significantly involved in the regulation of 100 different pathways ($p<0.05$).

Among these 18 miRNAs (**Table 2**), those predicted to be involved in the regulation of longitudinal growth and bone development were selected for validation, namely, miR-22-3p, miR-30c-5p, miR-106a-5p, miR-140-5p, miR-199a-5p, miR-335-5p, miR-340-5p, and miR-494-3p (**Figure 7**). These miRNAs were predicted to regulate genes involved in Wnt-β-catenin

signaling, Notch signaling, PI3K/AKT, and TGF-β signaling which are relevant for longitudinal growth (**Figure 7**).

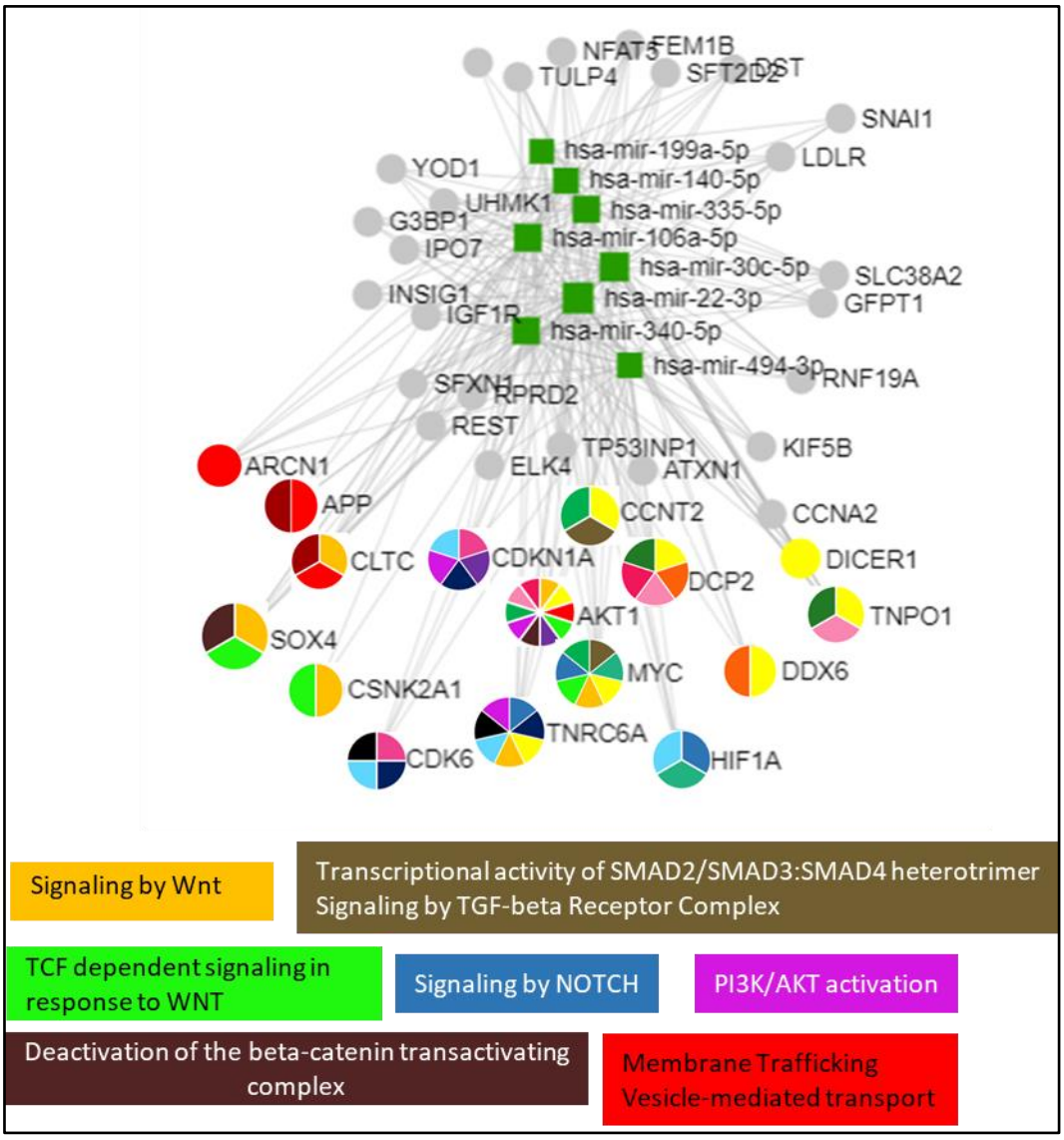

Figure 7. Genes and pathways, regulated by the 8 selected miRNAs, which are important for growth. *miRNAs are represented as green squares while genes are represented by circles. The different colors in the circles correspond to the pathways in which genes are involved. This network was obtained from miRNet v2.0 and only the significant pathways (p<0.05) involved with growth were selected to generate the figure. From: Catellani et al. Front Endocrinol (Lausanne). 2022 Jun 22;13:896640. doi: 10.3389/fendo.2022.896640 (154).*

Interestingly, among the 100 pathways in which the 18 miRNAs were involved, the three most significant were the pathway of the oncogene induced senescence, the SHC-related events triggered by IGF1R and the cyclin D associated events in G1 (**Table 3**).

Table 3 The 3 most significant pathways regulated by miRNAs. The pathway enrichment analysis was performed with miRNet v 2.0 and only significantly regulated pathways were considered ($p<0.05$). The genes targeted by miRNAs which are involved in these pathways are also reported.

Pathway	Genes
Oncogene Induced Senescence	CDK6 MDM2 MAPK1 TNRC6A
SHC-related events triggered by IGF1R	IGF1R KRAS MAPK1
Cyclin D associated events in G1	CCND1 CDK6 CDKN1A

The genes are all involved both in longitudinal growth and cancer: MDM2 is involved in bone mineralization but is also a negative regulator of p53; MAPK1 also known as ERK2 and TNRC6A are involved in both GH signalling and are associated with many cancers.

IGF1R is pivotal for growth but is also associated with many cancers, and KRAS is altered in RASopathies which are a kind of diseases charachterised both by reduced longitudinal growth and by an increased cancer risk. CDKN1A, also known as p21, is involved in chondrocyte development but is also deregulated in cancer and CDK6/CCND1 are involved in chondrocyte maturation but also in cell cycle progression.

4.4 miRNA validation step

MiR-22-3p, miR-30c-5p, miR-106a-5p, miR-140-5p, miR-199a-5p, miR-335-5p, miR-340-5p, and miR-494-3p were selected to be validated in single assay, at baseline and at 3 months on GH treatment in the larger group of 25 patients.

Among these miRNAs, miR-199a-5p (p=0.020), miR-335-5p (p=0.001) and miR-494-3p (p=0.026) were confirmed to be upregulated after 3 months on GH treatment with respect to the baseline (**Figure 8**).

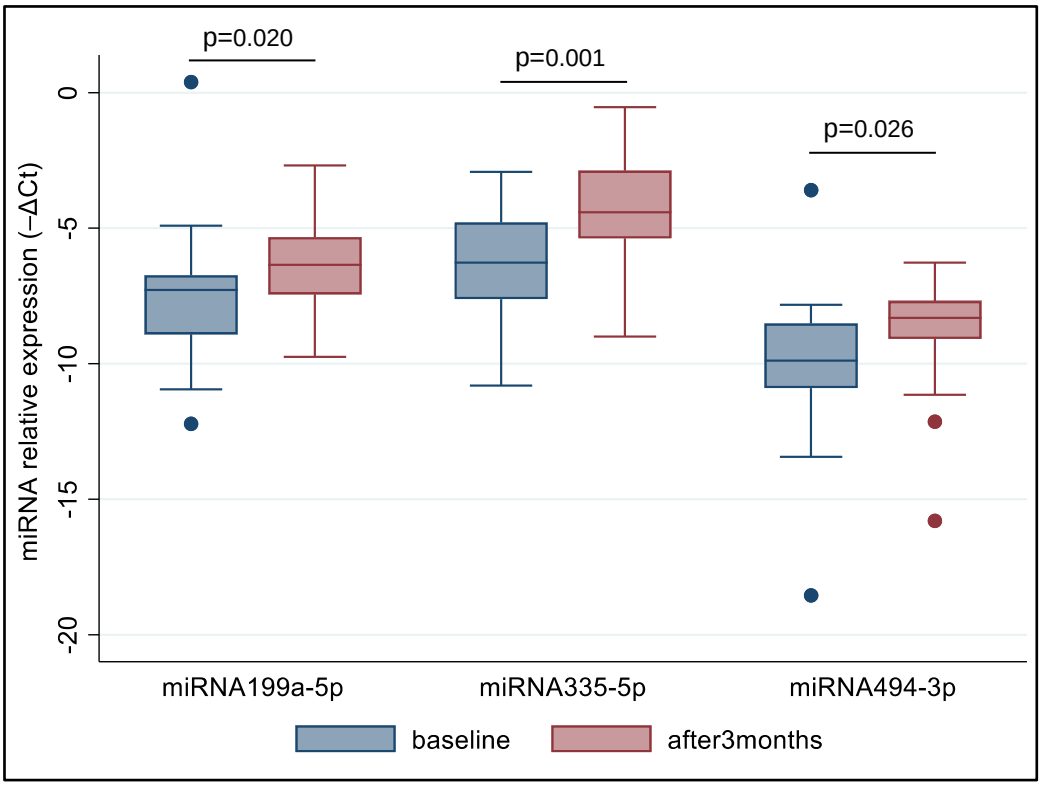

Figure 8. miR-199a-5p, miR-335-5p and miR-494-3p are upregulated after 3 months of GH treatment with respect to the baseline. *miRNA levels are expressed as -ΔCt where ΔCt is calculated as Ct miRNA-Ct miR-16-5p. The box plots represent in blue miRNA levels at baseline, and in red miRNA levels at 3 months on GH treatment. p<0.05 at paired Student's t-test. From: Catellani et al. Front Endocrinol (Lausanne). 2022 Jun 22;13:896640. doi: 10.3389/fendo.2022.896640 (154).*

The measurement of miRNA levels at 12 months on GH treatment evidenced that circulating levels of these three specific miRNAs were more stable and that the inter-individual variance was smaller than that oserved at baseline and at 3 months on treatment (**Figure 9 A, B, C**).

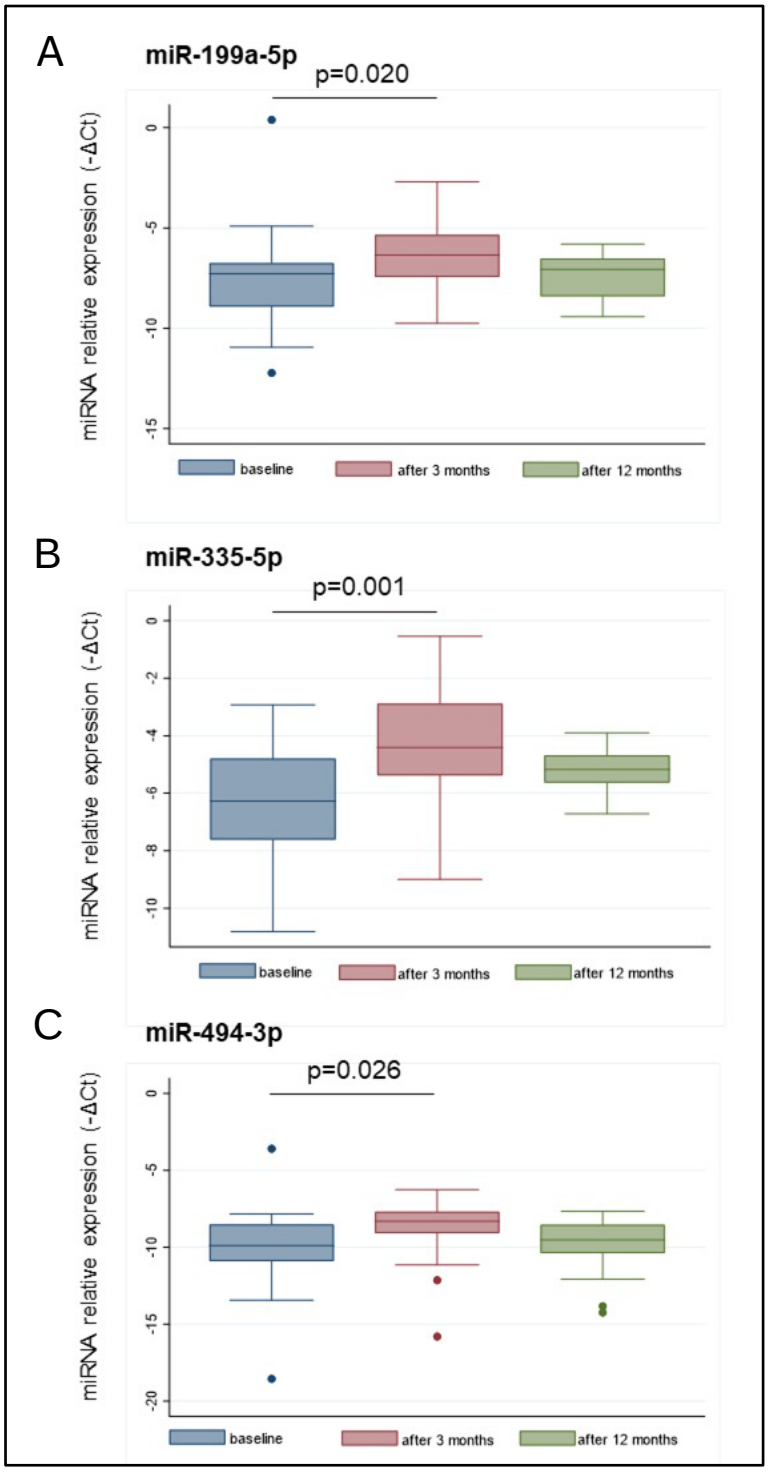

Figure 9. Distribution of miR-199a-5p (A), miR-335-5p (B) and miR-494-3p (C) levels at baseline, 3 and 12 months on GH treatment. *The boxplots represent miRNAs at baseline (blu boxes), at 3 months*

on treatment (red boxes) and at 12 months on treatment (green boxes). miRNA levels are expressed as -ΔCt where ΔCt is calculated as Ct miRNA-Ct miR-16-5p. p<0.05 at paired Student's t-test. From: Catellani et al. Front Endocrinol (Lausanne). 2022 Jun 22;13:896640. doi: 10.3389/fendo.2022.896640 (154).

The evaluation of miRNA kinetics over 12 months evidenced that miRNA levels tended to stabilize at 12 months (**Figure 10**).

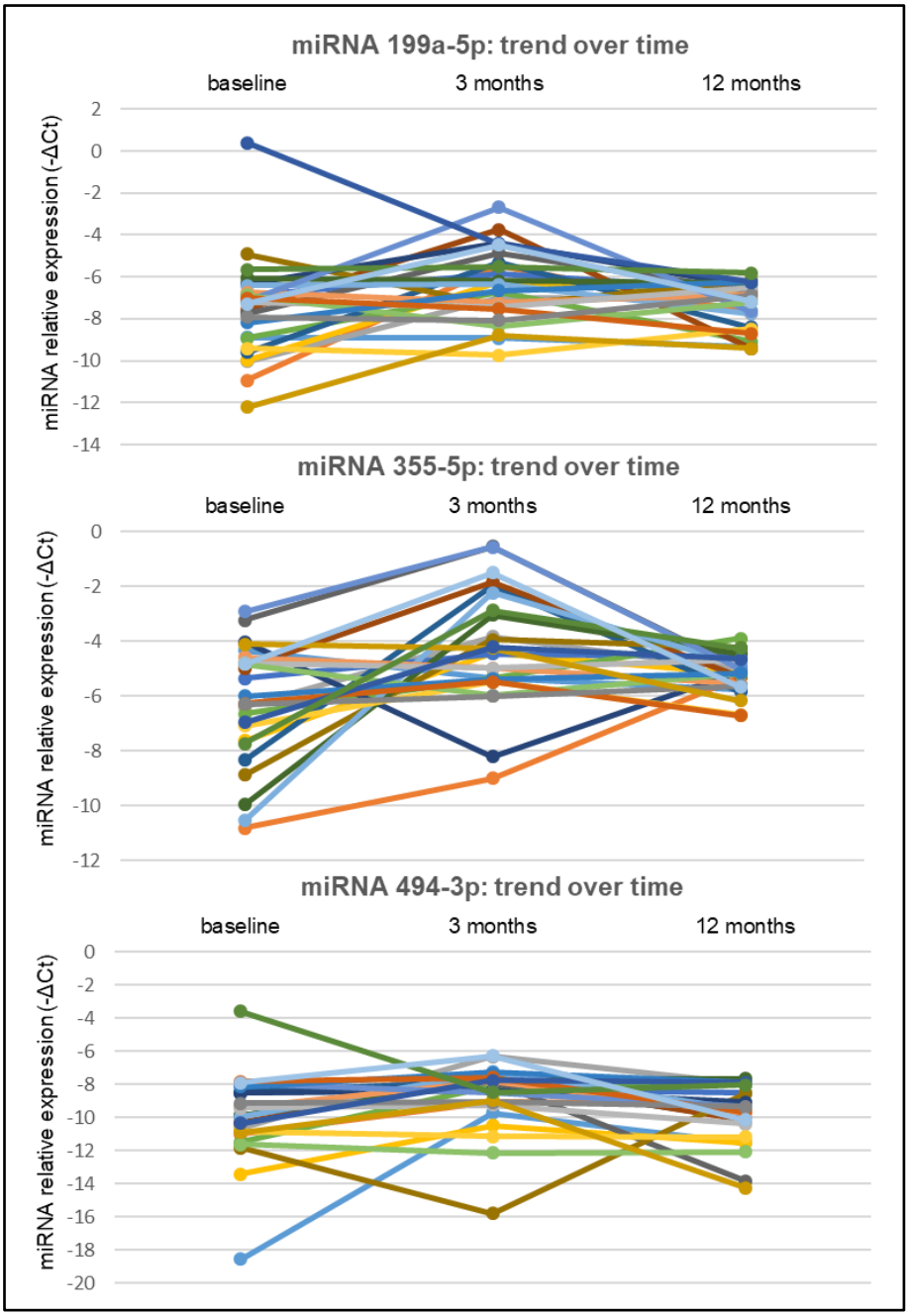

Figure 10. miRNA trend over time. *MiRNA levels are represented as points at baseline, 3 months and 12 months on treatment. Connectors evidence the trend of miRNA levels over 12 months on treatment. miRNA levels are expressed as -ΔCt where ΔCt is calculated as Ct miRNA-Ct miR-16-5p. $p<0.05$ at paired Student's t-test. From: Catellani et al. Front Endocrinol (Lausanne). 2022 Jun 22;13:896640. doi: 10.3389/fendo.2022.896640.(154).*

The subdivision of IIGHD patients in responders and non-responders to GH treatment, based on the change in height SDS after 12 months on treatment > or < +0.3 SDS, evidenced that miRNA levels were more variable in non-responder patients with respect to responders, however no significant differences were found between responders and non-responders (**Figure 11 A, B, C**).

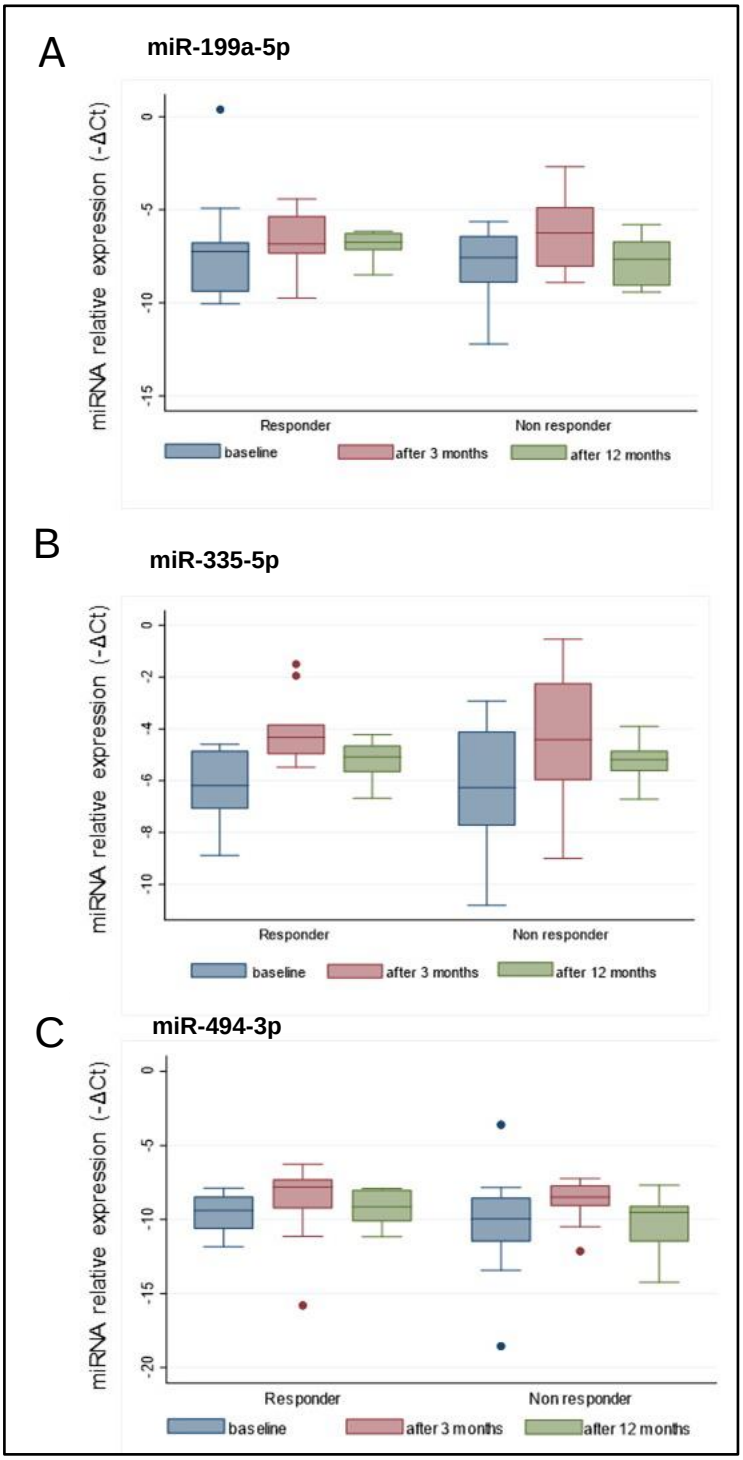

Figure 11. Distribution of miR-199a-5p (A), miR-335-5p (B) and miR-494-3p (C) levels at baseline, 3 and 12 months on GH treatment in responder and non-responder patients. *The boxplots represent miRNAs at baseline (blu boxes), at 3 months on treatment (red boxes) and at 12 months on treatment (green boxes). miRNA levels are expressed as -ΔCt where ΔCt is calculated as Ct miRNA-Ct miR-16-5p. p<0.05 at paired Student's t-test. From: Catellani et al. Front Endocrinol (Lausanne). 2022 Jun 22;13:896640. doi: 10.3389/fendo.2022.896640. (154)*

The subdivision of IIGHD patients based on GH peaks at testing (> or < 5 ng/ml) did not evidence changes in miRNA levels at baseline, 3 months or 12 months on treatment, nor in the change between 0 and 3 months (delta 0-3 months).

Moreover, no differences in miRNA levels were observed between patients grouped based on the type of GH used for treatment (biosimilar GH vs rhGH).

4.5 Simple linear regression analysis and multiple stepwise linear regression models to explain growth response

Possible associations between baseline parameters of patients and miRNA levels at baseline, at 3 months of GH treatment and miRNA levels variations during the first 3 months (ΔΔCt 0-3 months) were explored in order to evaluate whether a variable could be critical for the building of a model (**Table 4 A-C**). An association between miR-199a-5p levels at baseline (coef=3.34, p=0.009, 95% CI: 0.91-5.78) and delta-0-3 months (coef=-3.20, p=0.015, 95% CI=-5.71-0.70) with height SDS at baseline was found. Moreover, an association between miR-494-3p levels at baseline and IGF-I SDS at baseline was found (coef=2.14, p=0.014, 95% CI= 0.47-3.80).

Table 4. Associations between baseline characteristics, miR-199a-5p (A), miR-335-5p (B) and miR-494-3p (C) levels at baseline, their change between baseline and 3 months (delta) and after 3 months on treatment. Data are presented as linear regression coefficients, p-value and 95% CI. *From: Catellani et al. Front Endocrinol (Lausanne). 2022 Jun 22;13:896640. doi: 10.3389/fendo.2022.896640. (154)*

A: miRNA-199a-5p

Baseline characteristics	miRNA-199a-5p											
	baseline				delta 0-3 months				3 months			
	coef	p-value	95%CI		coef	p-value	95%CI		coef	p-value	95%CI	
Sex, M/F	0.49	0.646	-1.68	2.65	-0.72	0.503	-2.89	1.46	-0.23	0.767	-1.80	1.34
Bone age, yr	0.06	0.765	-0.35	0.46	-0.18	0.368	-0.58	0.23	-0.12	0.388	-0.40	0.16
CA, yr	0.03	0.876	-0.31	0.36	-0.15	0.361	-0.49	0.18	-0.13	0.288	-0.37	0.11
Height SDS	3.34	0.009	0.91	5.78	-3.20	0.015	-5.71	-0.70	0.14	0.891	-1.91	2.19
Weight SDS	0.81	0.222	-0.53	2.16	-0.28	0.687	-1.67	1.12	0.54	0.266	-0.44	1.52
BMI SDS	0.38	0.545	-0.91	1.67	0.37	0.567	-0.94	1.67	0.75	0.093	-0.14	1.64
IGF-I SDS	1.42	0.088	-0.23	3.06	-0.70	0.415	-2.45	1.05	0.72	0.242	-0.52	1.95
Alkaline phosphatase, U/l	0.01	0.136	-0.00	0.02	-0.00	0.936	-0.02	0.02	0.01	0.108	-0.00	0.02
GH peak at first stimulation test, ng/ml	-0.14	0.573	-0.64	0.36	0.12	0.616	-0.38	0.63	-0.01	0.938	-0.38	0.35
GH peak at second stimulation test, ng/ml	-0.11	0.666	-0.62	0.40	0.12	0.640	-0.40	0.64	0.01	0.955	-0.36	0.38
Biosimilar vs human recombinant GH	-0.24	0.807	-2.28	1.80	-0.00	0.999	-2.07	2.07	-0.24	0.737	-1.72	1.23
GH dose, mg/kg/day	34.16	0.796	-236.45	-304.78	24.37	0.856	-249.54	298.28	58.53	0.54	-136.05	253.12

B: miRNA-335-5p

Baseline characteristics	miRNA-335-5p											
	baseline				delta 0-3 months				3 months			
	coef	p-value	95%CI		coef	p-value	95%CI		coef	p-value	95%CI	
Sex, M/F	0.97	0.309	-0.96	2.91	-0.48	0.699	-2.99	2.04	0.50	0.592	-1.39	2.39
Bone age, yr	0.22	0.200	-0.13	0.57	-0.12	0.551	-0.54	0.29	0.10	0.520	-0.22	0.42
CA, yr	0.13	0.371	-0.17	0.44	-0.04	0.827	-0.44	0.35	0.09	0.525	-0.20	0.39
Height SDS	-0.07	0.954	-2.65	2.50	0.21	0.896	-3.07	3.49	0.14	0.909	-2.34	2.61
Weight SDS	0.31	0.611	-0.94	1.57	0.55	0.486	-1.05	2.14	-0.86	0.138	-2.02	0.30

BMI SDS	0.34	0.554	-0.83	1.52	0.46	0.529	-1.04	1.96	0.80	0.139	-0.28	1.89
IGF-I SDS	-1.26	0.097	-2.76	0.25	1.12	0.254	-0.86	3.1	-0.14	0.854	-1.67	1.40
Alkaline phosphatase, U/l	0.00	0.856	-0.02	0.02	0.01	0.253	-0.01	0.03	0.01	0.264	-0.01	0.03
GH peak at first stimulation test, ng/ml	-0.04	0.863	-0.50	0.42	-0.03	0.903	-0.62	0.55	-0.07	0.733	-0.51	0.37
GH peak at second stimulation test, ng/ml	0.24	0.413	-0.35	0.83	0.24	0.413	-0.35	0.83	0.23	0.296	-0.21	0.67
Biosimilar vs human recombinant GH	0.98	0.276	-0.83	2.79	-0.96	0.403	-3.3	1.37	0.02	0.985	-1.77	1.80
GH dose, mg/kg/day	87.36	0.466	-156.39	331.11	-215.9	0.151	-516.31	84.51	-128.54	0.260	-358.94	101.86

C: miRNA-494-3p

Baseline characteristics	**miRNA-494-3p**											
	baseline				**delta 0-3 months**				**3 months**			
	coef	**p-value**	**95%CI**		**coef**	**p-value**	**95%CI**		**coef**	**p-value**	**95%CI**	
Sex, M/F	0.08	0.942	-2.27	2.44	-1.65	0.142	-3.90	0.60	-1.57	0.066	-3.25	0.11
Bone age, yr	-0.31	0.141	-0.72	0.11	0.31	0.138	-0.11	0.72	-0.00	0.993	-0.34	0.34
CA, yr	-0.24	0.168	-0.59	0.11	0.18	0.318	-0.18	0.54	-0.06	0.638	-0.35	0.22
Height SDS	0.36	0.808	-2.70	3.43	-2.20	0.134	-5.12	0.73	-1.83	0.102	-4.05	0.39
Weight SDS	0.83	0.249	-0.63	2.30	-0.78	0.282	-2.25	0.69	0.05	0.927	-1.10	1.21
BMI SDS	1.17	0.078	-0.14	2.49	-0.75	0.272	-2.12	0.63	0.42	0.420	-0.64	1.49
IGF-I SDS	2.14	0.014	0.47	3.80	-1.66	0.065	-3.42	0.11	0.48	0.499	-0.97	1.93
Alkaline phosphatase, U/l	0.01	0.273	-0.01	0.04	-0.01	0.491	-0.03	0.02	0.01	0.058	-0.00	0.01
GH peak at first stimulation test, ng/ml	0.18	0.503	-0.36	0.72	0.03	0.903	-0.51	0.58	0.21	0.299	-0.20	0.62
GH peak at second stimulation test, ng/ml	-0.01	0.977	-0.57	0.55	-0.01	0.971	-0.57	0.55	-0.02	0.932	-0.45	0.41
Biosimilar vs human recombinant GH	-1.15	0.281	-3.31	1.01	0.24	0.822	-1.97	2.46	-0.91	0.268	-2.56	0.75
GH dose, mg/kg/day	-95.24	0.505	-385.97	195.49	50.98	0.722	-242.33	344.3	-44.25	0.688	-269.2	180.69

Abbreviations: BMI: body mass index; CA: chronological age; CI: confidence interval; FGB: fasting blood glucose; GH: growth hormone; IGF-I: insulin-like growth factor 1; SDS: Standard deviation score.

Several models were built starting from auxological parameters at baseline, and GH dose at the beginning of treatment, and then adding, GH peaks at testing, IGF-I SDS at baseline, difference between CA and bone age, miRNA levels at baseline and the delta 0-3 months in miRNA levels. These models were used to explain the change in height SDS over 6 and 12 months on treatment, and growth velocity during the first 6 months of treatment (**Table 5 A, B, C**).

Change in growth velocity from baseline to 12 month was non included, since the change in growth velocity was not constant over the 12 months of treatment as reported in **Figure 6**.

Table 5. Multiple stepwise linear regression models to explain the change in height SDS during the first 6 (A) and 12 months (B) on treatment, and growth velocity during the first 6 months on treatment (C). *From: Catellani et al. Front Endocrinol (Lausanne). 2022 Jun 22;13:896640. doi: 10.3389/fendo.2022.896640. (154)*

A

		Delta height 0-6	
		Adj R^2	**R^2 cv**
Model 1	Sex , CA (yr), GH dose (mg/Kg/day), height (SDS), weight (SDS), target height (SDS)	0.53	0.11
Model 2	sex, CA (yr) GH dose (mg/Kg/day), height (SDS), weight (SDS), target height (SDS), GH peaks (ng/ml)	0.49	0.04
Model 3	sex, CA (yr), GH dose (mg/Kg/day), height (SDS), weight (SDS), target height (SDS), IGF-I (SDS)	0.51	0.08
Model 4	sex, CA (yr), GH dose (mg/Kg/day), height (SDS), weight (SDS), target height (SDS), difference between CA and bone age	0.62	0.21
Model 5	sex, CA (yr), GH dose (mg/Kg/day), height (SDS), weight (SDS), target height (SDS) and:		
	miR-199a-5p (baseline and delta 0-3)	0.59	0.15
	miR-355-5p (baseline and delta 0-3)	0.49	0.07
	miR-494 -3p (baseline and delta 0-3)	0.48	0.06
Model 6 - STEPWISE	*selected variables: sex, CA (yr), target height (SDS), GH dose (mg/kg/day), height (SDS), weight (SDS), difference between CA and bone age (yr), GH peak at second test (ng/ml), miR-335-5p baseline, delta 0-3 months miR-335-5p, delta 0-3 months miR-494-3p.*	0.72	0.02

B

		Delta height 0-12	
		Adj R^2	**R^2 cv**
Model 1	sex, CA (yr), GH dose (mg/Kg/day), height (SDS), weight (SDS), target height (SDS)	0.36	0.15
Model 2	sex, CA (yr), GH dose (mg/Kg/day), height (SDS), weight (SDS), target height (SDS), GH peaks (ng/ml)	0.31	0.02
Model 3	sex, CA (yr), GH dose (mg/Kg/day), height (SDS), weight (SDS), target height (SDS), IGF-I (SDS)	0.36	0.10
Model 4	sex, CA (yr), GH dose (mg/Kg/day), height (SDS), weight (SDS), target height (SDS), difference between chronological age and bone age	0.67	0.44
Model 5	sex, CA (yr), GH dose (mg/Kg/day), height (SDS), weight (SDS), target height (SDS), and:		
	miR-199a-5p (baseline and delta 0-3)	0.41	0.20
	miR-355-5p (baseline and delta 0-3)	0.34	0.01
	miR-494 -3p (baseline and delta 0-3)	0.29	0.12
Model 6 - STEPWISE	*selected variables: sex, CA (yr), target height (SDS), GH dose (mg/kg/day), difference between CA and bone age, delta 0-3 months miR-335-5p, delta 0-3 months miR-494-3p*	0.79	0.43

C

		Delta growth rate 0-6	
		Adj R^2	**R^2 cv**
Model 1	Sex , CA (yr), GH dose (mg/Kg/day), height (SDS), weight (SDS), target height (SDS)	-0.12	0.07
Model 2	sex, CA (yr) GH dose (mg/Kg/day), height (SDS), weight (SDS), target height (SDS), GH peaks (ng/ml)	-0.23	0.14
Model 3	sex, CA (yr), GH dose (mg/Kg/day), height (SDS), weight (SDS), target height (SDS), IGF-I (SDS)	-0.17	0.08
Model 4	sex, CA (yr), GH dose (mg/Kg/day), height (SDS), weight (SDS), target height (SDS), difference between CA and bone age	0.00	0.00
Model 5	sex, CA (yr), GH dose (mg/Kg/day), height (SDS), weight (SDS), target height (SDS) and:		
	miR-199a-5p (baseline and delta 0-3)	0.39	0.23
	miR-355-5p (baseline and delta 0-3)	0.02	0.00
	miR-494 -3p (baseline and delta 0-3)	-0.05	0.01
Model 6 - STEPWISE	*selected variables: sex, CA (yr), GH dose (mg/Kg/day),* target height (SDS), *weight (SDS), difference between CA and bone age, GH peak at first test (ng/ml), GH peak at second test (ng/ml), miR-199a- 5p baseline, delta 0-3 months miR-335-5p, delta 0-3 months miR-199a-5p*	0.75	0.63

Abbreviations: CA: chronological age; GH: growth hormone; IGF-I: insulin-like growth factor 1; SDS: Standard deviation score

Concerning the change in height SDS 0-6 months, the addition of each single miRNA gave a contribution to the model comparable to that given by IGF-I SDS and by the value of GH peak, whithout giving a substantial improvement with respect to the model that used auxological parameters only. The difference between CA and bone age substantially increased the ability of the model to predict the outcome. The final model, which was obtained by a stepwise procedure, included miR-335-5p and miR-494-3p together with other variables commonly recorded during follow-up visits (**Table 5A**).

With regard to the change in height SDS 0-12 months (delta height SDS 0-12 months), miR-199a-5p was the miRNA that mostly improved the model containing the auxological parameters only, and its apport was more impacting than that of IGF-I SDS and values of GH peak. The difference between CA and bone age was the best predictor when added singularly to the auxological parameters. Interestinlgy, the stepwise procedure identified a model including miR-335-5p, miR-494-3p, sex, CA, target height SDS, GH dose at the beginning of treatment, and the difference between CA and bone age as the best predictive model (R^2=0.79, R^2 CV=0.43) (**Table 5B**).

Considering the change in growth velocity SDS 0-6 months (delta growth rate 0-6 months), only miR-199a-5p contributed to the model when miRNAs were added one by one. The variance of growth velocity over the first 6 months was explained better by this miRNA than by IGF-I SDS at baseline, values of GH at peaks, and the difference between chronological age and bone age. The stepwise procedure identified a highly predictive model which includes miR-335-5p, miR-199a-5p, sex, CA, weight SDS, target height SDS, GH dose, values of GH at peaks, and the difference between CA and bone age (R^2=0.75, R^2 CV=0.63) (**Table 5C**).

4.6 *In vitro* study

4.6.1 miR-199a-5p, miR-335-5p and miR-494-3p are expressed in HOB cells

As cell model for functional experiments we used primary human osteoblasts (HOB) isolated from femoral trabecular bone tissue from the knee or hip joint region (PromoCell). First we verified miR-199a-5p, miR-335-5p and miR-494-3p expression in HOB cells.

As reported in **Table 6**, HOB cells expressed all the three miRNAs of interest.

Table 6. Normalized expression of miR-199a-5p, miR-335-5p and miR-494-3p in HOB cells. MiRNA levels are reported as $2^{-\Delta Ct}$. Small nuclear RNA U6 was used as housekeeping gene and -ΔCt stands for: raw Ct miRNA- raw Ct U6. Data are reported as mean ±SD and are obtained from 5 independent experiments.

miRNA	**Relative expression ($2^{-\Delta Ct}$)**
miR-199a-5p	0,010 ± 0,003 (mean raw Ct: 29,1)
miR-335-5p	0,009 ± 0,004 (mean raw Ct: 29,1)
miR-494-3p	0,136 ± 0,123 (mean raw Ct: 25,5)

4.6.2 Study of the effects of GH treatment on miRNA levels in HOB cells

To investigate whether GH had an effect on miRNA levels in HOB cells as observed in circulating levels *in vivo*, HOB cells were treated with different doses of GH: 20 ng/ml, 100 ng/ml and 500 ng/ml for 24 hours.

Interestingly, the treatment with 20 ng/ml GH increased the levels of miR-335-5p (p=0.023, **Figure 12 B**), miR-494-3p (p=0.05, **Figure 12 C**) and slightly increased miR-199a-5p levels,

although not significantly (**Figure 12 A**). The treatment with 100 ng/ml or 500 ng/ml of GH had no significant impact on miRNA levels.

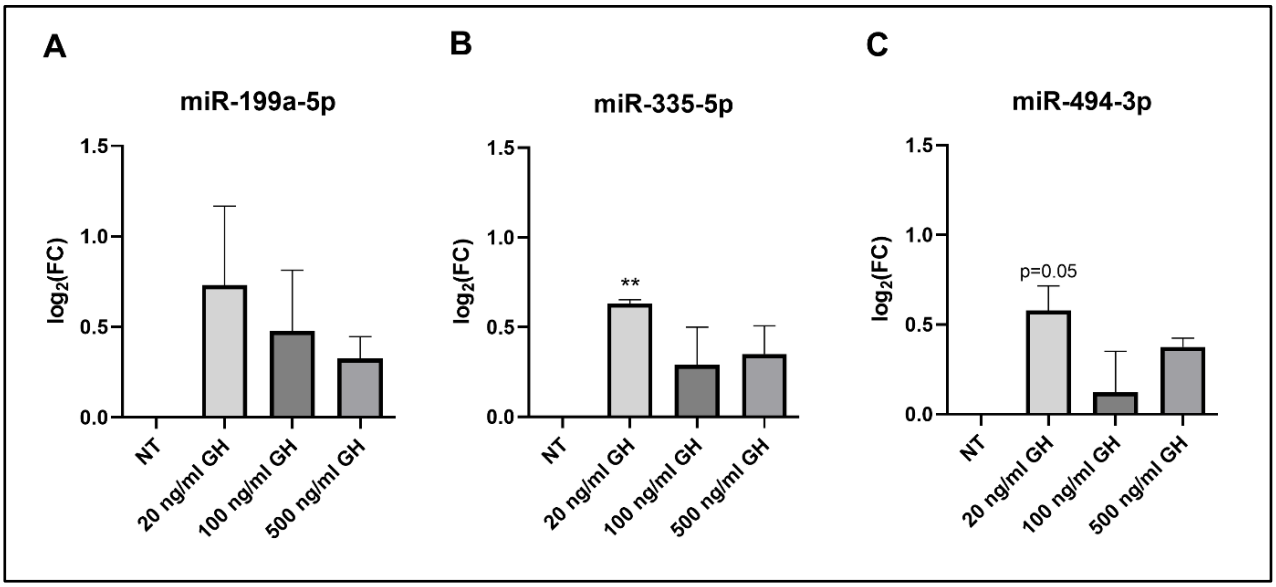

Figure 12. Analysis of miR-199a-5p, miR-335-5p, and miR-494-3p levels after GH treatment. *After 24 h seeding, HOB cells were treated with GH at 3 doses (20 ng/ml, 100 ng/ml and 500 ng/ml) for 24h. Small nuclear RNA U6 was used as housekeeping gene. FC (fold-change) with respect to untreated cells (NT) was calculated as* $2^{-\Delta\Delta Ct}$ *where -ΔCt stands for: raw Ct miRNA- raw Ct U6. Data are expressed as* $log_2 2^{-\Delta\Delta Ct}$*. Data are reported as mean ±SEM and are obtained from 3 independent experiments. *p<0.05 , **p<0.005 , ***p<0.0005 at Student's t-test, one-column statistics.*

4.6.3 *In silico* analysis of predicted targets of miR-199a-5p, miR-335-5p and miR-494-3p within bone

A target prediction analysis performed with Targetscan software and focused on miR-199a-5p, miR-335-5p and miR-494-3p evidenced that these 3 miRNAs have 2 common predicted targets: CLOCK, a gene involved in circadian clock regulation which is associated with bone development, and ROCK1 a serine/threonine kinase which controls cell adhesion and motility. Moreover, miR-199a-5p and miR-335-5p are both predicted to target CRIM1 which is known to regulate BMP4 and 7.

Interestingly, these three genes are also known to be involved in cancer. Aberrant CLOCK expression contributes to carcinogenesis, and ROCK1 and CRIM1 are increased in different types of cancers. In particular, ROCK1 is involved in osteosarcoma.

4.6.4 Analysis of CLOCK, ROCK1 and CRIM1 gene expression levels in HOB cells

A preliminar evaluation of gene expression levels of CLOCK, ROCK1 and CRIM1 in HOB cells evidenced that these 3 genes were expressed in this cell type (**Table 7**).

Table 7. Normalized expression of CLOCK, ROCK1, and CRIM1 in HOB. Gene expression levels are reported as $2^{-\Delta Ct}$. GAPDH was used as housekeeping gene and -ΔCt stands for: raw Ct miRNA- raw Ct GAPDH. Data are reported as mean ±SD and are obtained from 5 independent experiments.

Gene	**Relative expression ($2^{-\Delta Ct}$)**
CLOCK	0,005 ± 0,002 (mean raw Ct: 26,2)
ROCK1	0,018 ± 0,009 (mean raw Ct: 24,3)
CRIM1	0,048 ± 0,020 (mean raw Ct: 22,9)

4.6.5 Analysis of transfection efficiency

To identify the functions of the selected miRNAs in HOB cells, miRNAs were modulated *in vitro* by means of oligonucleotides which mimic miRNAs and oligonucleotides, complementary to the miRNAs, which inhibit miRNA activities. The analysis of transfection efficiency was performed in order to evaluate whether miRNA mimics and inhibitors exerted the expected effects of increasing or decreasing miRNA levels, respectively.

MiR-199a-5p mimic, miR-335-5p mimic, and miR-494-3p mimic significantly increased the respective miRNA levels after 48h of treatment (**Figure 13 A, B, C**). The mean increase was 57 fold for miR-199a-5p, 1451 fold for miR-335-5p, and 398 fold for miR-494-3p.

MiR-199a-5p inhibitor and miR-494-3p inhibitor significantly reduced the levels of the respective miRNAs. miR-335-inhibitor slightly reduced the levels of miR-335-5p, although not significantly.

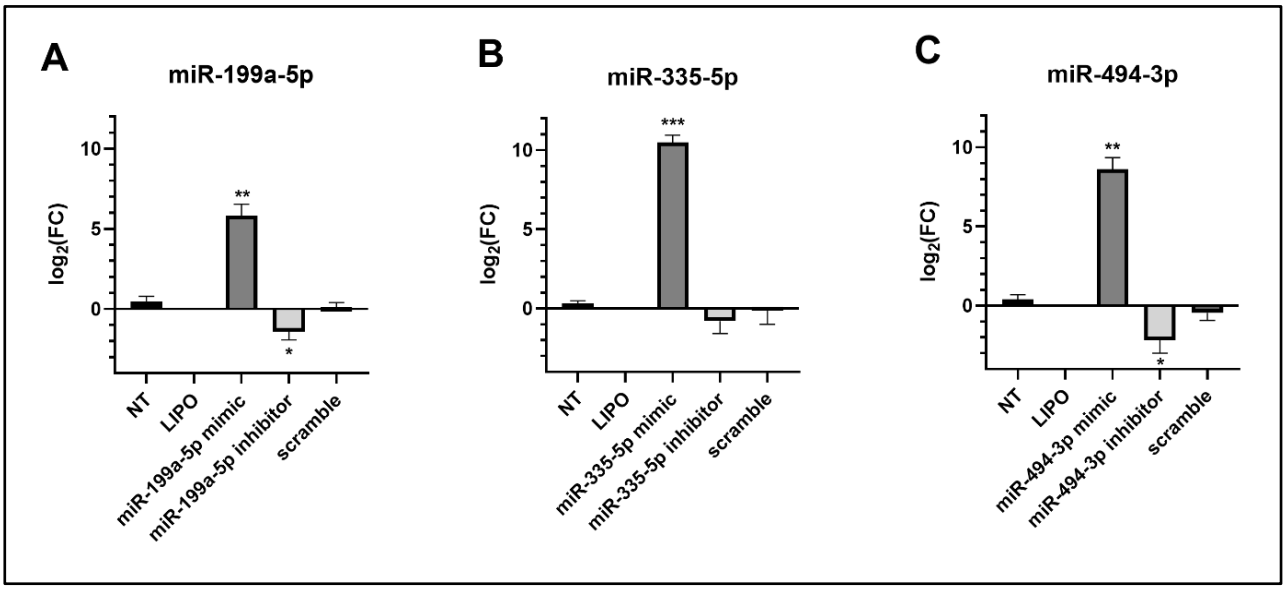

Figure 13. Transfection efficiency and effects of miRNA mimics and inhibitors on their respective miRNA targets. *Small nuclear RNA U6 was used as housekeeper gene. FC (fold-change) with respect to lipofectamine was calculated as* $2^{-\Delta\Delta Ct}$ *where -ΔCt stands for: raw Ct miRNA- raw Ct U6. Data are expressed as* $\log_2 2^{-\Delta\Delta Ct}$*. Data are reported as mean ± SD and are obtained from 3 independent experiments. *p<0.05 , **p<0.005 , ***p<0.0005 at one-column Student's t-test.*

4.6.6 Analysis of the effects of the miRNA mimics and inhibitors on CLOCK, ROCK1, and CRIM1 gene expression levels

CLOCK, ROCK1 and CRIM1 gene expression levels were analysed after 48h transfection with miR-199a-5p, miR-335-5p, and miR-494-3p mimics and inhibitors, to investigate whether these miRNAs had an effect on their predicted targets.

As represented in **Figure 14,** miR-199a-5p, miR-335-5p, and miR-494-3p mimics and inhibitors did not modulate significantly the gene expression of their predicted targets CLOCK (**A**), ROCK1 (**B**) and CRIM1 (**C**). Only ROCK1 showed a trend towards a reduction when cells were treated with miRNA mimics and a trend toward an increase when cells were treated with miRNA inhibitors.

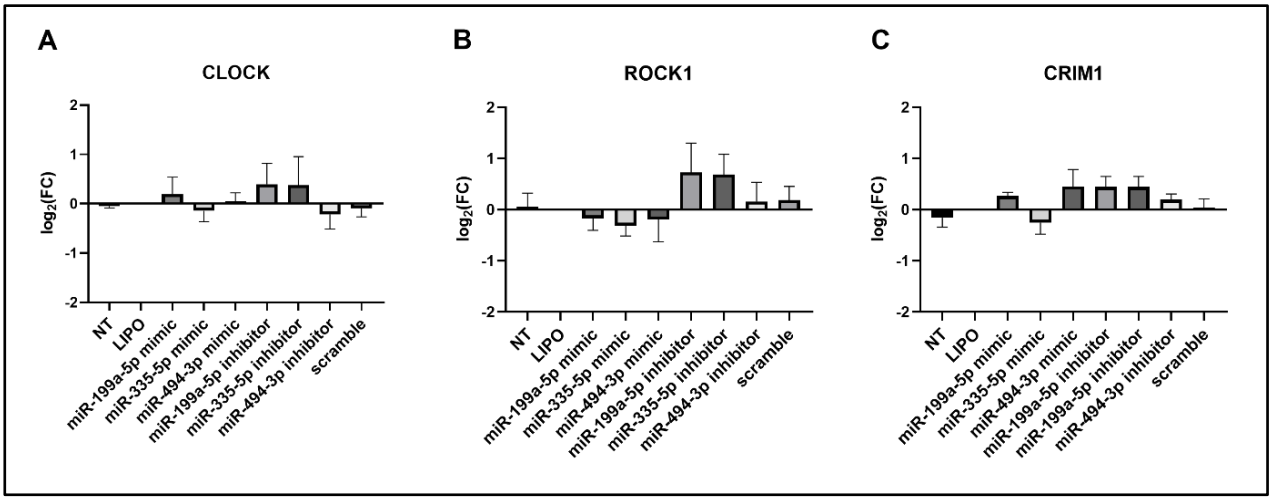

Figure 14. Gene expression levels of CLOCK (A), ROCK1 (B), and CRIM1 (C) after transfection with miRNA mimics and inhibitors. *GAPDH was used as housekeeping gene. FC (fold-change) with respect to lipofectamine was calculated as* $2^{-\Delta\Delta Ct}$ *where -ΔCt stands for: raw Ct gene- raw Ct GAPDH. Data are expressed as* $\log_2 2^{-\Delta\Delta Ct}$*. Data are reported as mean ±SEM and are obtained from 3 independent experiments.*

4.6.7 Analysis of the effects of the miRNA mimics and inhibitors on CLOCK and ROCK1 protein levels

Since CLOCK and ROCK1 are common predicted targets of all these 3 miRNAs, they were selected to evaluate the potential effects of miR-199a-5p, miR-335-5p, and miR-494-3p on CLOCK and ROCK1 protein levels.

As represented in **Figure 15**, CLOCK protein levels were not significantly modulated by miR-199a-5p, miR-335-5p, and miR-494-3p mimics or inhibitors.

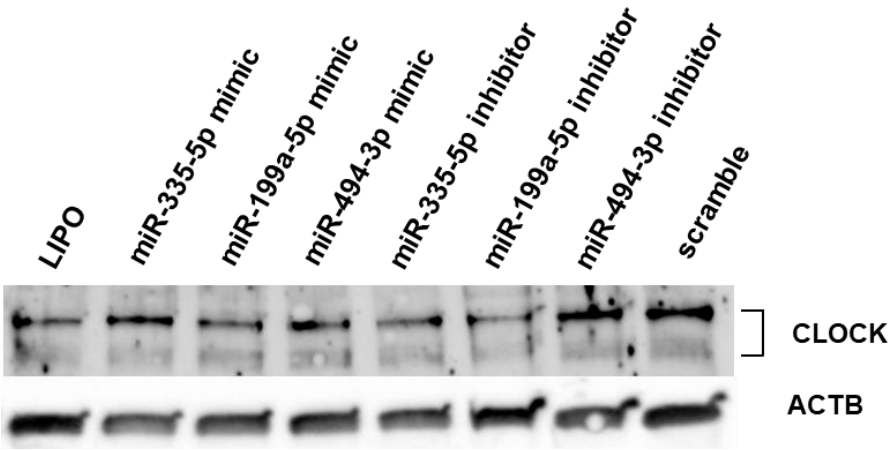

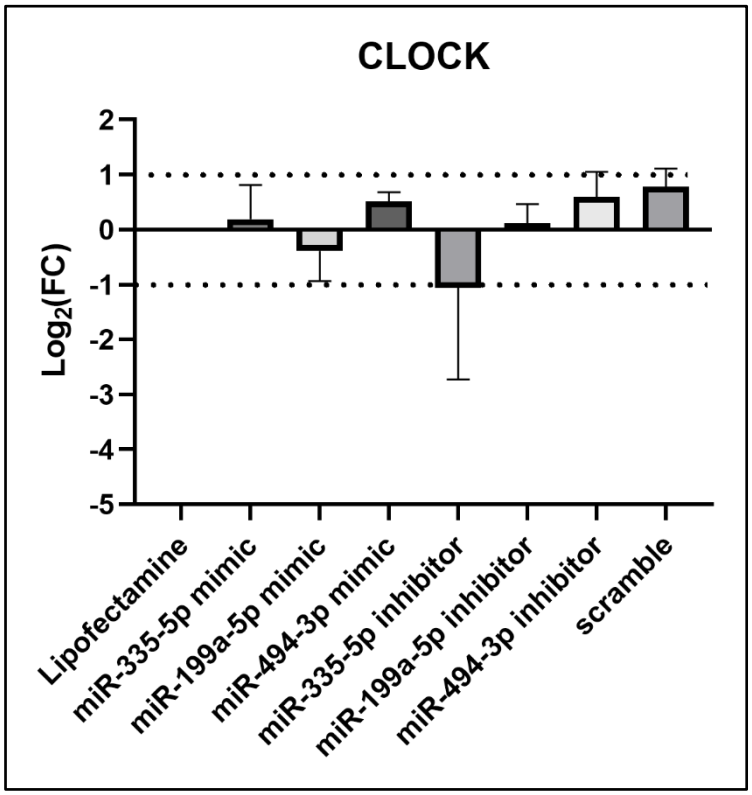

Figure 15. Western blot analysis of CLOCK protein levels after transfection with miR-199a-5p, miR-335-5p, and miR-494-3p mimics and inhibitors. *ECL plus reagent was used for the detection of CLOCK. ECL reagent was used for the detection of β-actin (ACTB). Exposures: 120 seconds for CLOCK, 10 seconds for ACTB (ChemiDoc, Bio-Rad). Western blot bands were quantified by densitometry (Image Lab) and the levels of CLOCK were normalized over ACTB. The change relative to lipofectamine treated cells (fold-change, FC) was calculated. Data are expressed as* log_2FC *and mean±SEM.*

ROCK1 protein levels were not significantly modulated by miR-335-5p or miR-494-3p mimics. MiR-199a-5p mimic reduced slightly ROCK1 protein levels, although not significantly. Moreover, ROCK1 protein levels were not significantly impacted by miR-199a-5p, miR-335-5p, and miR-494-3p inhibitors (**Figure 16**).

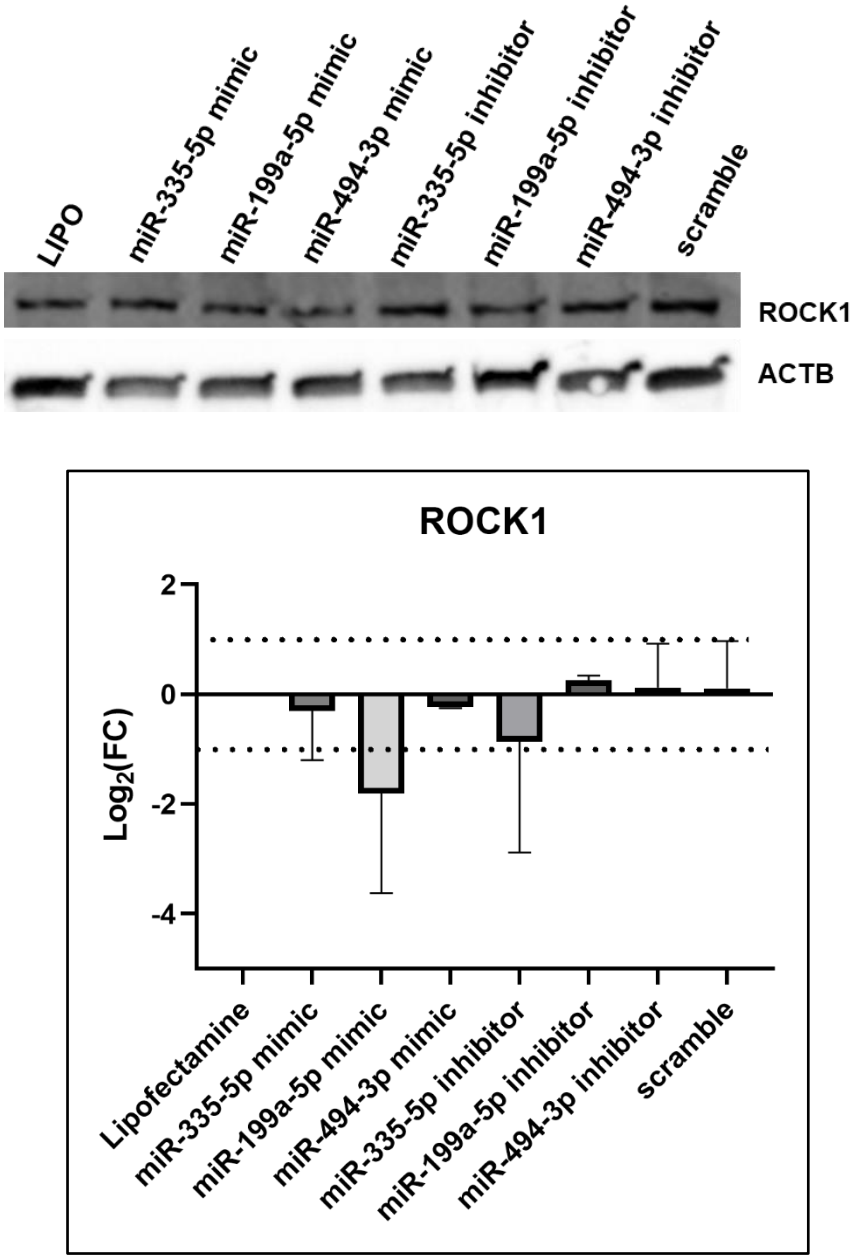

Figure 16. Western blot analysis of ROCK1 protein levels after transfection with miR-199a-5p, miR-335-5p, and miR-494-3p mimics and inhibitors. *ECL plus reagent was used for the detection of CLOCK. ECL reagent was used for the detection of* β-actin *(ACTB). Exposures: 120 seconds for ROCK1, 10 seconds for ACTB (ChemiDoc, Bio-Rad). Western blot bands were quantified by densitometry (Image Lab) and the levels of ROCK1 were normalized over ACTB. The change relative to lipofectamine treated cells (fold-change, FC) was calculated. Data are expressed as* log_2FC *and mean±SEM of two independent experiments is shown.*

4.6.8 Analysis of the effects of miRNA mimics and inhibitors on gene expression levels of the differentiation markers SPP1, COL1A1 and COL1A2

The differentiation markers osteopontin (SPP1), Collagen Type I Alpha 1 Chain (COL1A1) and Alpha 2 Chain (COL1A2) were selected to evaluate whether miR-199a-5p, miR-335-5p, and miR-494-3p could have an impact on osteoblast differentiation, possibly inducing de-differentiation.

MiR-199a-5p, miR-335-5p, and miR-494-3p mimics and inhibitors had no significant effects on the differentiation markers SPP1, COL1A1 and COL1A2, as reported in **Figure 17 A, B, C** respectively.

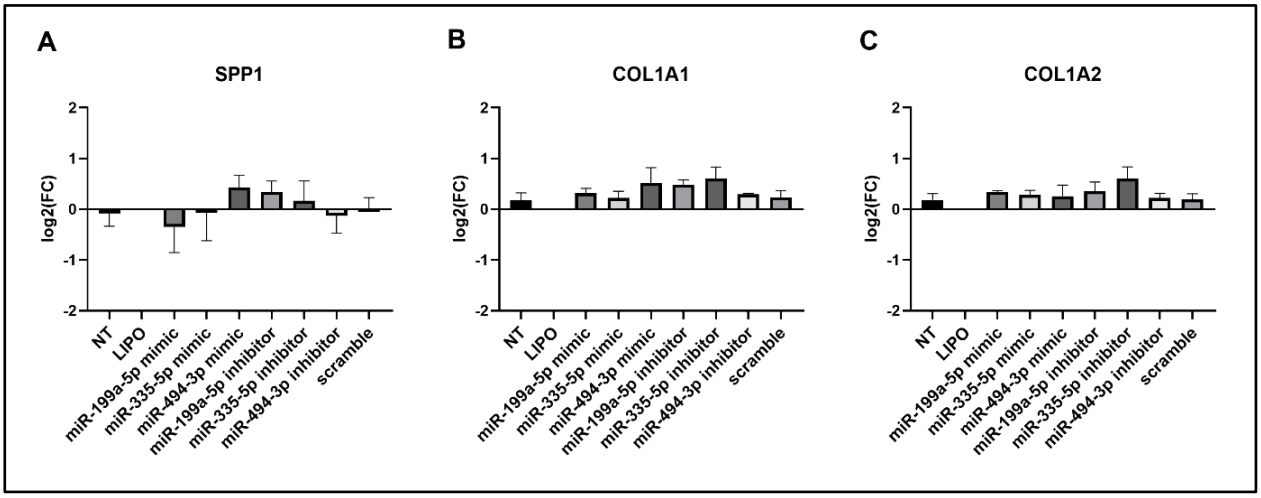

Figure 17. Gene expression levels of SPP1 (A), COL1A1 (B), and COL1A2 (C) after transfection with miRNA mimics and inhibitors. *GAPDH was used as housekeeping gene. FC (fold-change) with respect to lipofectamine was calculated as* $2^{-\Delta\Delta Ct}$ *where -ΔCt stands for: raw Ct gene- raw Ct GAPDH. Data are expressed as* $\log_2 2^{-\Delta\Delta Ct}$*. Data are reported as mean ±SEM and are obtained from 3 independent experiments.*

4.6.9 Analysis of the effects of miRNAs on cell viability/proliferation

In order to investigate the effects of miR-199a-5p, miR-335-5p, and miR-494-3p on cell viability, the WST-1 assay was performed. Absorbance results which derive from the cleavage of the tetrazolium salt WST-1 directly correlate with the number of living cells.

As represented in **Figure 18**, miR-199a-5p, miR-335-5p, and miR-494-3p mimics and inhibitors had no significant effects on cell viability after 48 hours of treatment.

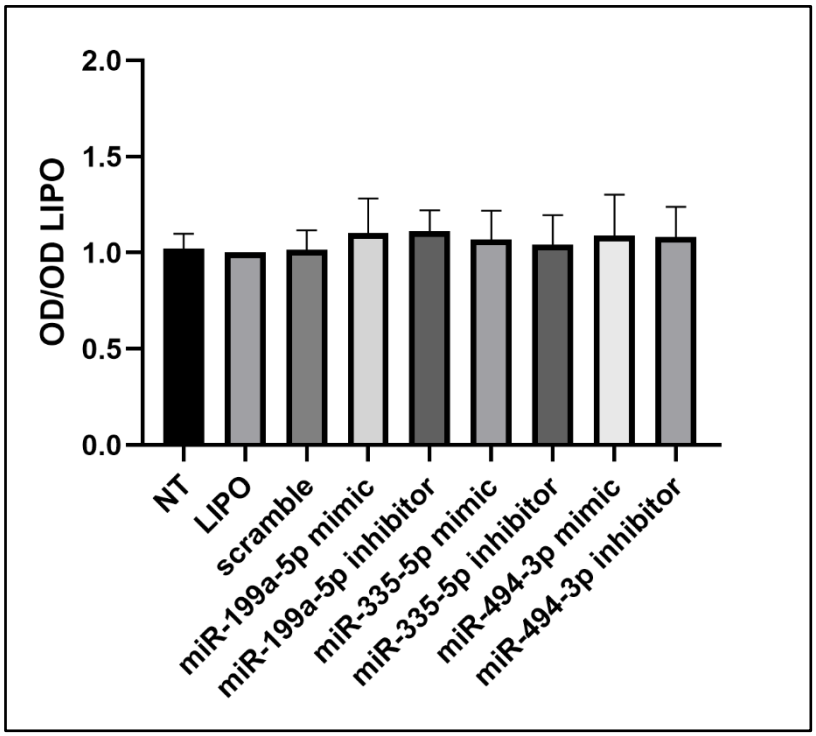

Figure 18. Cell viability of HOB cells after transfection with miR-199a-5p, miR-335-5p, and miR-494-3p mimics and inhibitors. *Cell viability was determined through the WST-1 colorimetric assay. Blank corrected OD is shown relative to that of lipofectamine (LIPO) treated cells. Data are reported as mean ± SD and are obtained from 3 independent experiments.*

5. Discussion

The need to improve growth response in GHD patients, the involvement of miRNAs in longitudinal growth, and their emerging role as potential diagnostic and prognostic biomarkers led us to investigate circulating miRNAs that changed early in IIGHD patients undergoing GH treatment and to evaluate whether these miRNAs contributed to explain the clinical outcome in terms of growth. Moreover, due to the debated potential oncogenic effect of GH especially concerning the risk of osteosarcoma, we evaluated the impact of the miRNAs, identified in the first part of the research project, on pathways related with cancer and we studied *in vitro* whether they could have a pro-oncogenic role.

The exploratory miRNA profiling analysis performed in serum samples from IIGHD patients showed that 18 miRNAs changed after 3 months of GH treatment with respect to the baseline. Of these, miR-199a-5p, miR-335-5p and miR-494-3p were confirmed to be up-regulated in a larger group of IIGHD patients. The collection of clinical, biochemical and auxological parameters of patients allowed to build multiple linear regression models. Interestingly, the inclusion of the baseline levels and the change (0-3 months) of these 3 miRNAs substantially improved the models and contributed to explain longitudinal growth of patients at 12 months of GH treatment.

To date, the change in circulating miRNA levels after GH administration in prepubertal patients with IIGHD has not been investigated yet. A previous paper by Kelly *et al.* investigated the role of miRNAs as potential biomarkers of GH administration in another population setting. Indeed, this study involved a population of 20 adult subjects: 6 subjects receving replacement dose of GH, 11 acromegalic patients and 3 subjects with normal GH secretion (*139*). In this population, miRNAs were analysed with the purpose to establish whether they could be useful to detect doping in sports. MiRNA microarray analysis was performed on samples from 4 acromegalic patients, 3 rhGH users and 2 subjects with normal GH secretion and showed that miR-2861,

miR-663, miR-3152, and miR-3185 were reduced when rhGH was delivered (*139*). However, these miRNAs were analysed in a population of adult patients and this could account for differences in findings in comparison with our study. In fact, the miRNA profile is known to change throughout life and to be influenced by age (*135,167*). A more recent study by Saccon *et al.* evidenced that 14 circulating miRNAs in adult patients and mice with untreated isolated congenital GHD were regulated by both age and genotype and 19 were regulated only by genotype with respect to controls, suggesting that miRNA expression is modulated by GH deficiency (*138*). Consistently, in our study we selected only prepubertal IIGHD patients and compared miRNA changes during GH treatment in these patients. Interestingly, Saccon *et al.* found that, among adults with untreated IGHD, miR-199a-5p was inversely correlated with parameters of glucose metabolism, as glucose and HbA1c (*138*). However, these parameters could be also related with body composition, which is altered in patients with severe GHD where often fat mass is increased and lean body mass is reduced, inducing hyperglicemia (*168*). We found increased miR-199a-5p after 3 months of GH replacement treatment in IIGHD patients, and this is consistent with the fact that GH is known to improve body composition and lean body mass (*168*). Consistently, miR-199a-5p was reported to regulate smooth muscle cell proliferation and hypertrophy which is important for organ remodeling (*169*). Furthermore, it should be taken into account that the study by *Saccon et al.* was performed in adults and old patients.

Our findings suggest that the early changes in miR-199a-5p, miR-335-5p and miR-494-3p could reflect both sensitivity to GH treatment and the degree of GH deficiency. Indeed, little differences have been observed in miRNA levels among patients at 12 months of GH treatment, whereas a change in miRNA levels occurred at 3 months of treatment. This could be dependent both on the initial GH deficiency status and on the innate sensitivity to GH treatment. Interestingly, in the regression models, GH dose was selected among the variables that gave an

important contribution to the explanation of growth response. The changes in miRNA levels were found to be independent from GH peak levels at diagnosis in response to stimulation tests, possibly confirming that GH peaks do not always reflect the degree of GH deficiency. This is consistent with the fact that the degree of response to stimulation tests is variable (*170*). Furthermore, the degree of response to treatment did not seem to affect the changes in miRNA levels during the first 3 months of GH treatment.

MiR-199a-5p, miR-335-5p and miR-494-3p baseline levels and their change 0-3 months gave considerable contribution to the capacity of the models to explain growth response compared with the use of biochemical and clinical parameters only, and compared with the currently available models (*68*). Good prediction models have been published in past years, but have never been used in routinary clinical practice due to their complexity. Among these, for example, one model used markers of bone metabolism in 24h urine samples collected at different time points besides auxological parameters (*73*).

The exploratory purpose of the study must be underlined and we are aware of the relatively small number of subjects investigated in the study. However, it should be taken into account that this population of children was quite difficult to collect. These data are worth be corroborated in a larger population. Moreover, further studies are needed to evaluate potential changes in these miRNAs at puberty, and to consider the potential use of these 3 miRNAs in prediction models also in other condition that have GH as a therapeutic indication. A group of healthy subjects could also be useful to compare results at baseline. A further possible use of these miRNAs could be the improvement of GH deficiency diagnosis. Intriguingly, the value of the information contained in miRNA levels at baseline and their change 0-3 months appeared to be greater than that contained in IGF-I serum levels, confirming that miRNAs are worth to be investigated further.

In the in *vitro* study we evaluated the effects of miR-199a-5p, miR-335-5p and miR-494-3p on cell viability/proliferation and differentiation in primary human osteoblasts (HOB) in order to evaluate any possible pro-oncogenic effects.

Contextually, an *in silico* analysis focused on these three specific miRNAs was performed to evaluate new and promising gene targets that could explain short stature. We found that these miRNAs are predicted to target CLOCK and ROCK1. Moreover, miR-199a-5p and miR-335-5p have CRIM1 as a common predicted target. CLOCK plays a pivotal role in the regulation of circadian rhythm which is known to be involved with bone remodeling and metabolism (*171,172*). ROCK1 a serine/threonine kinase which controls cell adhesion and motility (*173*). CRIM1 is a protein that regulates BMP4 and 7 in the Golgi, reduces the production and processing of preproteins to mature BMPs and reduces also their secretion (*174*). Interestingly, CLOCK, ROCK1, and CRIM1 have been studied in the context of cancer. For example, aberrant CLOCK expression was shown to increase tumor proliferation and growth in colon cancer (*175,176*) and ROCK1 is increased in osteosarcoma where reduces apoptosis and increases proliferation (*177*). CRIM1 was found to regulate adhesion and migration in lung cancer (*178*).

The transfections with miRNA mimics in HOB were very efficient. Nevertheless, it should be noticed that miRNA inhibitors do not necessarily reduce miRNA levels. Indeed, inhibitors can perform both a steric blocking of the complementary miRNA neutralizing its function, or promote miRNA degradation in the cell. The modulation of miRNA levels in HOB cells obtained by transfections, did not impact on CLOCK, ROCK1 and CRIM1 gene expression levels. Consistently, CLOCK and ROCK1 protein expression were unmodified. Of note, CLOCK and CRIM1 were only predicted targets of these miRNAs. Instead ROCK1 is reported as a validated target of miR-199a-5p (*179*), miR-335-5p (*152,180,181*) and miR-494-3p (*182*). These latter studies having ROCK1 as a target were performed in colorectal cancer (*179*),

osteosarcoma (*152*), melanoma (*180),* non-small cell lung cancer (*181)* and in MC3T3-E1 mouse preosteoblasts (*182*). Functional analyses were performed by using miRNA mimics only (*152,181,182*), both miRNA mimics and inhibitors (*180*), or plasmids expressing specific miRNAs (*179*). The direct effects on ROCK1 were evaluated by qPCR, western blot and luciferase reporter assay in these cell models. Interestingly, in MC3T3-E1 mouse preosteoblasts, miR-494-3p was reported to increase only mRNA levels of ROCK1 while protein levels were unchanged (*182*). However, none of these studies was performed in human primary osteoblasts.

The analysis of differentiation markers SPP1, COL1A1 and COL1A2 was performed to evaluate whether miR-199a-5p, miR-335-5p, and miR-494-3p could have an impact on osteoblast differentiation. SPP1 was selected as differentiation marker since it is expressed by mature osteoblasts, regulates bone mineralization toward terminal differentiation into osteocytes and is not expressed in precocious and less differentiated stages of osteoblast lineage (*165,166*). COL1, which is composed by two alpha 1 chains (COL1A1) and one alpha 2 chain (COL1A2), is the main component of the osteoid matrix and is highly expressed by osteoblasts while it is low in osteoprogenitors (*165,166).* SPP1, COL1A1 and COL1A2 gene expression levels were not significantly impacted by transfection with miRNA mimics and inhibitors. The studies that, to date, have investigated the role of miR-199a-5p, miR-335-5p and miR-494-3p in osteoblasts were conducted mainly in murine mesenchymal stem cells and not in human osteoblasts. MiR-199a-5p was found to promote osteoblast commitment in human bone marrow stromal cells (*183*). MiR-335-5p was reported to have a cell-specific regulatory function to promote osteogenic differentiation in a transgenic mouse model overexpressing miR-335-5p and in certain murine cell types: C3H10T-1/2 mesenchimal stem cells, MC3T3-E1 pre-osteoblast cells, immortalized MLO-A5 pre-osteocytes, MLO-Y4 osteocyte-like cells, NIH3T3 fibroblasts, and primary calvarial osteoblasts treated with ascorbic acid (*184,185*). Moreover,

miR-335-5p was found to promote chondrogenic differentiation of murine mesenchymal stem cells (*186*). MiR-494-3p was found to inhibit cell proliferation in murine pre-osteoblast MC3T3-E1 when treated with a compressive force (*182*). The analysis of miRNA effects on cell viability/proliferation evidenced that these miRNAs had no significant effects in osteoblasts.

The investigation of the effect of GH treatment on miRNA levels evidenced that in HOB miR-335-5p is increased after treatment at the dose of 20 ng/ml. Interestingly, this dose is similar to the doses administered to patients on GH treatment. We found also an effect on miR-494-3p at the same dose and a trend to increase of miR-199a-5p, although not significant. This suggests that the serum increase of miR-335-5p and miR-494-3p could be due to a direct effect of GH on miRNA expression.

6. Conclusions

In conclusion this exploratory study showed that miRNAs change on GH treatment, and that miR-199a-5p, miR-335-5p and miR-494-3p that change in the first three months of treatment contributed to explain the growth response in terms of height variation 0-12 months and growth velocity variation 0-6 months. These results are promising and, in the future, could contribute to improve timeliness and tailoring of treatment in the view of personalized therapy.

These three miRNAs were predicted to target genes involved both in bone development but also in cancer. However, the evaluation of the effects of miR-199a-5p, miR-335-5p and miR-494-3p in human primary osteoblasts showed that CLOCK, ROCK1 and CRIM1 putative targets were not significantly impacted by these miRNAs. Moreover, these miRNAs showed no effect on cell viability/proliferation or differentiation. These results are reassuring with respect to possible pro-oncogenic effects of GH which are still debated especially concerning osteosarcoma.

7. References

1. Strobl JS, Thomas MJ. Human growth hormone. Pharmacol Rev. 1994 Mar;46(1):1-34. PMID: 8190748.

2. Li CH, Evans HM. The isolation of pituitary growth hormone. Science. 1944 Mar 3;99(2566):183-4. doi: 10.1126/science.99.2566.183. PMID: 17736901.

3. Olarescu NC, Gunawardane K, Hansen TK, Møller N, Jørgensen JOL. Normal Physiology of Growth Hormone in Adults. 2019 Oct 16. In: Feingold KR, Anawalt B, Boyce A, Chrousos G, de Herder WW, Dhatariya K, Dungan K, Hershman JM, Hofland J, Kalra S, Kaltsas G, Koch C, Kopp P, Korbonits M, Kovacs CS, Kuohung W, Laferrère B, Levy M, McGee EA, McLachlan R, Morley JE, New M, Purnell J, Sahay R, Singer F, Sperling MA, Stratakis CA, Trence DL, Wilson DP, editors. Endotext [Internet]. South Dartmouth (MA): MDText.com, Inc.; 2000–. PMID: 25905284.

4. Mullis, P. E. (2005). Genetic control of growth, European Journal of Endocrinology eur j endocrinol, 152(1), 11-31.

5. Dehkhoda F, Lee CMM, Medina J, Brooks AJ. The Growth Hormone Receptor: Mechanism of Receptor Activation, Cell Signaling, and Physiological Aspects. Front Endocrinol (Lausanne). 2018 Feb 13;9:35. doi: 10.3389/fendo.2018.00035. PMID: 29487568; PMCID: PMC5816795.

6. Vélez EJ, Unniappan S. A Comparative Update on the Neuroendocrine Regulation of Growth Hormone in Vertebrates. Front Endocrinol (Lausanne). 2021 Feb 23;11:614981. doi: 10.3389/fendo.2020.614981. PMID: 33708174; PMCID: PMC7940767.

7. Boguszewski CL, Boguszewski MCDS. Growth Hormone's Links to Cancer. Endocr Rev. 2019 Apr 1;40(2):558-574. doi: 10.1210/er.2018-00166. PMID: 30500870.

8. Laron Z. Somatomedin-1 (recombinant insulin-like growth factor-1): clinical pharmacology and potential treatment of endocrine and metabolic disorders. BioDrugs. 1999 Jan;11(1):55-70. doi: 10.2165/00063030-199911010-00006. PMID: 18031115.

9. Wu S, Yang W, De Luca F. Insulin-Like Growth Factor-Independent Effects of Growth Hormone on Growth Plate Chondrogenesis and Longitudinal Bone Growth. Endocrinology. 2015 Jul;156(7):2541-51. doi: 10.1210/en.2014-1983. Epub 2015 Apr 24. PMID: 25910049.

10. Clemmons DR. Role of IGF-binding proteins in regulating IGF responses to changes in metabolism. J Mol Endocrinol. 2018 Jul;61(1):T139-T169. doi: 10.1530/JME-18-0016. Epub 2018 Mar 21. PMID: 29563157.

11. Firth SM, Baxter RC. Cellular actions of the insulin-like growth factor binding proteins. Endocr Rev. 2002 Dec;23(6):824-54. doi: 10.1210/er.2001-0033. PMID: 12466191.

12. Brooks AJ, Waters MJ. The growth hormone receptor: mechanism of activation and clinical implications. Nat Rev Endocrinol. 2010 Sep;6(9):515-25. doi: 10.1038/nrendo.2010.123. Epub 2010 Jul 27. PMID: 20664532.

13. Carter-Su C, Schwartz J, Kikuchi G. Identification of a high affinity growth hormone receptor in rat adipocyte membranes. J Biol Chem. 1984 Jan 25;259(2):1099-104. PMID: 6319377.

14. Zhao L, Dong H, Zhang CC, Kinch L, Osawa M, Iacovino M, Grishin NV, Kyba M, Huang LJ. A JAK2 interdomain linker relays Epo receptor engagement signals to kinase activation. J Biol Chem. 2009 Sep 25;284(39):26988-98. doi: 10.1074/jbc.M109.011387. Epub 2009 Jul 28. PMID: 19638629; PMCID: PMC2785384.

15. Jin H, Lanning NJ, Carter-Su C. JAK2, but not Src family kinases, is required for STAT, ERK, and Akt signaling in response to growth hormone in preadipocytes and hepatoma cells.

Mol Endocrinol. 2008 Aug;22(8):1825-41. doi: 10.1210/me.2008-0015. Epub 2008 May 22. PMID: 18499741; PMCID: PMC2505331.

16. Rowlinson SW, Yoshizato H, Barclay JL, Brooks AJ, Behncken SN, Kerr LM, Millard K, Palethorpe K, Nielsen K, Clyde-Smith J, Hancock JF, Waters MJ. An agonist-induced conformational change in the growth hormone receptor determines the choice of signalling pathway. Nat Cell Biol. 2008 Jun;10(6):740-7. doi: 10.1038/ncb1737.

17. Han Y, Leaman DW, Watling D, Rogers NC, Groner B, Kerr IM, Wood WI, Stark GR. Participation of JAK and STAT proteins in growth hormone-induced signaling. J Biol Chem. 1996 Mar 8;271(10):5947-52. doi: 10.1074/jbc.271.10.5947. PMID: 8621469.

18. Hwa V, Little B, Adiyaman P, Kofoed EM, Pratt KL, Ocal G, Berberoglu M, Rosenfeld RG. Severe growth hormone insensitivity resulting from total absence of signal transducer and activator of transcription 5b. J Clin Endocrinol Metab. 2005 Jul;90(7):4260-6. doi: 10.1210/jc.2005-0515. Epub 2005 Apr 12. PMID: 15827093.

19. Kurzer, J.H., Carter-Su, C. Growth Hormone Induced Activation and Regulation of JAK2 and STAT Proteins. 2003 In: Sehgal, P.B., Levy, D.E., Hirano, T. (eds) Signal Transducers and Activators of Transcription (STATs). Springer, Dordrecht. https://doi.org/10.1007/978-94-017-3000-6_12

20. Manabe N, Kubota Y, Kitanaka A, Ohnishi H, Taminato T, Tanaka T. Src transduces signaling via growth hormone (GH)-activated GH receptor (GHR) tyrosine-phosphorylating GHR and STAT5 in human leukemia cells. Leuk Res (2006) 30(11):1391–8. doi:10.1016/j.leukres.2006.03.024

21. Hansen JA, Lindberg K, Hilton DJ, Nielsen JH, Billestrup N. Mechanism of inhibition of growth hormone receptor signaling by suppressor of cytokine signaling proteins. Mol Endocrinol. 1999 Nov;13(11):1832-43. doi: 10.1210/mend.13.11.0368. PMID: 10551777.

22. Carter-Su C, Schwartz J, Argetsinger LS. Growth hormone signaling pathways. Growth Horm IGF Res. 2016 Jun;28:11-5. doi: 10.1016/j.ghir.2015.09.002. Epub 2015 Sep 10. PMID: 26421979; PMCID: PMC7644140.

23. Piwien-Pilipuk G, Van Mater D, Ross SE, MacDougald OA, Schwartz J. Growth hormone regulates phosphorylation and function of CCAAT/enhancer-binding protein beta by modulating Akt and glycogen synthase kinase-3. J Biol Chem. 2001 Jun 1;276(22):19664-71. doi: 10.1074/jbc.M010193200. Epub 2001 Mar 13. PMID: 11278638.

24. Thirone AC, Carvalho CR, Saad MJ. Growth hormone stimulates the tyrosine kinase activity of JAK2 and induces tyrosine phosphorylation of insulin receptor substrates and Shc in rat tissues. Endocrinology. 1999 Jan;140(1):55-62. doi: 10.1210/endo.140.1.6417.

25. Ridderstråle M, Degerman E, Tornqvist H. Growth hormone stimulates the tyrosine phosphorylation of the insulin receptor substrate-1 and its association with phosphatidylinositol 3-kinase in primary adipocytes. J Biol Chem. 1995 Feb 24;270(8):3471-4. doi: 10.1074/jbc.270.8.3471.

26. Dominici FP, Argentino DP, Muñoz MC, Miquet JG, Sotelo AI, Turyn D. Influence of the crosstalk between growth hormone and insulin signalling on the modulation of insulin sensitivity. Growth Horm IGF Res. 2005 Oct;15(5):324-36. doi: 10.1016/j.ghir.2005.07.001.

27. Emanuelli B, Peraldi P, Filloux C, Sawka-Verhelle D, Hilton D, Van Obberghen E. SOCS-3 is an insulin-induced negative regulator of insulin signaling. J Biol Chem. 2000 May 26;275(21):15985-91. doi: 10.1074/jbc.275.21.15985.

28. Feng X, Tang H, Leng J, Jiang Q. Suppressors of cytokine signaling (SOCS) and type 2 diabetes. Mol Biol Rep. 2014;41(4):2265-74. doi: 10.1007/s11033-014-3079-8. Epub 2014 Jan 12. PMID: 24414000.

29. Wu CT, Morris JR. Genes, genetics, and epigenetics: a correspondence. Science. 2001 Aug 10;293(5532):1103-5. doi: 10.1126/science.293.5532.1103. PMID: 11498582.

30. Wang J, Zhou J, Cheng CM, Kopchick JJ, Bondy CA. Evidence supporting dual, IGF-I-independent and IGF-I-dependent, roles for GH in promoting longitudinal bone growth. J Endocrinol. 2004 Feb;180(2):247-55. doi: 10.1677/joe.0.1800247. PMID: 14765976.

31. Møller N, Jørgensen JO. Effects of growth hormone on glucose, lipid, and protein metabolism in human subjects. Endocr Rev. 2009 Apr;30(2):152-77. doi: 10.1210/er.2008-0027. Epub 2009 Feb 24. PMID: 19240267.

32. Rizza RA, Mandarino LJ, Gerich JE. Effects of growth hormone on insulin action in man. Mechanisms of insulin resistance, impaired suppression of glucose production, and impaired stimulation of glucose utilization. Diabetes. 1982 Aug;31(8 Pt 1):663-9. doi: 10.2337/diab.31.8.663. PMID: 6761205.

33. Martini FH, Nath JL, Bartholomew E. Fundamentals of Anatomy and Physiology 11th edition. 2017 Pearson Ed. UK

34. Lieke G.E. Cox, B. van Rietbergen, C.C. van Donkelaar, K. Ito. The turnover of mineralized growth plate cartilage into bone may be regulated by osteocytes Journal of Biomechanics 2011 44 (9) 1765-1770.

35. Emons J, Chagin AS, Sävendahl L, Karperien M, Wit JM. Mechanisms of growth plate maturation and epiphyseal fusion. Horm Res Paediatr. 2011;75(6):383-91. doi: 10.1159/000327788. Epub 2011 May 4. PMID: 21540578.

36. Blum WF, Alherbish A, Alsagheir A, El Awwa A, Kaplan W, Koledova E, Savage MO. The growth hormone-insulin-like growth factor-I axis in the diagnosis and treatment of growth

disorders. Endocr Connect. 2018 Jun;7(6):R212-R222. doi: 10.1530/EC-18-0099. Epub 2018 May 3. PMID: 29724795; PMCID: PMC5987361.

37. Daughaday WH, Kipnis DM. The growth-promoting and anti-insulin actions of somatotropin. Recent Prog Horm Res. 1966;22:49-99. doi: 10.1016/b978-1-4831-9825-5.50005-1. PMID: 5334632.

38. Salmon WD, Daughaday WH. A hormonally controlled serum factor which stimulates sulfate incorporation by cartilage in vitro. J Lab Clin Med. 1957 Jun;49(6):825-36. PMID: 13429201.

39. Schlechter NL, Russell SM, Spencer EM, Nicoll CS. Evidence suggesting that the direct growth-promoting effect of growth hormone on cartilage in vivo is mediated by local production of somatomedin. Proc Natl Acad Sci U S A. 1986 Oct;83(20):7932-4. doi: 10.1073/pnas.83.20.7932. PMID: 3464007; PMCID: PMC386837.

40. Isaksson OG, Lindahl A, Nilsson A, Isgaard J. Mechanism of the stimulatory effect of growth hormone on longitudinal bone growth. Endocr Rev. 1987 Nov;8(4):426-38. doi: 10.1210/edrv-8-4-426. PMID: 3319530.

41. Yakar S, Liu JL, Stannard B, Butler A, Accili D, Sauer B, LeRoith D. Normal growth and development in the absence of hepatic insulin-like growth factor I. Proc Natl Acad Sci U S A. 1999 Jun 22;96(13):7324-9. doi: 10.1073/pnas.96.13.7324. PMID: 10377413; PMCID: PMC22084.

42. Hunziker EB, Wagner J, Zapf J. Differential effects of insulin-like growth factor I and growth hormone on developmental stages of rat growth plate chondrocytes in vivo. J Clin Invest. 1994 Mar;93(3):1078-86. doi: 10.1172/JCI117058. PMID: 8132746; PMCID: PMC294043.

43. Ohlsson C, Nilsson A, Isaksson O, Lindahl A. Growth hormone induces multiplication of the slowly cycling germinal cells of the rat tibial growth plate. Proc Natl Acad Sci U S A. 1992 Oct 15;89(20):9826-30. doi: 10.1073/pnas.89.20.9826. PMID: 1409707; PMCID: PMC50226.

44. Green H, Morikawa M, Nixon T. A dual effector theory of growth-hormone action. Differentiation. 1985;29(3):195-8. doi: 10.1111/j.1432-0436.1985.tb00316.x. PMID: 3908201.

45. Russell SM, Spencer EM. Local injections of human or rat growth hormone or of purified human somatomedin-C stimulate unilateral tibial epiphyseal growth in hypophysectomized rats. Endocrinology. 1985 Jun;116(6):2563-7. doi: 10.1210/endo-116-6-2563. PMID: 4039658.

46. Isaksson OG, Jansson JO, Gause IA. Growth hormone stimulates longitudinal bone growth directly. Science. 1982 Jun 11;216(4551):1237-9. doi: 10.1126/science.7079756. PMID: 7079756.

47. Wang J, Zhou J, Bondy CA. Igf1 promotes longitudinal bone growth by insulin-like actions augmenting chondrocyte hypertrophy. FASEB J. 1999 Nov;13(14):1985-90. doi: 10.1096/fasebj.13.14.1985. PMID: 10544181.

48. DiGirolamo DJ, Mukherjee A, Fulzele K, Gan Y, Cao X, Frank SJ, Clemens TL. Mode of growth hormone action in osteoblasts. J Biol Chem. 2007 Oct 26;282(43):31666-74. doi: 10.1074/jbc.M705219200. Epub 2007 Aug 13. PMID: 17698843.

49. Kassem M, Blum W, Ristelli J, Mosekilde L, Eriksen EF. Growth hormone stimulates proliferation and differentiation of normal human osteoblast-like cells in vitro. Calcif Tissue Int. 1993 Mar;52(3):222-6. doi: 10.1007/BF00298723. PMID: 7683248.

50. Tritos NA, Klibanski A. Effects of Growth Hormone on Bone. Prog Mol Biol Transl Sci. 2016;138:193-211. doi: 10.1016/bs.pmbts.2015.10.008. Epub 2016 Jan 6. PMID: 26940392.

51. Crane JL, Cao X. Function of matrix IGF-1 in coupling bone resorption and formation. J Mol Med (Berl). 2014 Feb;92(2):107-15. doi: 10.1007/s00109-013-1084-3. Epub 2013 Sep 26. PMID: 24068256; PMCID: PMC3946714.

52. Savage, M.O. The Changing Face of Paediatric Human Growth Hormone Therapy. Endocrines 2022, 3, 419-427. https://doi.org/10.3390/endocrines3030033

53. Ranke MB. Short and Long-Term Effects of Growth Hormone in Children and Adolescents With GH Deficiency. Front Endocrinol (Lausanne). 2021 Sep 1;12:720419. doi: 10.3389/fendo.2021.720419. PMID: 34539573; PMCID: PMC8440916.

54. Vimpani GV, Vimpani AF, Lidgard GP, Cameron EH, Farquhar JW. Prevalence of Severe Growth Hormone Deficiency. Br Med J (1977) 2:427–30. doi: 10.1136/bmj.2.6084.427

55. Beck JC, McGarry EE, Dyrenfurth I, Venning EH. The metabolic effects of human and monkey growth hormone in man. Ann Intern Med. 1958 Nov;49(5):1090-105. doi: 10.7326/0003-4819-49-5-1090. PMID: 13595475.

56. Schweizer R, Blumenstock G, Mangelsdorf K, Ehehalt S, Rössner L, Dorn T, et al. Prevalence and Incidence of Endocrine Disorders in Children: Results of a Survey in Baden-Wuerttemberg and Bavaria (EndoPrIn BB) 2000-2001. Klin Padiatr (2010) 222:67–72. doi: 10.1055/s-0029-1241868

57. Stochholm K, Gravholt CH, Laursen T, Jørgensen JO, Laurberg P, Andersen M, et al. Incidence of GH Deficiency - A Nationwide Study. Eur J Endocrinol (2006) 155:61–71. doi: 10.1530/eje.1.02191

58. Ranke MB, Wit JM. Growth hormone - past, present and future. Nat Rev Endocrinol. 2018 May;14(5):285-300. doi: 10.1038/nrendo.2018.22. Epub 2018 Mar 16. PMID: 29546874.

59. Alatzoglou KS, Webb EA, Le Tissier P, Dattani MT. Isolated growth hormone deficiency (GHD) in childhood and adolescence: recent advances. Endocr Rev. 2014 Jun;35(3):376-432. doi: 10.1210/er.2013-1067. Epub 2014 Jan 22. PMID: 24450934.

60. Chinoy A, Murray PG. Diagnosis of growth hormone deficiency in the paediatric and transitional age. Best Pract Res Clin Endocrinol Metab. 2016 Dec;30(6):737-747. doi: 10.1016/j.beem.2016.11.002. Epub 2016 Nov 4. PMID: 27974187.

61. Dauber A, Rosenfeld RG, Hirschhorn JN. Genetic evaluation of short stature. J Clin Endocrinol Metab. 2014 Sep;99(9):3080-92. doi: 10.1210/jc.2014-1506. Epub 2014 Jun 10. PMID: 24915122; PMCID: PMC4154097.

62. Rogol A, Anhalt H, Schorr Haines M, George Vogiatzi M. "Growth Hormone Deficiency | Endocrine Society." Endocrine.org, Endocrine Society, 23 December 2022, https://www.endocrine.org/patient-engagement/endocrine-library/growth-hormone-deficiency

63. Aguiar-Oliveira MH, Bartke A. Growth Hormone Deficiency: Health and Longevity. Endocr Rev. 2019 Apr 1;40(2):575-601. doi: 10.1210/er.2018-00216. PMID: 30576428; PMCID: PMC6416709.

64. Savage MO, Bang P. The variability of responses to growth hormone therapy in children with short stature. Indian J Endocrinol Metab. 2012 Dec;16(Suppl 2):S178-84. doi: 10.4103/2230-8210.104034. PMID: 23565373; PMCID: PMC3603021.

65. Cappa M, Iughetti L, Loche S, Maghnie M, Vottero A; GeNeSIS National Board on behalf of the GeNeSIS Italian Investigators. Efficacy and safety of growth hormone treatment in children with short stature: the Italian cohort of the GENeSIS clinical study. J Endoocrinol Invest. 2016 Jun;39(6):667-77.

66. Sävendahl L, Pournara E, Pedersen BT, Blankenstein O. Is safety of childhood growth hormone therapy related to dose? Data from a large observational study. Eur J Endocrinol. 2016 May;174(5):681-91

67. Shimatsu A, Tai S, Imori M, Ihara K, Taketsuna M, Funai J, Tanaka T, Teramoto A, Irie M, Chihara K. Efficacy and safety of growth hormone replacement therapy in Japanese adults with growth hormone deficiency: a postmarketing observational study. Endocr J. 2013;60(10):1131-1144.

68. Loftus J, Lindberg A, Aydin F, Gomez R, Maghnie M, Rooman R, Steinkamp H, Doerr H, Ranke M, Camacho-Hubner C. Individualised growth response optimisation (iGRO) tool: an accessible and easy-to-use growth prediction system to enable treatment optimisation for children treated with growth hormone J Pediatr Endocrinol Metab. 2017 Oct 26;30(10):1019-1026. doi: 10.1515/jpem-2017-0120.

69. Koledova E, Stoyanov G, Ovbude L, Davies PSW. Adherence and long-term growth outcomes: results from the easypod connect observational study (ECOS) in paediatric patients with growth disorders. Endocr Connect. 2018;7(8):914–923. doi: 10.1530/EC-18-0172

70. Wit JM, Ranke MB, Albertsson-Wikland K, Carrascosa A, Rosenfeld RG, Van Buuren S, Kristrom B, Schoenau E, Audi L, Hokken-Koelega AC, Bang P, Jung H, Blum WF, Silverman LA, Cohen P, Cianfarani S, Deal C, Clayton PE, de Graaff L, Dahlgren J, Kleintjens J, Roelants M. Personalized approach to growth hormone treatment: clinical use of growth prediction models. Horm Res Paediatr. 2013;79(5):257-70. doi: 10.1159/000351025. Epub 2013 May 28. PMID: 23735882.

71. Kaspers, S.; Ranke, M.B.; Han, D.; Loftus, J.; Wollmann, H.; Lindberg, A.; Roelants, M.; Kleintjens, J. Implications of a data-driven approach to treatment with growth hormone in

children with growth hormone deficiency and Turner syndrome. Appl. Health Econ. Health Policy 2013, 11, 237–249.

72. Ranke, M.B.; Lindberg, A.; KIGS International Board. Observed and predicted growth responses in prepubertal children with growth disorders: Guidance of growth hormone treatment by empirical variables. J. Clin. Endocrinol. Metab. 2010, 95, 1229–1237.

73. Schonau, E.; Westermann, F.; Rauch, F.; Stabrey, A.; Wassmer, G.; Keller, E.; Bramswig, J.; Blum, W.F.; German Lilly Growth Response Study Group. A new and accurate prediction model for growth response to growth hormone treatment in children with growth hormone deficiency. Eur. J. Endocrinol. 2001, 144, 13–20.

74. Wikland, K.A.; Kriström, B.; Rosberg, S.; Svensson, B.; Nierop, A.E. Validated multivariate models predicting the growth response to growth hormone treatment in individual short children with a broad range in GH secretion capacities. Pediatr. Res. 2000, 48, 475–484.

75. Brittain AL, Basu R, Qian Y, Kopchick JJ. Growth Hormone and the Epithelial-to-Mesenchymal Transition. J Clin Endocrinol Metab. 2017 Oct 1;102(10):3662-3673. doi: 10.1210/jc.2017-01000. PMID: 28938477.

76. Boguszewski CL, Boguszewski MC, Kopchick JJ. Growth hormone, insulin-like growth factor system and carcinogenesis. Endokrynol Pol. 2016;67(4):414-26. doi: 10.5603/EP.a2016.0053. Epub 2016 Jul 8. PMID: 27387246.

77. Harvey S, Martínez-Moreno CG, Luna M, Arámburo C. Autocrine/paracrine roles of extrapituitary growth hormone and prolactin in health and disease: An overview. Gen Comp Endocrinol. 2015 Sep 1;220:103-11. doi: 10.1016/j.ygcen.2014.11.004. Epub 2014 Nov 15. PMID: 25448258.

78. Perry JK, Starling Emerald B, Mertani HC, Lobie PE. The oncogenic potential of growth hormone, Growth Hormone & IGF Research, Volume 16, Issues 5–6, 2006, Pages 277-289

79. Chesnokova V, Melmed S. Growth hormone in the tumor microenvironment. Arch Endocrinol Metab. 2019 Nov-Dec;63(6):568-575. doi: 10.20945/2359-3997000000186. PMID: 31939481; PMCID: PMC7025769.

80. Guevara-Aguirre J, Balasubramanian P, Guevara-Aguirre M, Wei M, Madia F, Cheng CW, Hwang D, Martin-Montalvo A, Saavedra J, Ingles S, de Cabo R, Cohen P, Longo VD. Growth hormone receptor deficiency is associated with a major reduction in pro-aging signaling, cancer, and diabetes in humans. Sci Transl Med. 2011 Feb 16;3(70):70ra13. doi: 10.1126/scitranslmed.3001845. PMID: 21325617; PMCID: PMC3357623.

81. Chhabra Y, Wong HY, Nikolajsen LF, Steinocher H, Papadopulos A, Tunny KA, Meunier FA, Smith AG, Kragelund BB, Brooks AJ, Waters MJ. A growth hormone receptor SNP promotes lung cancer by impairment of SOCS2-mediated degradation. Oncogene. 2018 Jan 25;37(4):489-501. doi: 10.1038/onc.2017.352. Epub 2017 Oct 2. PMID: 28967904; PMCID: PMC5799715.

82. Kopchick JJ, List EO, Kelder B, Gosney ES, Berryman DE. Evaluation of growth hormone (GH) action in mice: discovery of GH receptor antagonists and clinical indications. Mol Cell Endocrinol. 2014 Apr 5;386(1-2):34-45. doi: 10.1016/j.mce.2013.09.004. Epub 2013 Sep 11. PMID: 24035867; PMCID: PMC3943600.

83. Laron Z, Kauli R, Lapkina L, Werner H. IGF-I deficiency, longevity and cancer protection of patients with Laron syndrome. Mutat Res Rev Mutat Res. 2017 Apr-Jun;772:123-133. doi: 10.1016/j.mrrev.2016.08.002. Epub 2016 Aug 5. PMID: 28528685.

84. Sävendahl L, Cooke R, Tidblad A, Beckers D, Butler G, Cianfarani S, Clayton P, Coste J, Hokken-Koelega ACS, Kiess W, Kuehni CE, Albertsson-Wikland K, Deodati A, Ecosse E,

Gausche R, Giacomozzi C, Konrad D, Landier F, Pfaeffle R, Sommer G, Thomas M, Tollerfield S, Zandwijken GRJ, Carel JC, Swerdlow AJ. Long-term mortality after childhood growth hormone treatment: the SAGhE cohort study. Lancet Diabetes Endocrinol. 2020 Aug;8(8):683-692. doi: 10.1016/S2213-8587(20)30163-7. PMID: 32707116.

85. Poidvin A, Carel JC, Ecosse E, Levy D, Michon J, Coste J. Increased risk of bone tumors after growth hormone treatment in childhood: A population-based cohort study in France. Cancer Med. 2018 Jul;7(7):3465-3473. doi: 10.1002/cam4.1602. Epub 2018 Jun 14. PMID: 29905027; PMCID: PMC6051149.

86. Swerdlow AJ, Cooke R, Beckers D, Borgström B, Butler G, Carel JC, Cianfarani S, Clayton P, Coste J, Deodati A, Ecosse E, Gausche R, Giacomozzi C, Hokken-Koelega ACS, Khan AJ, Kiess W, Kuehni CE, Mullis PE, Pfaffle R, Sävendahl L, Sommer G, Thomas M, Tidblad A, Tollerfield S, Van Eycken L, Zandwijken GRJ. Cancer Risks in Patients Treated With Growth Hormone in Childhood: The SAGhE European Cohort Study. J Clin Endocrinol Metab. 2017 May 1;102(5):1661-1672. doi: 10.1210/jc.2016-2046. PMID: 28187225; PMCID: PMC6061931.

87. Carel JC, Ecosse E, Landier F, Meguellati-Hakkas D, Kaguelidou F, Rey G, Coste J. Long-term mortality after recombinant growth hormone treatment for isolated growth hormone deficiency or childhood short stature: preliminary report of the French SAGhE study. J Clin Endocrinol Metab. 2012 Feb;97(2):416-25. doi: 10.1210/jc.2011-1995. Epub 2012 Jan 11. PMID: 22238382.

88. Swerdlow AJ, Higgins CD, Adlard P, Preece MA. Risk of cancer in patients treated with human pituitary growth hormone in the UK, 1959-85: a cohort study. Lancet. 2002 Jul 27;360(9329):273-7. doi: 10.1016/s0140-6736(02)09519-3. PMID: 12147369.

89. Waddington CH (1939) An introduction to modern genetics/by C. H. Waddington. George Allen & Unwin, London

90. O'Brien J, Hayder H, Zayed Y, Peng C. Overview of MicroRNA Biogenesis, Mechanisms of Actions, and Circulation Front Endocrinol (Lausanne). 2018 Aug 3;9:402. doi: 10.3389/fendo.2018.00402. eCollection 2018.

91. Catalanotto C, Cogoni , Zardo G. MicroRNA in Control of Gene Expression: An Overview of Nuclear Functions Int J Mol Sci. 2016 Oct 13;17(10):1712. doi: 10.3390/ijms17101712.

92. Volinia S, Calin GA, Liu CG, Ambs S, Cimmino A, Petrocca F, Visone R, Iorio M, Roldo C, Ferracin M, Prueitt RL, Yanaihara N, Lanza G, Scarpa A, Vecchione A, Negrini M, Harris CC, Croce CM. A microRNA expression signature of human solid tumors defines cancer gene targets. Proc Natl Acad Sci U S A. 2006 Feb 14;103(7):2257-61. doi: 10.1073/pnas.0510565103. Epub 2006 Feb 3. PMID: 16461460; PMCID: PMC1413718.

93. Friedman R.C., Farh K.K., Burge C.B., Bartel D.P. Most mammalian mRNAs are conserved targets of microRNAs. Genome Res. 2009;19:92–105. doi: 10.1101/gr.082701.108

94. Filipowicz W, Bhattacharyya SN, Sonenberg N. Mechanisms of post-transcriptional regulation by microRNAs: are the answers in sight? Nat Rev Genet. 2008 Feb;9(2):102-14. doi: 10.1038/nrg2290. PMID: 18197166.

95. Morselli M, Dieci G. Epigenetic regulation of human non-coding RNA gene transcription. Biochem Soc Trans. 2022 Apr 29;50(2):723-736. doi: 10.1042/BST20210860. PMID: 35285478.

96. Ferreira HJ, Esteller M. Non-coding RNAs, epigenetics, and cancer: tying it all together. Cancer Metastasis Rev. 2018 Mar;37(1):55-73. doi: 10.1007/s10555-017-9715-8. PMID: 29374363.

97. Zealy RW, Wrenn SP, Davila S, Min KW, Yoon JH. microRNA-binding proteins: specificity and function. Wiley Interdiscip Rev RNA. 2017 Sep;8(5). doi: 10.1002/wrna.1414. Epub 2017 Jan 28. PMID: 28130820.

98. Vishnoi A, Rani S. MiRNA Biogenesis and Regulation of Diseases: An Overview. Methods Mol Biol. 2017;1509:1-10. doi: 10.1007/978-1-4939-6524-3_1. PMID: 27826912.

99. Bartel DP. MicroRNAs: target recognition and regulatory functions. Cell. 2009 Jan 23; 136(2):215-233

100. Denli AM, Tops BB, Plasterk RH, Ketting RF, Hannon GJ. Processing of primary microRNAs by the Microprocessor complex. Nature. 2004 Nov 11;432(7014):231-5. doi: 10.1038/nature03049. Epub 2004 Nov 7. PMID: 15531879.

101. McGeary SE, Lin KS, Shi CY, Pham T, Bisaria N, Kelley GM, Bartel DP. The biochemical basis of microRNA targeting efficacy. Science Dec 5, (2019).

102. Broughton JP, Lovci MT, Huang JL, Yeo GW, Pasquinelli AE. Pairing beyond the Seed Supports MicroRNA Targeting Specificity. Mol Cell. 2016 Oct 20;64(2):320-333. doi: 10.1016/j.molcel.2016.09.004. Epub 2016 Oct 6. PMID: 27720646; PMCID: PMC5074850.

103. Miao L, Yao H, Li C, Pu M, Yao X, Yang H, Qi X, Ren J, Wang Y. A dual inhibition: microRNA-552 suppresses both transcription and translation of cytochrome P450 2E1. Biochim Biophys Acta. 2016 Apr;1859(4):650-62. doi: 10.1016/j.bbagrm.2016.02.016. Epub 2016 Feb 27. PMID: 26926595.

104. Benhamed M, Herbig U, Ye T, Dejean A, Bischof O. Senescence is an endogenous trigger for microRNA-directed transcriptional gene silencing in human cells. Nat Cell Biol. 2012 Feb 26;14(3):266-75. doi: 10.1038/ncb2443. PMID: 22366686; PMCID: PMC5423543.

105. Blazie SM, Geissel HC, Wilky H, Joshi R, Newbern J, Mangone M. Alternative Polyadenylation Directs Tissue-Specific miRNA Targeting in Caenorhabditis elegans Somatic Tissues. Genetics. 2017 Jun;206(2):757-774. doi: 10.1534/genetics.116.196774. Epub 2017 Mar 27. PMID: 28348061; PMCID: PMC5499184.

106. Nam JW, Rissland OS, Koppstein D, Abreu-Goodger C, Jan CH, Agarwal V, Yildirim MA, Rodriguez A, Bartel DP. Global analyses of the effect of different cellular contexts on microRNA targeting. Mol Cell. 2014 Mar 20;53(6):1031-1043. doi: 10.1016/j.molcel.2014.02.013. Epub 2014 Mar 13. PMID: 24631284; PMCID: PMC4062300.

107. Pillai RS, Bhattacharyya SN, Filipowicz W. Repression of protein synthesis by miRNAs: how many mechanisms? Trends Cell Biol. 2007 Mar;17(3):118-26. doi: 10.1016/j.tcb.2006.12.007. Epub 2007 Jan 2. PMID: 17197185.

108. Truesdell SS, Mortensen RD, Seo M, Schroeder JC, Lee JH, LeTonqueze O, Vasudevan S. MicroRNA-mediated mRNA translation activation in quiescent cells and oocytes involves recruitment of a nuclear microRNP. Sci Rep. 2012;2:842. doi: 10.1038/srep00842. Epub 2012 Nov 13. PMID: 23150790; PMCID: PMC3496365.

109. Ørom UA, Nielsen FC, Lund AH. MicroRNA-10a binds the 5'UTR of ribosomal protein mRNAs and enhances their translation. Mol Cell. 2008 May 23;30(4):460-71. doi: 10.1016/j.molcel.2008.05.001. PMID: 18498749.

110. Tsang, J., Zhu, J. & van Oudenaarden, A. (2007). MicroRNA-mediated feedback and feedforward loops are recurrent network motifs in mammals. Mol. Cell, 26, 753–767.

111. Ebert, M. S. & Sharp, P. A. (2012). Roles for microRNAs in conferring robustness to biological processes. Cell, 149, 515–524

112. Shkumatava, A., Stark, A., Sive, H. & Bartel, D. P.(2009). Coherent but overlapping expression of microRNAs and their targets during vertebrate development. Genes Dev. 23, 466–481.

113. Barman B, Bhattacharyya SN. mRNA Targeting to Endoplasmic Reticulum Precedes Ago Protein Interaction and MicroRNA (miRNA)-mediated Translation Repression in Mammalian Cells. J Biol Chem. 2015 Oct 9;290(41):24650-6. doi: 10.1074/jbc.C115.661868. Epub 2015 Aug 24. PMID: 26304123; PMCID: PMC4598978.

114. Nishi K, Takahashi T, Suzawa M, Miyakawa T, Nagasawa T, Ming Y, Tanokura M, Ui-Tei K. Control of the localization and function of a miRNA silencing component TNRC6A by Argonaute protein. Nucleic Acids Res. 2015 Nov 16;43(20):9856-73. doi: 10.1093/nar/gkv1026. Epub 2015 Oct 7. PMID: 26446993; PMCID: PMC4787778.

115. Gibbings DJ, Ciaudo C, Erhardt M, Voinnet O. Multivesicular bodies associate with components of miRNA effector complexes and modulate miRNA activity. Nat Cell Biol. 2009 Sep;11(9):1143-9. doi: 10.1038/ncb1929. Epub 2009 Aug 16. Erratum in: Nat Cell Biol. 2009 Oct;11(10):1272. PMID: 19684575.

116. Mori MA, Ludwig RG, Garcia-Martin R, Brandão BB, Kahn CR. Extracellular miRNAs: From Biomarkers to Mediators of Physiology and Disease. Cell Metab. 2019 Oct 1;30(4):656-673. doi: 10.1016/j.cmet.2019.07.011. Epub 2019 Aug 22. PMID: 31447320; PMCID: PMC6774861.

117. Turchinovich A, Tonevitsky AG, Burwinkel B. Extracellular miRNA: A Collision of Two Paradigms. Trends Biochem Sci. 2016 Oct;41(10):883-892. doi: 10.1016/j.tibs.2016.08.004. Epub 2016 Sep 3. PMID: 27597517.

118. Krützfeldt J. Strategies to use microRNAs as therapeutic targets. Best Pract Res Clin Endocrinol Metab. 2016 Oct;30(5):551-561. doi: 10.1016/j.beem.2016.07.004. Epub 2016 Aug 1. PMID: 27923450.

119. El-Awady RA, Herzi F, Al-Tunaiji H, Saleh EM, Abdel-Wahab AH, Al Homossi A, Suhail M, El-Sarafi A, Al-Tel T. Epigenetics and miRNA as predictive markers and targets for lung cancer chemotherapy. Cancer Biol Ther; 2015 16(7):1056-1070.

120. Yan S, Cao Y, Mao AW. MicroRNAs in colorectal cancer: potential biomarkers and therapeutic targets. Front Biosci 2015; 20:1092-1103.

121. Mitchell PS, Parkin RK, Kroh EM, Fritz BR, Wyman SK, Pogosova-Agadjanyan EL, Peterson A, Noteboom J, O'Briant KC, Allen A, Lin DW, Urban N, Drescher CW, Knudsen BS, Stirewalt DL, Gentleman R, Vessella RL, Nelson PS, Martin DB, Tewari M. Circulating microRNAs as stable blood-based markers for cancer detection. Proc Natl Acad Sci U S A. 2008 Jul 29;105(30):10513-8. doi: 10.1073/pnas.0804549105. Epub 2008 Jul 28. PMID: 18663219; PMCID: PMC2492472.

122. Lee RC, Feinbaum RL, Ambros V. The C.elegans heterochronic gene lin-4 encodes small RNAs with antisense complementarity to lin-14. Cell. 1993;75:843–854.

123. Lui JC. Regulation of body growth by microRNAs. Mol Cell Endocrinol. 2017 Nov 15;456:2-8. doi: 10.1016/j.mce.2016.10.024. Epub 2016 Oct 24. PMID: 27789392; PMCID: PMC7202226.

124. Kobayashi T, Lu J, Cobb BS, Rodda SJ, McMahon AP, Schipani E, Merkenschlager M, Kronenberg HM. Dicer-dependent pathways regulate chondrocyte proliferation and differentiation. Proc Natl Acad Sci U S A. 2008 Feb 12;105(6):1949-54. doi: 10.1073/pnas.0707900105. Epub 2008 Jan 31. PMID: 18238902; PMCID: PMC2538863.

125. Jee YH, Wang J, Yue S, Jennings M, Clokie SJ, Nilsson O, Lui JC, Baron J. mir-374-5p, mir-379-5p, and mir-503-5p Regulate Proliferation and Hypertrophic Differentiation of Growth Plate Chondrocytes in Male Rats. Endocrinology. 2018 Mar 1;159(3):1469-1478. doi: 10.1210/en.2017-00780. PMID: 29390136; PMCID: PMC5839730.

126. Papaioannou G. miRNAs in Bone Development. Curr Genomics. 2015 Dec;16(6):427-34. doi: 10.2174/1389202916666150817202425. PMID: 27019617; PMCID: PMC4765530.

127. Papaioannou G, Mirzamohammadi F, Kobayashi T. MicroRNAs involved in bone formation. Cell Mol Life Sci. 2014 Dec;71(24):4747-61. doi: 10.1007/s00018-014-1700-6. Epub 2014 Aug 10. PMID: 25108446; PMCID: PMC4234685.

128. Cirillo F, Catellani C, Lazzeroni P, Sartori C, Street ME. The Role of MicroRNAs in Influencing Body Growth and Development Horm Res Paediatr. 2020;93(1):7-15. doi: 10.1159/000504669.

129. Jing J, Xiong S, Li Z, Wu J, Zhou L, Gui JF, Mei J. A feedback regulatory loop involving p53/miR-200 and growth hormone endocrine axis controls embryo size of zebrafish. Sci Rep. 2015 Oct 28;5:15906. doi: 10.1038/srep15906. PMID: 26507500; PMCID: PMC4623745.

130. Elzein S, Goodyer CG. Regulation of human growth hormone receptor expression by microRNAs. Mol Endocrinol. 2014 Sep;28(9):1448-1459

131. Lin S, Li H, Mu H, Luo W, Li Y, Jia X, Wang S, Jia X, Nie Q, Li Y, Zhang X. Let-7b regulates the expression of the growth hormone receptor gene in deletion-type dwarf chickens. BMC Genomics. 2012 Jul 10;13:306. doi: 10.1186/1471-2164-13-306. PMID: 22781587; PMCID: PMC3428657.

132. Zhang H, Qi Q, Chen T, Luo J, Xi Q, Jiang Q, Sun J, Zhang Y. Age-Related Changes in MicroRNA in the Rat Pituitary and Potential Role in GH Regulation. Int J Mol Sci. 2018 Jul 15;19(7):2058. doi: 10.3390/ijms19072058. PMID: 30011963; PMCID: PMC6073141.

133. Qi QE, Xi QY, Ye RS, Chen T, Cheng X, Li CY, Zhu XT, Shu G, Wang LN, Jiang QY, Zhang YL. Alteration of the miRNA expression profile in male porcine anterior pituitary cells in response to GHRH and CST and analysis of the potential roles for miRNAs in regulating GH. Growth Horm IGF Res. 2015 Apr;25(2):66-74. doi: 10.1016/j.ghir.2014.12.002. Epub 2014 Dec 9. PMID: 25613666.

134. Ye RS, Li M, Qi QE, Cheng X, Chen T, Li CY, Wang SB, Shu G, Wang LN, Zhu XT, Jiang QY, Xi QY, Zhang YL. Comparative Anterior Pituitary miRNA and mRNA Expression Profiles of Bama Minipigs and Landrace Pigs Reveal Potential Molecular Network Involved in Animal Postnatal Growth. PLoS One. 2015 Jul 2;10(7):e0131987. doi: 10.1371/journal.pone.0131987. PMID: 26134288; PMCID: PMC4489742.

135. Lai CY, Wu YT, Yu SL, Yu YH, Lee SY, Liu CM, Hsieh WS, Hwu HG, Chen PC, Jeng SF, Chen WJ. Modulated expression of human peripheral blood microRNAs from infancy to adulthood and its role in aging. Aging Cell. 2014 Aug;13(4):679-89. doi: 10.1111/acel.12225. Epub 2014 May 6. PMID: 24803090; PMCID: PMC4326935.

136. Wang X, Yang L, Wang H, Shao F, Yu J, Jiang H, Han Y, Gong D, Gu Z. Growth hormone-regulated mRNAs and miRNAs in chicken hepatocytes. PLoS One. 2014 Nov 11;9(11):e112896. doi: 10.1371/journal.pone.0112896. PMID: 25386791; PMCID: PMC4227886.

137. Galimov A, Hartung A, Trepp R, Mader A, Flück M, Linke A, Blüher M, Christ E, Krützfeldt J. Growth hormone replacement therapy regulates microRNA-29a and targets

involved in insulin resistance. J Mol Med (Berl). 2015 Dec;93(12):1369-79. doi: 10.1007/s00109-015-1322-y. Epub 2015 Jul 23. PMID: 26199111; PMCID: PMC4661224.

138. Saccon TD, Schneider A, Marinho CG, Nunes ADC, Noureddine S, Dhahbi J, Nunez Lopez YO, LeMunyan G, Salvatori R, Oliveira CRP, Oliveira-Santos AA, Musi N, Bartke A, Aguiar-Oliveira MH, Masternak MM. Circulating microRNA profile in humans and mice with congenital GH deficiency. Aging Cell. 2021 Jul;20(7):e13420. doi: 10.1111/acel.13420. Epub 2021 Jun 12. PMID: 34118183; PMCID: PMC8282278.

139. Kelly BN, Haverstick DM, Lee JK, Thorner MO, Vance ML, Xin W, Bruns DE. Circulating microRNA as a biomarker of human growth hormone administration to patients. Drug Test Anal. 2014 Mar;6(3):234-238.

140. Calin GA, Dumitru CD, Shimizu M, Bichi R, Zupo S, Noch E, Aldler H, Rattan S, Keating M, Rai K, Rassenti L, Kipps T, Negrini M, Bullrich F, Croce CM. Frequent deletions and down-regulation of micro- RNA genes miR15 and miR16 at 13q14 in chronic lymphocytic leukemia. Proc Natl Acad Sci U S A. 2002 Nov 26;99(24):15524-9. doi: 10.1073/pnas.242606799. Epub 2002 Nov 14. PMID: 12434020; PMCID: PMC137750.

141. Peng Y, Croce CM. The role of MicroRNAs in human cancer. Signal Transduct Target Ther. 2016 Jan 28;1:15004. doi: 10.1038/sigtrans.2015.4. PMID: 29263891; PMCID: PMC5661652.

142. Otmani K, Lewalle P. Tumor Suppressor miRNA in Cancer Cells and the Tumor Microenvironment: Mechanism of Deregulation and Clinical Implications. Front Oncol. 2021 Oct 15;11:708765. doi: 10.3389/fonc.2021.708765. PMID: 34722255; PMCID: PMC8554338.

143. Catellani C, Ravegnini G, Sartori C, Angelini S, Street ME. GH and IGF System: The Regulatory Role of miRNAs and lncRNAs in Cancer. Front Endocrinol (Lausanne). 2021 Aug 16;12:701246. doi: 10.3389/fendo.2021.701246. PMID: 34484116; PMCID: PMC8415755.

144. Cheng M, Huang W, Cai W, Fang M, Chen Y, Wang C, Yan W. Growth hormone receptor promotes osteosarcoma cell growth and metastases. FEBS Open Bio. 2020 Jan;10(1):127-134. doi: 10.1002/2211-5463.12761. Epub 2019 Dec 18. PMID: 31725956; PMCID: PMC6943229.

145. Tzanakakis GN, Giatagana EM, Berdiaki A, Spyridaki I, Hida K, Neagu M, Tsatsakis AM, Nikitovic D. The Role of IGF/IGF-IR-Signaling and Extracellular Matrix Effectors in Bone Sarcoma Pathogenesis. Cancers (Basel). 2021 May 19;13(10):2478. doi: 10.3390/cancers13102478. PMID: 34069554; PMCID: PMC8160938.

146. Wang YH, Han XD, Qiu Y, Xiong J, Yu Y, Wang B, Zhu ZZ, Qian BP, Chen YX, Wang SF, Shi HF, Sun X. Increased expression of insulin-like growth factor-1 receptor is correlated with tumor metastasis and prognosis in patients with osteosarcoma. J Surg Oncol. 2012 Mar;105(3):235-43. doi: 10.1002/jso.22077. Epub 2011 Aug 22. PMID: 21866554.

147. Chen L, Wang Q, Wang GD, Wang HS, Huang Y, Liu XM, Cai XH. miR-16 inhibits cell proliferation by targeting IGF1R and the Raf1-MEK1/2-ERK1/2 pathway in osteosarcoma. FEBS Lett. 2013 May 2;587(9):1366-72. doi: 10.1016/j.febslet.2013.03.007. Epub 2013 Mar 15. PMID: 23507142.

148. Liu Y, Zhu ST, Wang X, Deng J, Li WH, Zhang P, Liu BS. MiR-100 Inhibits Osteosarcoma Cell Proliferation, Migration, and Invasion and Enhances Chemosensitivity by Targeting IGFIR. Technol Cancer Res Treat. 2016 Oct;15(5):NP40-8. doi: 10.1177/1533034615601281. Epub 2015 Aug 25. PMID: 26306402.

149. Chen G, Fang T, Huang Z, Qi Y, Du S, Di T, Lei Z, Zhang X, Yan W. MicroRNA-133a Inhibits Osteosarcoma Cells Proliferation and Invasion via Targeting IGF-1R. Cell Physiol Biochem. 2016;38(2):598-608. doi: 10.1159/000438653. Epub 2016 Feb 5. PMID: 26845446.

150. Xie Y, Deng H, Wei R, Sun W, Qi Y, Yao S, Cai L, Wang Y, Deng Z. Overexpression of miR-335 inhibits the migration and invasion of osteosarcoma by targeting SNIP1. Int J Biol

Macromol. 2019 Jul 15;133:137-147. doi: 10.1016/j.ijbiomac.2019.04.016. Epub 2019 Apr 4. PMID: 30954590.

151. Liu ZF, Liang ZQ, Li L, Zhou YB, Wang ZB, Gu WF, Tu LY, Zhao J. MiR-335 functions as a tumor suppressor and regulates survivin expression in osteosarcoma. Eur Rev Med Pharmacol Sci. 2016 Apr;20(7):1251-7. PMID: 27097943.

152. Wang Y, Zhao W, Fu Q. miR-335 suppresses migration and invasion by targeting ROCK1 in osteosarcoma cells. Mol Cell Biochem. 2013 Dec;384(1-2):105-11. doi: 10.1007/s11010-013-1786-4. Epub 2013 Aug 22. PMID: 23975506.

153. Heyn H, Engelmann M, Schreek S, Ahrens P, Lehmann U, Kreipe H, Schlegelberger B, Beger C. MicroRNA miR-335 is crucial for the BRCA1 regulatory cascade in breast cancer development. Int J Cancer. 2011 Dec 15;129(12):2797-806. doi: 10.1002/ijc.25962. Epub 2011 May 25. PMID: 21618216.

154. Catellani C, Ravegnini G, Sartori C, Righi B, Lazzeroni P, Bonvicini L, Poluzzi S, Cirillo F, Predieri B, Iughetti L, Giorgi Rossi P, Angelini S, Street ME. Specific miRNAs Change After 3 Months of GH treatment and Contribute to Explain the Growth Response After 12 Months. Front Endocrinol (Lausanne). 2022 Jun 22;13:896640. doi: 10.3389/fendo.2022.896640. PMID: 35813630; PMCID: PMC9256936.

155. Cole TJ, Freeman JV, Preece MA. Body Mass Index Reference Curves for the UK, 1990. Arch Dis Child (1995) 73:25–9. doi: 10.1136/adc.73.1.25

156. Tanner JM, Whitehouse RH, Takaishi M. Standards From Birth to Maturity for Height, Weight, Height Velocity, and Weight Velocity: British Children 1965, Part II. Arch Dis Child (1966) 41:613–36. doi: 10.1136/adc.41.220.613

157. Greulich WW, Pyle SI. Radiographic Atlas Of Skeletal Development Of The Hand And Wrist. 2nd Edition. Stanford, California: Stanford University Press (1959). ISBN: 0804703981.

158. Marshall WA, Tanner JM. Variations in the Pattern of Pubertal Changes In Boys. Arch Dis Child (1970) 45(239):13–23. doi: 10.1136/adc.45.239.13

159. Marshall WA, Tanner J. Variations in Pattern of Pubertal Changes in Girls. Arch Dis Child (1969) 44:291–303. doi: 10.1136/adc.44.235.291

160. Schwarzenbach H, da Silva AM, Calin G, Pantel K. Data Normalization Strategies for MicroRNA Quantification. Clin Chem (2015) 61:1333–42. doi:10.1373/clinchem.2015.239459

161. Livak KJ, Schmittgen TD. Analysis of relative gene expression data using real-time quantitative PCR and the 2(-Delta Delta C(T)) Method. Methods. 2001 Dec;25(4):402-8. doi: 10.1006/meth.2001.1262. PMID: 11846609.

162. Chang L, Zhou G, Soufan O, Xia J. miRNet 2.0: network-based visual analytics for miRNA functional analysis and systems biology. Nucleic Acids Res. 2020 Jul 2;48(W1):W244-W251. doi: 10.1093/nar/gkaa467. PMID: 32484539; PMCID: PMC7319552.

163. Agarwal V, Bell GW, Nam J, Bartel DP. Predicting effective microRNA target sites in mammalian mRNAs. eLife, 4:e05005, (2015). eLife Lens view.

164. Lewis BP, Burge CB, Bartel DP. Conserved seed pairing, often flanked by adenosines, indicates that thousands of human genes are microRNA targets. Cell. 2005 Jan 14;120(1):15-20. doi: 10.1016/j.cell.2004.12.035. PMID: 15652477.

165. Amarasekara DS, Kim S, Rho J. Regulation of Osteoblast Differentiation by Cytokine Networks. Int J Mol Sci. 2021 Mar 11;22(6):2851. doi: 10.3390/ijms22062851. PMID: 33799644; PMCID: PMC7998677.

166. Vrahnas, C., & Sims, N. A. (2020). Basic Aspects of Osteoblast Function. In B. Z. Leder, & M. N. Wein (Eds.), Osteoporosis: Pathophysiology and Clinical Management (3 ed., pp. 1-16). (Contemporary Endocrinology). Humana Press Inc. https://doi.org/10.1007/978-3-319-69287-6_1

167. Noren Hooten N, Fitzpatrick M, Wood WH 3rd, De S, Ejiogu N, Zhang Y, Mattison JA, Becker KG, Zonderman AB, Evans MK. Age-related changes in microRNA levels in serum. Aging (Albany NY). 2013 Oct;5(10):725-40. doi: 10.18632/aging.100603. PMID: 24088671; PMCID: PMC3838776.

168. Mukherjee A, Murray RD, Shalet SM. Impact of growth hormone status on body composition and the skeleton. Horm Res. 2004;62 Suppl 3:35-41. doi: 10.1159/000080497. PMID: 15539797.

169. Hashemi Gheinani A, Burkhard FC, Rehrauer H, Aquino Fournier C, Monastyrskaya K. MicroRNA MiR-199a-5p regulates smooth muscle cell proliferation and morphology by targeting WNT2 signaling pathway. J Biol Chem. 2015 Mar 13;290(11):7067-86. doi: 10.1074/jbc.M114.618694. Epub 2015 Jan 16. PMID: 25596533; PMCID: PMC4358129.

170. Hilczer M, Smyczynska J, Lewinski A. Limitations of clinical utility of growth hormone stimulating tests in diagnosing children with short stature. Endocr Regul. 2006 Sep;40(3):69-75. PMID: 17100548.

171. Luo B, Zhou X, Tang Q, Yin Y, Feng G, Li S, Chen L. Circadian rhythms affect bone reconstruction by regulating bone energy metabolism. J Transl Med. 2021 Sep 27;19(1):410. doi: 10.1186/s12967-021-03068-x. PMID: 34579752; PMCID: PMC8477514.

172. Song C, Wang J, Kim B, Lu C, Zhang Z, Liu H, Kang H, Sun Y, Guan H, Fang Z, Li F. Insights into the Role of Circadian Rhythms in Bone Metabolism: A Promising Intervention

Target? Biomed Res Int. 2018 Sep 27;2018:9156478. doi: 10.1155/2018/9156478. PMID: 30363685; PMCID: PMC6180976.

173. Patel RA, Liu Y, Wang B, Li R, Sebti SM. Identification of novel ROCK inhibitors with anti-migratory and anti-invasive activities. Oncogene. 2014 Jan 30;33(5):550-5. doi: 10.1038/onc.2012.634. Epub 2013 Feb 11. PMID: 23396364; PMCID: PMC3977753.

174. Wilkinson L, Kolle G, Wen D, Piper M, Scott J, Little M. CRIM1 regulates the rate of processing and delivery of bone morphogenetic proteins to the cell surface. J Biol Chem. 2003 Sep 5;278(36):34181-8. doi: 10.1074/jbc.M301247200. Epub 2003 Jun 12. PMID: 12805376.

175. Shafi AA, Knudsen KE. Cancer and the Circadian Clock. Cancer Res. 2019 Aug 1;79(15):3806-3814. doi: 10.1158/0008-5472.CAN-19-0566. Epub 2019 Jul 12. PMID: 31300477; PMCID: PMC8121183.

176. Sakamoto W, Takenoshita S. OVEREXPRESSION OF BOTH CLOCK AND BMAL1 INHIBITS ENTRY TO S PHASE IN HUMAN COLON CANCER CELLS. Fukushima J Med Sci. 2015;61(2):111-24. doi: 10.5387/fms.2015-11. Epub 2015 Sep 11. PMID: 26370682; PMCID: PMC5131586.

177. Liu X, Choy E, Hornicek FJ, Yang S, Yang C, Harmon D, Mankin H, Duan Z. ROCK1 as a potential therapeutic target in osteosarcoma. J Orthop Res. 2011 Aug;29(8):1259-66. doi: 10.1002/jor.21403. Epub 2011 Mar 8. PMID: 21387396.

178. Zeng H, Zhang Y, Yi Q, Wu Y, Wan R, Tang L. CRIM1, a newfound cancer-related player, regulates the adhesion and migration of lung cancer cells. Growth Factors. 2015;33(5-6):384-92. doi: 10.3109/08977194.2015.1119132. Epub 2015 Dec 10. PMID: 26653968.

179. Zhu QD, Zhou QQ, Dong L, Huang Z, Wu F, Deng X. MiR-199a-5p Inhibits the Growth and Metastasis of Colorectal Cancer Cells by Targeting ROCK1. Technol Cancer Res Treat.

2018 Jan 1;17:1533034618775509. doi: 10.1177/1533034618775509. PMID: 29807462; PMCID: PMC5974564.

180. Cheng Y, Shen P. miR-335 Acts as a Tumor Suppressor and Enhances Ionizing Radiation-Induced Tumor Regression by Targeting ROCK1. Front Oncol. 2020 Mar 11;10:278. doi: 10.3389/fonc.2020.00278. Erratum in: Front Oncol. 2021 Feb 04;11:650811. PMID: 32219065; PMCID: PMC7078682.

181. Du W, Tang H, Lei Z, Zhu J, Zeng Y, Liu Z, Huang JA. miR-335-5p inhibits TGF-β1-induced epithelial-mesenchymal transition in non-small cell lung cancer via ROCK1. Respir Res. 2019 Oct 21;20(1):225. doi: 10.1186/s12931-019-1184-x. PMID: 31638991; PMCID: PMC6805547.

182. Iwawaki Y, Mizusawa N, Iwata T, Higaki N, Goto T, Watanabe M, Tomotake Y, Ichikawa T, Yoshimoto K. MiR-494-3p induced by compressive force inhibits cell proliferation in MC3T3-E1 cells. J Biosci Bioeng. 2015 Oct;120(4):456-62. doi: 10.1016/j.jbiosc.2015.02.006. Epub 2015 Mar 17. PMID: 25795570.

183. Qi XB, Jia B, Wang W, Xu GH, Guo JC, Li X, Liu JN. Role of miR-199a-5p in osteoblast differentiation by targeting TET2. Gene. 2020 Feb 5;726:144193. doi: 10.1016/j.gene.2019.144193. Epub 2019 Oct 26. PMID: 31669647.

184. Zhang L, Tang Y, Zhu X, Tu T, Sui L, Han Q, Yu L, Meng S, Zheng L, Valverde P, Tang J, Murray D, Zhou X, Drissi H, Dard MM, Tu Q, Chen J. Overexpression of MiR-335-5p Promotes Bone Formation and Regeneration in Mice. J Bone Miner Res. 2017 Dec;32(12):2466-2475. doi: 10.1002/jbmr.3230. Epub 2017 Aug 28. PMID: 28846804; PMCID: PMC5732062.

185. Zhang J, Tu Q, Bonewald LF, He X, Stein G, Lian J, Chen J. Effects of miR-335-5p in modulating osteogenic differentiation by specifically downregulating Wnt antagonist DKK1. J

Bone Miner Res. 2011 Aug;26(8):1953-63. doi: 10.1002/jbmr.377. PMID: 21351149; PMCID: PMC3810406.

186. Lin X, Wu L, Zhang Z, Yang R, Guan Q, Hou X, Wu Q. MiR-335-5p promotes chondrogenesis in mouse mesenchymal stem cells and is regulated through two positive feedback loops. J Bone Miner Res. 2014 Jul;29(7):1575-85. doi: 10.1002/jbmr.2163. PMID: 24347469.

List of papers published during the 3 years of PhD

1. Moghetti P, **Catellani C**, Sartori C, Migazzi M, Cirillo F, Villani M, Buia V, Righi B, Dauriz M, Fiers T, Tosi F, Street ME. Serum HMGB1 levels are independently associated with glucose clamp-derived measures of insulin resistance in women with PCOS. Journal of Endocrinological Investigation. 2023 *Accepted for publication article*

2. **Catellani C**, Ravegnini G, Sartori C, Righi B, Lazzeroni P, Bonvicini L, Poluzzi S, Cirillo F, Predieri B, Iughetti L, Giorgi Rossi P, Angelini S, Street ME. Specific miRNAs Change After 3 Months of GH treatment and Contribute to Explain the Growth Response After 12 Months. Front Endocrinol (Lausanne). 2022 Jun 22;13:896640. doi: 10.3389/fendo.2022.896640. *article*

3. **Catellani C***, Cirillo F*, Graziano S, Montanini L, Marmiroli N, Gullì M, Street ME. MicroRNA global profiling in cystic fibrosis cell lines reveals dysregulated pathways related with inflammation, cancer, growth, glucose and lipid metabolism, and fertility. Acta Biomed. 2022 Jul 1;93(3):e2022133. doi: 10.23750/abm.v93i3.12842.**Co-first author article*

4. Mansueto ML, Zagni G, Sartori C, Olivares Bermudez BA, Righi B, **Catellani C**, Fusco C, Frasoldati A, De Fanti A, Iughetti L, Street ME. Late diagnosis of severe long-standing autoimmune hypothyroidism after the first lockdown for the Covid-19 pandemic: clinical features and follow-up. Acta Biomed. 2022 Mar 8;92(S1):e2021239. doi: 10.23750/abm.v92iS1.11730. PMID: 35261392. *case report*

5. **Catellani C**, Ravegnini G, Sartori C, Angelini S, Street ME. GH and IGF System: The Regulatory Role of miRNAs and lncRNAs in Cancer. Front Endocrinol (Lausanne). 2021 Aug 16;12:701246. doi: 10.3389/fendo.2021.701246. PMID: 34484116; PMCID: PMC8415755. *Review*

6. Street ME, Sartori C, **Catellani C**, Righi B. Precocious Puberty and Covid-19 Into Perspective: Potential Increased Frequency, Possible Causes, and a Potential Emergency to Be Addressed Front Pediatr. 2021; 9: 734899. *Review*

7. Street ME, Cirillo F, **Catellani C**, Dauriz M, Lazzeroni P, Sartori C, Moghetti P. Current treatment for polycystic ovary syndrome: focus on adolescence. Minerva Pediatr. 2020 Aug;72(4):288-311. doi: 10.23736/S0026-4946.20.05861-2. Epub 2020 May 15. PMID: 32418411. *review*